NEW METHODS FOR THE EXAMINATION OF POOR QUALITY MEDICINES

A Thesis
Presented to
The Academic Faculty

By

Dana M. Hostetler

In Partial Fulfillment
Of the Requirements for the Degree
Master of Science in Chemistry

Georgia Institute of Technology

May 2011

NEW METHODS FOR THE EXAMINATION OF POOR QUALITY MEDICINES

Approved by:

Dr. Facundo M. Fernández, Advisor
School of Chemistry and Biochemistry
Georgia Institute of Technology

Dr. Julia Kubanek
School of Chemistry and Biochemistry
Georgia Institute of Technology

Dr. Lawrence Bottomley
School of Chemistry and Biochemistry
Georgia Institute of Technology

Date Approved: March 31, 2011

ACKNOWLEDGMENTS

I am very grateful to my advisor, Dr. Facundo Fernández for his support and guidance throughout the process of my research. Additionally, there were many others who assisted in this work: Michael D. Green, Paul N. Newton, Harparkash Kaur, Christina Y. Hampton, Leonard Nyadong, Arti Navare, Mark Kwasnik, Glenn Harris, Dr. Manshui Zhou, Dr. Asiri Galhena, and Christina Jones. Additionally, I am grateful to my committee and to all others that worked with me during my time at Georgia Tech.

I am grateful for the funding that was provided by the Gates Foundation. I am very grateful for all the collaborators I have had the privilege of working with for the duration of my time at Georgia Tech, including the Centers for Disease Control and Prevention, the London School of Hygiene and Tropical Medicine, and Oxford University.

I am extremely grateful for my friends and family who were there to support me during my academic endeavors at Georgia Tech, particularly my husband, Ryan Hostetler, and my parents, Dan and Mary DePotter. Thank you for always supporting me in everything I do.

TABLE OF CONTENTS

LIST OF TABLES

LIST OF FIGURES

LIST OF ABBREVIATIONS

AAS ..... Atomic Absorption Spectroscopy

ACT ..... Artemisinin Combination Therapy

APCI ..... Atmospheric Pressure Chemical Ionization

APTDI ..... Atmospheric Pressure Thermal Desorption Ionization

API ..... Active Pharmaceutical Ingredient

BMGF ..... Bill and Melinda Gates Foundation

CI ..... Confidence Interval

CID ..... Collision Induced Dissociation

CODFIN ..... Counterfeit Drug Forensic Investigation Network

DART ..... Direct Analysis in Real Time

DDA ..... Dodecylamine

DESI ..... Desorption Electrospray Ionization

$\mathbf{E_{int}}$ ..... Internal Energy

$\mathbf{E_o}$ ..... Critical Energy

ESI ..... Electrospray Ionization

FDA ..... Food and Drug Administration

FI-GR-SA Flow Injection Gradient Ratio Standard Addition

GPHF Global Pharma Health Fund

GR-SA Gradient Ratio Standard Addition

HPLC High Performance Liquid Chromatography

LC-MS Liquid Chromatography-Mass Spectrometry

LED Light Emitting Diode

LQAS Lot Quality Assurance Sampling

LSHTM London School of Hygiene and Tropical Medicine

MQCL Medicine Quality Control Laboratory

MRA Medicine Regulatory Agency

MS Mass Spectrometry

MSD Metastable-Stimulated Desorption

PEG Polyethylene Glycol

PTFE Polytetrafluoroethylene

Q-TOF Quadrupole Time-of-Flight

SP Sulfalene- Pyrimethamine

SY Survival Yield

TLC ..... Thin Layer Chromatography

TOF ..... Time-of-Flight

WHO ..... World Health Organization

XRD ..... X-ray Diffraction

SUMMARY

The production and distribution of counterfeit drugs is a critical health problem that plagues nations worldwide. The presence of counterfeit antimalarials has become especially worrying, as these drugs are most often needed by those living in nations whose resources to verify the medicine supply are lacking. Rapid analysis methods used for screening large quantities of poor quality antimalarials are critical in the battle to protect those in less developed regions of the world. Simple, cost effective analysis methods that can be used in the field must be developed so those whose governments cannot afford to maintain medicine regulatory agencies can still have faith in their medicinal supply.

A very powerful screening method, Direct Analysis in Real Time Mass Spectrometry (DART-MS) has been used to investigate thousands of poor quality medicines. This method, however, is known to fragment molecules more readily than commonly used, 'softer' ionization methods, such as electrospray ionization. Excess fragmentation in 'harder' ionization sources is due to deposition of additional internal energy to the ionized molecules. This internal energy deposition can be measured, so the analyst can be knowledgeable as to what to expect when examining unknowns using this recently developed ionization source.

Quantitation of the active pharmaceutical ingredient (API) in pharmaceuticals is crucial to the determination of what class a poor quality medicine fits into. Because poor quality drugs can be of different types, it is important to accurately classify them, in hopes of improving the supply of medicines available to those in less developed regions

of the world. High performance liquid chromatography (HPLC) is most commonly used to quantify the active pharmaceutical ingredient in poor quality medicines, however, this method is time consuming, preventing its use in high throughput settings.

During the course of my research, hundreds of poor quality pharmaceuticals were analyzed using DART-MS. The active pharmaceutical ingredient was detected during the rapid screening for many of these drugs, however, a more in depth analysis would often reveal less than the expected quantity of active ingredient. A rapid non-chromatographic quantitation method was developed using a mass spectrometer as the detector. This method allows for both quantitative and qualitative information regarding a specific sample to be obtained simultaneously, saving the analyst time and resources. Utilizing this non- chromatographic mass spectrometric method, degradation products have been identified, thus increasing our ability to classify drugs into their respective divisions.

CHAPTER 1

INTRODUCTION

Since the late 1990's, detection of counterfeit antimalarial medicines, the most commonly used drugs in tropical regions, has been increasing[1]. The World Health Organization (WHO) now recommends artemisinin-based combination therapies (ACTs) be used to treat malaria in most areas of Africa and South East Asia, where the multi-drug resistant strain of malaria, *Plasmodium falciparum* malaria, is most commonly present[2]. This treatment combines a short-lived artemisinin derivative and a longer-lasting antimalarial, such as piperaquine or lumefantrine. This new treatment has proved to be very effective against malaria, creating great hope. Unfortunately, ACTs are already being counterfeited worldwide due to their high demand and higher cost.

Drugs can fall in one of four groups: genuine, degraded, substandard and counterfeit (fake). A medicine is considered genuine when it contains the correct active pharmaceutical ingredient (API) in the correct amount, with the correct dissolution profile, and is contained in the correct packaging. A medicine is classified as degraded when it is produced by the claimed legitimate manufacturers and known to have once contained the correct amount of active ingredient, but no longer present does so due to suboptimal storage conditions. Medicines classified as degraded can be verified as such through detection of API degradation products. A medicine is classified as substandard when it contains the correct packaging and can be traced to the manufacturer stated on the packaging, however, the drug was not correctly manufactured, possesses

unacceptable levels of impurities, exhibits incorrect dissolution properties, or the dosage of the active ingredient outside of the accepted range. The final category of classification for medicines is counterfeit. A drug is considered counterfeit when there is evident intent to deceive the customer: the packaging may be a copy, the expected API may not be present (or present in a trace amount), or an unexpected active ingredient not listed on the packaging may be detected in the drug.

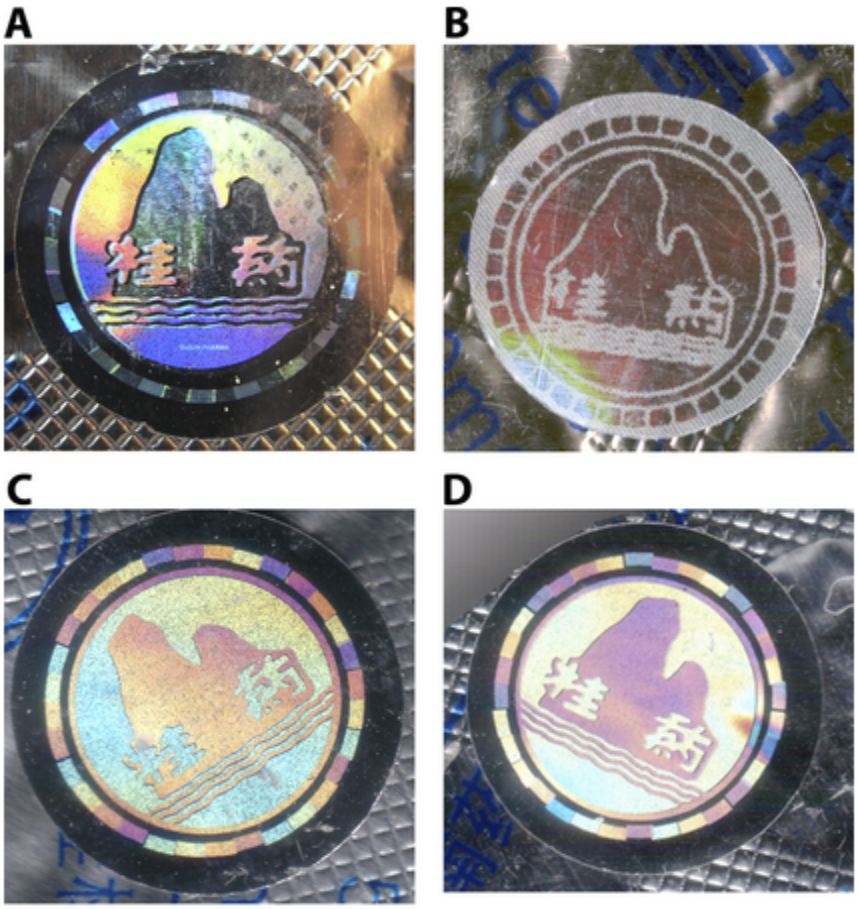

Figure 1: Images of genuine and counterfeit artesunate packaging holograms. A genuine Guilin Pharmaceutical artesunate blister pack hologram can be seen in 1a, while counterfeit copies of this hologram can be seen in 1b-d.

Counterfeit drugs harm those taking them because these patients actually receive little to no effective treatment[3, 4]. The presence of poor quality drugs also damages the pharmaceutical industry whose products are copied, causing billion-dollar losses. During my investigations of poor quality medicines, I have found that counterfeiters will go to great lengths to fool whatever regulatory agency (MRA) may be in place. In order to deceive the MRA or to cause a placebo effect, counterfeiters will often include different active ingredients than stated on the packaging (most common) or sub-therapeutic amounts of the stated active pharmaceutical ingredient in the counterfeit medicine. Infected people who take fake drugs that contain a lower dose of a therapeutic treatment are then effectively selecting parasites or bacteria that are resistant to this medicine. This process could render some anti-infective drugs useless for the treatment of a particular strain of the infectious agent. This issue, together with lack of compliance by patients, has rendered many monotherapy treatments for diseases such as malaria, completely ineffective. Examples include mefloquine around the border of Thailand[5], chloroquine in many regions of Africa and Southeast Asia[6], and more recently reports have been made in Southeast Asia of resistance to artemisinin combination therapies[7].

The ability to quickly and easily identify poor quality medicines is a critical component of drug quality assurance. Many techniques are currently used to establish medicine quality. However, most of these require technologies that are not available in the countries that need them. The countries where poor quality drugs are most prevalent tend to be less developed and have less resources, so many times these countries cannot afford to put a medicine regulatory agency in place to assure the quality of drugs available in that country. Access to an affordable medicine quality control laboratory

(MQCL) is therefore essential. The WHO encourages members to maintain such a laboratory[2], but unfortunately this is not always possible due to lack of economic resources.

Visual and physical inspection is the simplest of the techniques used to identify poor quality medicines. Manufacturers do their best to employ anti-counterfeiting measures, such as unique holograms on the packaging as well as invisible covert features to ensure the authenticity of their products. Unfortunately, with every development, it seems the counterfeiters are only one step behind. The holograms adhered to packages of artesunate manufactured by Guilin Pharmaceutical Co. Ltd. have been extensively counterfeited. Thus far, 16 different counterfeits have been indentified[8]. Visual inspection of packaging involves inspection of the batch number, expiration date, and a close look at any insert that may be provided with the medicine. The tablet is examined for size, markings, color, and chipped edges, indicators that the medicine being examined is not good quality. In order to be absolutely sure that the packaging is not counterfeit, it is important to compare these packages with known genuine packages from all manufacturing plants for the medicine being inspected.

Collaborators have used pollen analysis to determine the region of origin for drugs verified as counterfeit by other analytical methods[9]. This method involves an analyst looking closely at the pollen under a microscope and possibly using an imaging technique to determine the type of pollen, if a grain is detected. The types and amounts of different pollen grains found can narrow down the regions where these counterfeit drugs are being manufactured, assisting officials in stopping these harmful medicines from being traded.

Thin layer chromatography (TLC) is a simple and inexpensive tool that can be very effective in identifying poor quality medicines. TLC plates and a variety of chemical reagents are necessary, along with minimal training for the person performing the experiment. A genuine medicine from the same manufacturer is also required in order confirm results of the TLC experiment. TLC is useful as a pass/fail mechanism, but cannot distinguish between the types of poor quality medicines. A method has been reported which utilizes TLC and 2,4-dinitrophenylhydrazine or 4-benzoylamino-2,5-dimethoxybenzenediasonium chloride hemi (zinc chloride) salt as the reagents, resulting in pink or blue products, respectively, only if a derivative of artemisinin is present[10].

As discussed previously, many developing countries do not have the technical, financial, or human resources required to inspect and police the drug supply. Simple and affordable field methods, therefore, provide a practical means of rapidly monitoring drug quality. Portable laboratories provide a versatile means of initial screening of most antimalarial formulations. The GPHF MiniLab, a field laboratory compiled specifically for the analysis of antimalarials, uses a four-stage process to examine the quality of drugs: Visual inspection of solid dosage forms and packages, tablet and capsule disintegration test for a preliminary assessment of drug solubility, simple color reactions to identify drugs, and semi-quantitative TLC to check for quantities of API present, which requires the user to be trained prior to utilizing the MiniLab. The Tanzanian Food and Drugs Authority piloted the use of the MiniLab kits and found it to be relatively inexpensive and rapid, but only grossly substandard or counterfeited samples could be distinguished. While the MiniLab is a useful tool, it is recommended that it be used to complement drug analysis completed by a MQCL[11].

High Performance Liquid Chromatography (HPLC) is the standard in determining quantity of active pharmaceutical ingredient present in medicines. HPLC, which separates compounds based on their polarity or size, is a more complicated technique than the analytical methods used in the MiniLab and must therefore be performed in an MQCL. Based on the retention time and area of the analyte peak, HPLC identifies and quantifies active pharmaceutical ingredients present in a drug, but requires a clean laboratory for sample preparation and many high purity solvents for analysis. Additionally, a standard is necessary to verify the identification of a particular drug when using HPLC to match retention times. Between instrumentation and necessary consumables, HPLC is a quite costly analysis method, which results in this technique not being widely available in the poorest countries of the developing world. .

HPLC instruments can be coupled with many types of detectors. Most commonly, UV/Visible absorbance detector, though other options include single wavelength, fluorescence, photo diode array, electrochemical, refractive index, or mass spectrometry detectors. Liquid chromatography-mass spectrometry (LC-MS) enables abundant chemical information to be obtained from each sample analysis, however, this technique relies on tedious, time-consuming sample preparation and requires a great deal of analysis time.

Mass spectrometric analysis of poor quality drugs provides the analyst with qualitative information on every compound that is ionized in the medicine. Because of this ability to detect the majority of ionizable compounds present, mass spectrometric analysis has the ability to distinguish between counterfeit, degraded, and substandard medicine, thought this analysis and classification is usually done in conjunction with

other analytical techniques. For the screening of suspect poor quality medicines, Direct Analysis in Real Time (DART) is commonly used as the ionization source, as it allows for rapid analysis and does not require any type of sample preparation. Desorption Electrospray Ionization (DESI) is an ionization technique that is also often used in the analysis of poor quality medicines. DESI utilizes an ESI needle directed at a stage where the sample is placed[12]. The charged solvent dissolves a small portion of the tablet and is sucked into the mass spectrometer inlet through an extended capillary. This ionization technique, like DART, takes place in open air and requires no sample preparation, resulting in very high sample. Despite the usefulness of mass spectrometry as an analytical technique, instrumentation and consumables necessary for analysis make it very costly and the analyst must have extensive training.

Inexpensive hand-held LED photometers are useful in measuring the absorbance associated with colorimetric reactions specific for active ingredients in pharmaceutical preparations. Colorimetric methods have been published for many antimalarials, including artemisinin derivatives[10, 13-15]. Simple refractometers have also proven very useful in measuring dissolved active pharmaceutical ingredients in appropriate solvents[15]. Other inexpensive and portable instruments are useful in measuring physicochemical characteristics such as pH, tablet weight, viscosity of syrups, and density of suspensions and solutions. The pH of a genuine artesunate tablet, for example, in aqueous alcohol is approximately 3.5, whereas some tested poor quality medicines had a pH of approximately 6.5. Tablet weight of a particular class of counterfeited Guilin artesunate tablet tends to be approximately 10% more than then genuine tablet[4]. While these portable instruments can provide the analyst with useful information, analysis should

always be run in conjunction a MQCL, to ensure accurate classification of poor quality medicines.

Nondestructive portable spectroscopic technologies are available for field-testing of poor quality medicines. Infrared spectroscopy and Raman spectroscopy are currently being evaluated for rapid detection of poor quality medicines. With these techniques, drug samples may be scanned through the plastic of the blisterpack while still in its original packaging and no toxic chemicals or flammable solvents are necessary. Raman spectroscopy is based on the Raman effect, the scattering of light interacting with the different vibrational modes of the drug and excipient molecules contained in the tablet. One potential drawback of using Raman spectroscopy is that only the sample surface is probed, so if the active pharmaceutical ingredient is not distributed homogeneously throughout the entire tablet, the resulting content information may be inaccurate. The spectra obtained using Raman spectroscopy cannot be deconvoluted into specific signals from different chemicals as it presents information regarding the functional groups in a molecule. In order to identify genuine samples, a fingerprinting method is used where a Raman spectrum is compared against a spectral database. It is also important to ensure that interference from an excipient does not cause the sample to be wrongly characterized as a fake. Because of this, it is crucial to have a database of every genuine formulation from every manufacturer, thus decreasing the risk of incorrectly identifying a genuine drug as a poor quality medicine. A common disadvantage seen when Raman has been tested to analyze pharmaceutical preparations is that many drugs contain highly fluorescent excipients, thus negatively affecting the quality of the spectrum.

Nevertheless, Raman spectroscopy has been successfully tested in the field for detection of counterfeits[16].

Infrared spectroscopy utilizes the fact that different drug molecules absorb differently when excited with infrared light. Unlike Raman spectroscopy, infrared radiation has a larger penetration depth, with the potential advantage being that the larger area examined can detect an active ingredient that is not perfectly homogeneous throughout the entire tablet. Infrared spectroscopy, like Raman, uses the fingerprinting method in order to match the sample spectrum to a compound in the database. Near-infrared spectroscopy uses the near-infrared region of the electromagnetic spectrum (from approximately 800–2500 nm) and entails exciting the molecules in a sample and recording the unique fingerprint obtained. The method has been used to analyze excipients and may be used to demonstrate that they are not in the correct proportion, thus suggesting that the medicine is counterfeit[17].

X-ray fluorescence (XRF) is a nondestructive technique that utilizes X-rays to determine which chemical elements are contained in a sample. When X-ray fluorescence is used for analysis, X-rays bombard the sample and characteristic emissions result from different elements. This technique requires no sample preparation and is most commonly used for elemental analysis and to detect metals present. Although the active pharmaceutical ingredient is not measured directly, the elemental composition of counterfeit drugs tends to be quite different from that of the genuine. XRF, like Raman and infrared methods, requires a genuine tablet to verify whether a medicine can be classified as genuine or poor quality.

X-ray diffraction (XRD) is based on the elastic scattering of X-rays by the crystalline structures organized and aligned in crystals. Powder diffraction is often used in identifying unknown samples. This technique compares the spectrum obtained from a specific sample to a database containing spectra from every expected possibility. This method is destructive, as the tablet must be crushed into a powder. This method can also be used to measure the relative abundance of the major components in the sample, and usually provides information regarding excipients that is not easily obtained by mass spectrometry and other common analytical methods[18].

Many of the methods stated previously are used on a regular basis by CODFIN for analysis of poor quality medicines. The analytical workflow currently in use by CODFIN to test samples collected in country-level drug quality surveys can be seen in Figure 2, below. Steps colored with light green background can be performed in the field or in the laboratory depending on the logistics of the study.

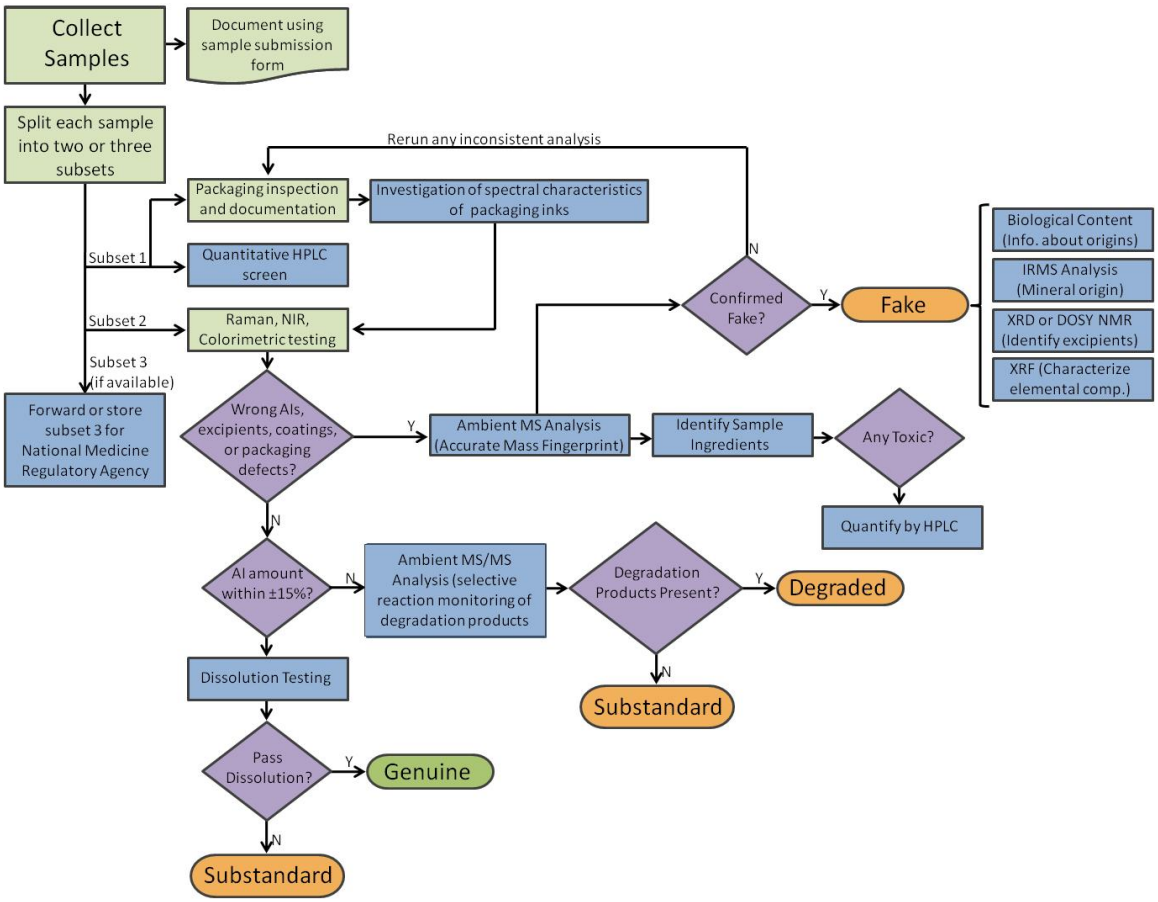

Figure 2: Protocol of poor quality medicine analysis used by CODFIN.

There are increasing reports of poor quality antimalarials in Africa[19]. Since 1999 there have been reports of counterfeit artesunate tablets from Nigeria, Chad, the Democratic Republic of the Congo (DRC) and Cameroon, counterfeit dihydroartemisinin tablets from Tanzania, Nigeria, Kenya and the DRC, counterfeit artemether tablets from DRC, substandard artesunate from Kenya, Ghana and Burkina Faso, poor quality artesunate tablets from Ghana, Nigeria, Tanzania and Uganda, poor quality artemether tablets from Kenya and Uganda and poor quality dihydroartemisinin tablets from Ghana, Kenya, Nigeria and Tanzania[3, 20-26]. Monotherapy formulations, however, even when of good quality, should no longer be generally available[27] and are being replaced by ACTs. Although, poor quality ACTs have yet to be reported in Asia there is an alarming increase of reported poor quality ACTs in Africa, e.g. artemether- lumefantrine tablets from Ghana, Nigeria and Uganda[26], counterfeit artemether- lumefantrine from Ghana and Nigeria[28-31] and counterfeit dihydroartemisinin- piperaquine from Kenya[20]. In response to this apparent epidemic of poor-quality ACTs in Africa, we offered to analyze antimalarial medicines of suspicious quality in sub-Saharan Africa via meetings, word of mouth, INTERPOL and the Counterfeit Drug Forensic Investigation Network (CODFIN; www.codfin.org). The study referred to reports these findings and assesses their implications for malaria control in Africa (See Appendix A.1).

DART is an ionization technique often used in combination with mass spectrometry. This ionization source is optimal for the screening of poor quality medicines, as it requires no sample preparation and has very high throughput. This ion generation technology, first reported in 2005 by Cody *et al.*, is becoming one of the most popular surface analysis methodologies amenable to open air operation (Figure 3). DART

utilizes a heated helium metastable plasma produced by a point-to-plane atmospheric pressure glow discharge. Most often, helium is used as the discharge gas, though nitrogen can be used as the discharge gas as well. The discharge gas molecules are subject to an electrical potential of around 3600 V, generating a glow discharge containing ionized gas, electrons, and metastable species (atoms in an excited state). These metastables are heated and directed through a grid electrode that prevents ion-ion and ion-electron recombination of ionic species generated within the DART ionization source. The most prevalent mechanism proposed for the formation of positive ions by DART involves Penning ionization of atmospheric water molecules induced by collisions with electronically-excited metastable helium atoms (He* $^3S_1$, 19.8 eV) (Eq. 1)[32]:

$$He^*(g) + nH_2O(g) \longrightarrow He(g) + (H_2O)_{n-1}H^+(g) + OH^-(g) \quad \text{(Eq. 1)}$$

Protonated water clusters of different sizes react with thermally-desorbed molecules (AB) (Eq. 2a) to undergo proton transfer to different extents depending on *n* (Eq. 2b)[33].

$$AB(s) \xrightarrow{heat} AB(g) \quad \text{(Eq. 2a)}$$

$$AB(g) \xrightarrow{(H_2O)_{n-1}H^+(g)} AB(H_2O)_{n-2}H^+(g) + H_2O(g) \xrightarrow{-(n-2)H_2O} ABH^+(g) \quad \text{(Eq. 2b)}$$

Another ionization mechanism that has been observed under high grid voltages, small DART to mass inlet spacing, and low humidity conditions is direct Penning ionization of desorbed analytes[34]. This mechanism produces electron ionization-like spectra (Eq. 3) for low polarity compounds with low proton affinities. Under these conditions, charge exchange reactions with diatomic oxygen molecular ions can also occur (Eq. 4a and 4b)[34].

$$He^*(g) + AB(g) \longrightarrow He(g) + AB^+(g) + e^- \quad \text{(Eq. 3)}$$

$$He^*(g)+O_2(g)\longrightarrow He(g)+O_2^+(g)+e^- \quad \text{(Eq. 4a)}$$

$$O_2^+(g)+AB(g)\longrightarrow O_2(g)+AB^+(g) \quad \text{(Eq. 4b)}$$

These ionization processes occur in the sampling region between the DART ionization source and the mass spectrometer inlet. Placement of a solid, liquid or gaseous sample in this region causes molecules on the sample surface to be desorbed as a result of the high temperatures and interaction with metastables, after which, reaction with water clusters occurs, resulting in a singly charged ion that is analyzed by the mass spectrometer.

Although many applications of DART MS have been demonstrated in the literature[35-37], this technique has not yet reached maturity. Many compounds exist that will not be readily ionized by DART. For example, if a molecule is very large, heat alone may not provide enough energy to desorb a sufficient number of molecules into the gas phase to be detectable. Also, in a case where a target compound does not have a higher proton affinity than water, analyte ions may not be formed when DART is run in the more commonly used positive mode. Another stumbling block in the path of more efficient DART ionization is the choice of discharge gas used. When nitrogen is used instead of helium, differences in excitation energies and heat conductivity cause a marked difference in sensitivity. This phenomenon demonstrates that nitrogen excited states are lower in energy than most commonly populated electronic levels in metastable helium atoms, and that sample heating is much slower when nitrogen is used, limiting the number of neutrals available for proton transfer reactions.

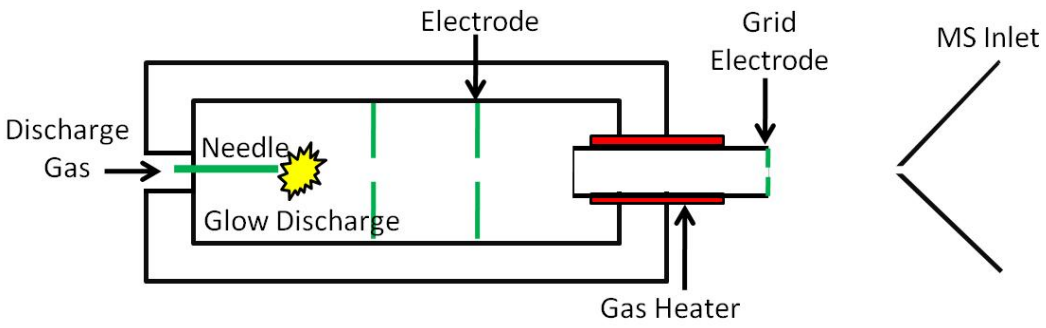

Figure 3: Schematic of a DART ionization source.

The focus of this research was applying DART to the field of counterfeit drug detection. One outcome of this research is the first database consolidating chemical analysis results from fake drugs collected in developing countries. Hundreds of suspicious pharmaceuticals were analyzed using high-resolution DART time-of-flight (TOF) mass spectrometry and accurate mass measurements to identify their ingredients (See Appendix A.2). This work was carried out as part of the Bill and Melinda Gates Foundation (BMGF)-funded ACT consortium led by the London School of Hygiene and Tropical Medicine (LSHTM). DART ionization is optimal for screening of suspect poor quality medicines because there is no need for sample preparation and each sample requires only seconds of analysis time. Although the benefits of DART ionization outweigh the negatives for the screening of drugs, DART is a technique that causes more fragmentation to analytes than softer 'soft' techniques, like electrospray ionization. The extent of fragmentation of a compound during ionization is directly proportional to the internal energy deposited to this analyte. Internal energy deposition in DART becomes extremely relevant when applying it to the investigation of samples of unknown content. If several signals are detected in a mass spectrum due to fragmentation, the analyst may be tricked into considering each of them as individual sample components, severely complicating data analysis and possibly the experimental results. Because analytes of interest are being unintentionally fragmented when a 'hard' ion generation technique is used, the intensity of the target peak is decreased, resulting in decreased sensitivity for the analyte of interest.

When choosing an ionization method, the optimal situation would be one in which ionization causes no fragmentation unless the user chooses to purposely do so, for

example in a controlled tandem MS experiment. The higher the internal energy deposition associated with a particular ion generation technology is, the more in-source induced fragmentation will be observed, resulting in a more complicated mass spectrum with lower sensitivity.

The extent of internal energy deposition can be determined by several methods[38-40]. The "survival yield method" was chosen for this study. In this method, a series of *p*-substituted benzylpyridinium salts whose dissociation energies are well known is used to probe the extent of internal energy in the system (Figure 4). When these analytes are subject to DART, the energy imparted during ionization causes a certain degree of fragmentation. The intensity of the precursor ion peak is compared to the intensity of the product fragment ion peak; the ratio is converted to a survival yield. By comparing the survival yields of the ions in the benzylpyridinium series to their known dissociation energies, the internal energy distribution produced by DART under various conditions can be investigated.

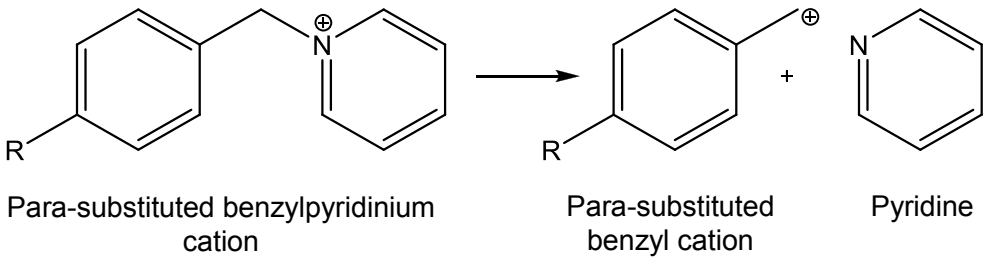

Figure 4: Structure of p-substituted benzylpyridinium ions and their fragments**.**

To date, the majority of internal energy (E_{int}) deposition studies have focused primarily on spray-[38-40] and laser-[41, 42] based desorption/ionization techniques. E_{int} deposition studies of ions generated by atmospheric pressure chemical ionization (APCI) have focused on post-source E_{int} contributions to fragmentation[43, 44] or isomerization[45] during in-source and tandem MS collision induced dissociation (CID). Previously, the E_{int} deposition of desorption electrospray ionization (DESI) has been investigated yielding insight on ion formation and energetics of this ambient ionization technique[40].

One of the most difficult tasks in screening of poor quality drugs is determining whether a drug fits into the classification defined as substandard or degraded. In both classes, a lower than expected quantity of API is found. The ability to distinguish between these classes, however, is crucial, as the solutions to these problems are very different. If the poor quality medicines are substandard, the problem must be presented to the manufacturers, as the error is occurring during the production of the medicine. Degraded drugs, however, are caused by poor storage conditions, so the problem must be addressed with the pharmacies and other distributors.

The ACT Consortium has begun a multi-year stability study to examine the stability of many ACTs under tropical conditions and to identify their degradation products. In addition, many of these medicines are not stored as directed by the manufacturer. Thus, many of these drugs may be degrading prior to their distribution to patients. This is especially likely in countries with weak or no medicine regulatory agencies (MRAs). The sheer number of samples involved in the ACT Consortium study implies that analysis by HPLC will require years of instrument time. To obtain quantitative data without HPLC analysis, a rapid quantitative method utilizing mass

spectrometry was developed. This method utilizes a gradient ratio standard addition approach.

The gradient ratio standard addition method was initially developed as a calibration method for flame atomic absorption spectrometry[46]. It was applied first to Flame Atomic Absorption Spectrometry (AAS), for detecting calcium in the presence of severe matrix effects. This method has not been applied outside the field of atomic absorption spectrometry until now, despite its potential usefulness. The gradient ratio standard addition method consists of consecutive injections, the first with analyte concentration C_s, and the second composed of the sample and the standard, with total analyte concentration $C_{s+r}=C_s+C_r$, where C_r is analyte concentration in the added standard alone. Two traces are thus recorded: the sample trace with intensity vs. time I_s, and the standard plus sample trace, with intensity I_{s+r}. These traces (chronograms) are overlaid and aligned so the initial edges match up. Because the compounds that cause matrix effects are diluted as the peak decreases from the maximum to an intensity of zero but the ratio of the two traces remains constant, this method allows the analyst to treat the trailing part of the chronograms as a series of multiple standard additions with only a single physical addition of the standard.

The ionization technique that was used for the flow injection gradient ratio standard addition method presented here is electrospray ionization (ESI). ESI is a commonly used method of ionization in many applications. During ESI, a solution is sprayed from a charged needle, leading to the formation of a Taylor cone[47, 48]. The droplets being emitted from the cone break down due to Coulombic explosions and produce "naked" ions following, most likely, a combination of two proposed models.

The first is the ion evaporation model[49], which suggests that as the charged droplet is decreasing in size due to collisions with the heated dry gas, the charge density on its surface becomes large enough to induce desorption of a charged analyte molecule. The second model, known as the charged residue model[50], proposes that electrospray droplets are continually evaporating and splitting off, eventually leading to a bare molecule that remains charged.

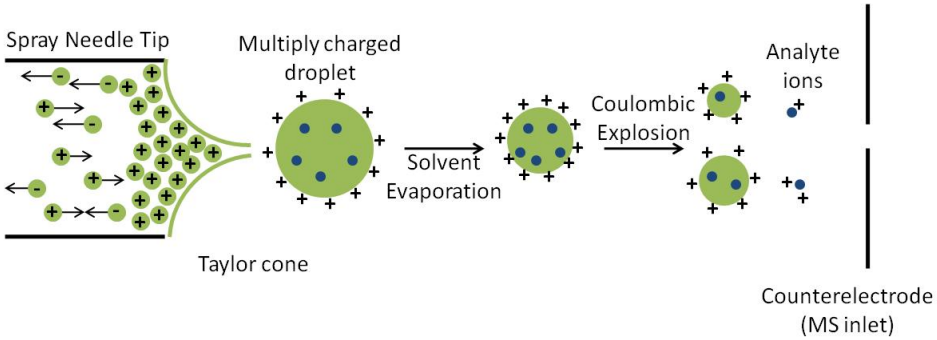

Figure 5: Schematic of electrospray ionization.

Although ESI has been used extensively for quantitation[51] of APIs, quantitation can be done reliably only by using an internal standard[52] to compensate for potential ion suppression effects, and by coupling to chromatography to simplify the resulting mass spectrum. The optimal internal standard is a compound with the same ionization efficiency and a similar mass to the analyte. The ionization efficiency will be similar for molecules with similar chemistries, thus the response by the mass spectrometer for these two compounds will be comparable. The best internal standard is a stable isotope-labeled version of the analyte. Deuterated or ^{13}C analogs, however, may be very expensive or may not be available at all. The quantitative method presented here does not require such standards and avoids chromatography, thereby decreasing analysis time and increasing the number of samples that can be analyzed per hour. This method is well suited for classifying medicine quality.

CHAPTER 2

EXPERIMENTAL

2.1 DART Screening of Poor-Quality Medicines

2.1.1 Solvents, Standards, Instrumentation

DART-MS was used to rapidly screen drugs for the expected active ingredient or any other compounds that may be present in drug samples. The DART 100 ion source was purchased from Ionsense (Saugus, MA, US). The mass spectrometers used for detection were a JMS-100TLC (AccuTOF) orthogonal acceleration time-of-flight mass spectrometer (JEOL USA, Peabody, MA, US) and a quadrupole time-of-flight hybrid instrument (Bruker MicroTOF Q I, Billerica, MA, US). Standards were purchased for artesunate (Apin Chemicals Ltd., Abingdon, Oxon, UK; Sigma, St. Louis, MO, US), dihydroartemisinin (Apin Chemicals Ltd., Abingdon, Oxon, UK), amodiaquine (Sigma, St. Louis, MO, US), pyrimethamine (Sigma, St. Louis, MO, US), mefloquine (Sigma, St. Louis, MO, US), quinine (Sigma, St. Louis, MO, US), chloroquine (Fluka, St. Louis, MO, US), sulfadiazine (Sigma, St. Louis, MO, US), and acetaminophen (Sigma, St. Louis, MO, US). For calibration of the mass spectrometers, a 1.5 μM solution of PEG 400 (Sigma-Aldrich, St. Louis, MO, US) in methanol (VWR, Radnor, PA, US) was used. The excitation gas used for all DART experiments was helium (Airgas, Atlanta, GA, US).

The DART settings used for analysis of suspect poor quality medicines were as follows: gas temperature of 200°C, grid 1 voltage of 50 V and grid 2 voltage of 150 V.

The discharge needle was set to 3600 V. The flow rate of helium when the AccuTOF was used was most commonly 4 L min^{-1}, while analysis on the MicroTOF Q required a lower flow rate of 1 L min^{-1}. When DART was used in conjunction with the MicroTOF Q, a Vapur® vacuum interface had to be employed to maintain the low pressure required by the instrument. This interface utilized a ceramic tube and aluminum vestibule connected to the mass spectrometer interface. This vestibule was directly connected to a small diaphragm pump (Vacuubrand, Wertheim, Germany). In this additional vacuum interface, neutrals are removed, and ions are guided into the mass spectrometer, resulting in the ability to use much lower gas flow rates while gaining sensitivity, as more of the ions in the ionization region are sampled into the mass spectrometer.

2.1.2 Sample Collection

Collaborating members of the Counterfeit Drug Forensic Investigation Network (CODFIN) collected samples throughout Africa and South East Asia using both random and convenience sampling methods. The most commonly used sampling method in studies of drug quality is convenience sampling. Convenience sampling involves shoppers purchasing medicines without specific guidance as to which outlets to purchase medicines from. Convenience sampling is a cheap, simple method that does not require a complete list of all outlets in the sampled region. Compilation of such a list is most often a difficult task due to poor documentation in developing countries and unregistered or illegally run outlets. Convenience sampling is very prone to bias, however, as the shopper may only purchase medicines from reputable outlets, poorly run outlets, or illegal outlets, depending on the outcome they prefer or expect. As a result, convenience

sampling produces outcomes that may not accurately represent the true distribution of types of medicines in the region.

Random sampling results in a more accurate sampling of a region's medicines. With a sufficient sample size, random sampling will result in reliable estimates of the prevalence of outlets providing poor quality medicines and their distributions in a defined geographical area. This sampling method allows for comparisons to be made with subsequent estimates and allows for the evaluation of the effectiveness of any interventions taken to assist in solving the problems found. The main drawback to the random sampling method is the fact that a very large sample size is required for accurate, usable data. The costs associated with this large sample size can be quite high, a reason why many do not use this strategy.

Lot Quality Assurance Sampling (LQAS) method determines whether the prevalence of outlets selling poor quality medicines exceeds a certain threshold[18]. This method is often used by companies to assure product quality. LQAS helps keep the cost of determining the distribution of medicine types in a region low and it is often used as a precursor to the random sampling method. Although this method is very useful, it also requires an accurate list of registered pharmaceutical distributors, which is difficult to attain.

2.1.3 Data Processing

Spectra resulting from DART screening of poor quality medicines are first examined for the drug stated on the packaging. If there is no active ingredient specified or the packaging is not available, the spectra are examined for common antimalarials.

After this step, the (x, y) data is imported into an in-house developed database of many common drugs and excipients. In most cases, the majority of intense peaks are identified as compounds in the database through their accurate masses. If major peaks have not been identified at this point, SmartFormula, a software program provided by Bruker compares exact mass and isotopic ratios to determine the most likely candidates for the elemental formula of the selected peak. To ensure the existence of a compound before that peak is labeled, ChemSpider, an online chemical database, is used to identify compounds with the elemental formula generated by SmartFormula. In this way, the compounds contained in poor quality medicines are identified.

Once compounds are identified, all the MS, packaging and HPLC data is entered into a database that was created specifically for the compilation of all information on poor quality medicines. Collaborators and MRAs can have immediate access to the data. See Appendix A.2 for more information on this database.

2.2 DART-MS Internal Energy Deposition Studies

2.2.1 Synthesis and Preparation of Para-Substituted Benzylpyridinium Salts

The *p*-substituted methyl- (CH_3), chloro- (Cl), cyano- (CN), and nitro (NO_2) benzylpyridinium compounds were synthesized by condensation of the *p*-substituted benzyl halide with pyridine followed by recrystallization from diethyl ether as described by Katritzky *et al*.[41]. Pyridine, nitromethane, anhydrous diethyl ether, anhydrous ethanol, and the benzyl halide starting reagents were all used without further purification (Sigma-Aldrich, St. Louis, MO, US). The methoxy- (OCH_3) substituted compound was purchased (Arkat US, Inc. Gainesville, FL, US). All samples were stored in a -80 °C

freezer when not in use to minimize degradation. For DART experiments, an equimolar thermometer ion mixture (100 μM) was prepared in nanopure water (Barnstead International, Dubuque, IA, US), while for ESI experiments, a 1 μM mixture was prepared in either a nanopure water or a 50% methanol (Sigma-Aldrich, St. Louis, MO, US) solution.

2.2.2 DART-TOF MS Sampling, Instrumentation, and Data Acquisition

DART samples were prepared by pipetting 5 μL aliquots of the sample mixture onto the tips of DIP-it™ sample capillaries (IonSense, Inc. Saugus, MA, US) and allowing the drops to dry for 30 minutes. Sample deposition was repeated eight times so a total of 4 nanomoles of each compound was deposited on each capillary. Capillaries were affixed to an in-house built sample holder attached to a hinged right-angle sample arm (Thorlabs, Newton, NJ, US) for reproducible sample placement during all experiments.

MS analysis was performed with a commercial DART 100 ionization source (IonSense, Inc. Saugus, MA, US) and a JMS-100TLC (AccuTOF™) orthogonal acceleration time-of-flight (TOF) mass spectrometer (JEOL, USA, Peabody, MA). All experiments were performed in positive ion mode. Ion optics and detector settings can be found in Appendix A.5. A lower orifice 1 voltage was required for DART than for ESI, since it improved sensitivity. Preliminary experiments with DART at higher orifice 1 voltages (40 V and 60 V) resulted in overall low sensitivity, with the higher E_o ions remaining undetected, thus withholding the ability to conduct reliable E_{int} statistical calculations.

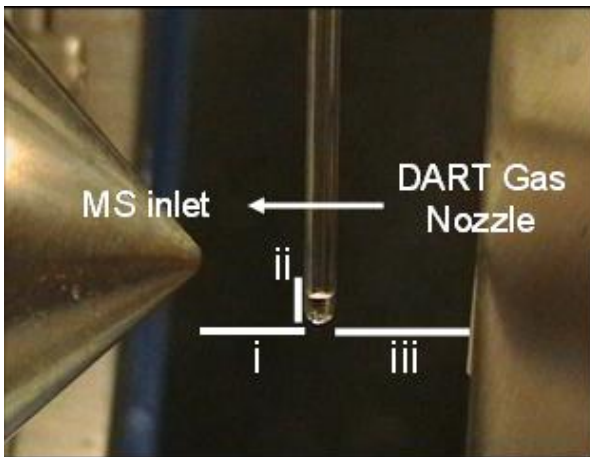

Figure 6: Sample placement for DART-TOF MS analysis of thermometer compounds. Samples were applied to Dip-it™ (diameter 0.16 cm) sample capillaries affixed to a stable sampling arm. Sample positioning distances: (i) center of MS orifice to capillary, 0.60 cm, (ii) capillary depth below center of MS orifice, 0.16 cm, and (iii) capillary to center of gas outlet distance, 0.74 cm.

DART ion source settings were as follows: discharge needle voltage: 3600 V, discharge electrode voltage: 150 V, grid electrode voltage: 100 V, distance between ion source and spectrometer inlet: 1.5 cm, distance of sample capillary to MS orifice: 0.60 cm, capillary depth below MS orifice: 0.16 cm, and capillary distance to the center of the DART gas nozzle: 0.74 cm (Figure 6). The rate of helium gas flow through the DART was 2, 4, or 6 L min^{-1}, and the set heater temperature was 175, 250, or 325 ºC. A solution of polyethylene glycol 600 (PEG, Sigma Aldrich, St. Louis, MO) prepared in 50% methanol was used as the mass calibration standard. A sample capillary dipped in the PEG solution was placed in front of the helium stream for 60 s, and a reference mass spectrum was obtained. Ultra high purity helium (99.999 %, Airgas, Atlanta, GA, US) was used in all DART experiments. Sample capillaries were held in the ionization region for 60 s. Mass spectral data processing, calibration, and background subtraction were performed using the built-in mass spectrometer software (MassCenter, v. 1.3). The temperature at the tip of the DIP-it™ capillary was determined with an 80BK temperature probe connected to a digital multimeter (Fluke 179-True RMS, Everett, WA, US). Ultra high purity nitrogen (99.995 %. Airgas, Atlanta, GA, US) was used following the exact procedure as helium experiments, but only the low dissociation energy compounds (*p*-OCH_3, *p*-CH_3, and *p*-Cl) were detected in this case. This result made E_{int} calculations impossible due to the lack of data points on the fitted survival yield curves. The lower vibronic metastable energy level of nitrogen, and its lower thermal conductivity are believed to be the primary responsible factor for the low sensitivity[32].

2.2.3 ESI-TOF MS Experiments, Instrumentation, and Data Acquisition

For ESI-TOF MS experiments, the DART ion source mounted onto the TOF mass spectrometer was replaced by the a pneumatically-assisted micro-ESI source (JEOL, USA, Peabody, MA). In this source, the nebulizing gas flows orthogonally (pointing downwards) to the mass spectrometer inlet orifice, while the drying (desolvating) gas is applied coaxially to the ESI needle assembly passing through a heated metal block to enhance desolvation. All mass spectrometer settings were identical to those used for DART-TOF MS experiments, with the exception that the orifice 1 voltage was set to 50 V for ESI, the minimum setting that produced sufficient sensitivity. A 1 μM solution containing all five *p*-substituted benzylpyridinium compounds prepared in either nanopure water or 50% methanol was delivered to the ion source with a liquid handling pump (Valco Instruments Co., VICI M6, Houston, TX, US). For the 50% methanol solution, the flow rate used was 200 μL min^{-1}. Due to the difficulty of desolvating aqueous droplets, however, a lower flow rate (150 μL min^{-1}) was required to produce a stable spray from the aqueous solution. A 1:10 000 dilution of the PEG solution was used as the mass calibration standard. Ion source settings were as follows: desolvation and nebulizing gas: nitrogen (99.995%, Airgas, Atlanta, GA), desolvation gas flow rate: 1 L min^{-1}, nebulizing gas flow rate: 2.5 L min^{-1}, desolvating chamber temperature: 175, 250, or 325 ºC, and needle voltage: 2500 V. Mass spectral data acquisition, processing, and calibration settings were identical to those used in DART-TOF MS experiments.

2.2.4 Survival Yield Method and Data Analysis

Uncontrolled ion activation within the ion source leads to an increase in the ions' E_{int}[42]. Defined by Vékey as the "amount of energy an ion contains above the ground electronic, vibrational, and rotational states"[43], E_{int} is a significant factor in determining ion fragmentation yields[38]. Because of the heterogeneity of the processes occurring in atmospheric pressure and ambient ionization, the extent of ion activation is better described by P(E), the normalized probability distribution that an ion has a given E_{int}[38,43]. Many methods have been developed to determine P(E) including the "thermometer molecule" method[53], the "deconvolution method"[54], and the method used in this study, the "survival yield" (SY) method[55, 56]. The SY method assumes that: (1) all ions with E_{int} below a critical energy, E_o, do not dissociate and appear as intact ionic species, and (2) all ions with E_{int} above E_o will dissociate into fragment ions[38, 40]. Experiments are performed with a series of *p*-substituted benzylpyridinium salts with well characterized thermodynamic properties and a similar number of degrees of freedom. The prevailing fragmentation pathway commonly observed for these salts is dissociation forming pyridine and a *p*-substituted benzyl cation at a known E_o. Following ionization, the ratio of the precursor (I_{prec}) and fragment (I_{frag}) ion intensities is calculated (Eq. 5)[55, 56].

$$SY_{exp} = \frac{I_{prec}}{I_{prec} + I_{frag}} \qquad \text{(Eq. 5)}$$

SY values are then plotted against their respective E_o and two points corresponding to a SY value of 0 at 0 eV (indicating that no precursor ions would survive if the associated critical energy was 0 eV) and a SY value of 1 at 3.5 eV (indicating that at high critical energies, no fragment ions would be observed) are added in order to fit the data to a sigmoidal function (Eq. 6).

$$SY_{Fitted} = \frac{a}{1+e^{-\left(\frac{Energy-x_0}{b}\right)}} = \int_0^{\infty} P(E)dE \quad \text{(Eq. 6)}$$

The SY_{Fitted} curve parameters, a, b, and $x_{0,}$ are experimentally fitted variables. The E_{int} distribution is determined by taking the first derivative of the sigmoid curve, generating the P(E) curve. The mean E_{int}, $<E_o>$, is then calculated by determining the centroid of P(E) (Eq. 7).

$$< E_0 >= \frac{E \cdot P(E)dE}{\int_0^{\infty} P(E)dE} \quad \text{(Eq. 7)}$$

An example of experimental data fitted to the sigmoidal function, then integrated can be found below, in Figure 7. For data analysis, each chronogram was averaged for one minute using the built-in mass spectrometer software (MassCenter, v. 1.3) and the spectrum was exported into Excel (Microsoft, Auburn, WA, US). After manually selecting peak maxima for the ions of interest, and calculating survival yields of each (Eq. 1), the data were treated with an in-house programmed macros to fit the survival yields to a sigmoid curve and to calculate the residual error of the fit, E_{int} distribution, mean E_{int}, and the full width half-maximum of the distribution.

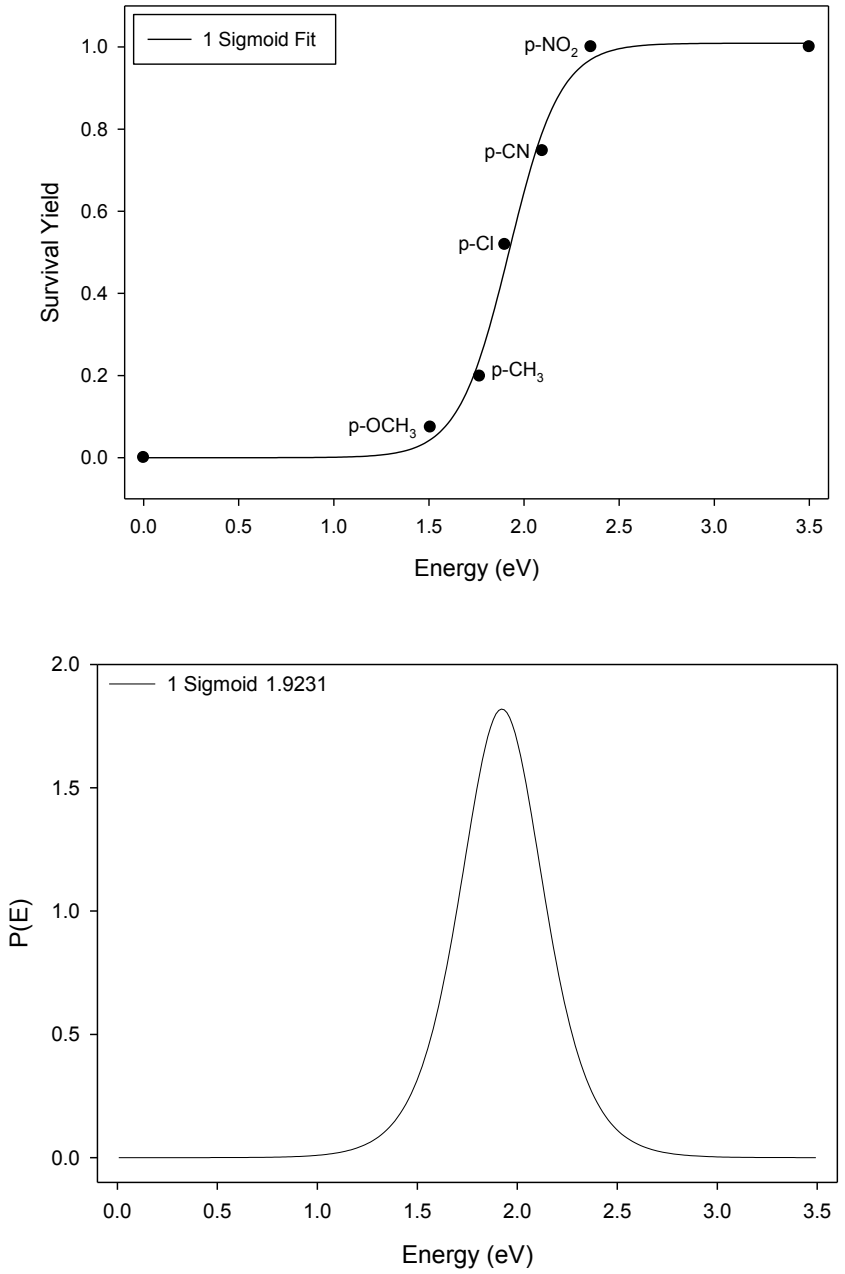

Figure 7: The upper panel represents the survival yield of each investigated benzylpyridinium ion versus its known critical energy is fit to a sigmoidal function using Equation 6. Theoretical data points of (0,0) and (3.5,1) were added to fit the sigmoidal function to the data. The lower panel represents the integral of the data fit in the top panel. The peak of this integral is the average internal energy for these compounds under the conditions used for the experiment, in this case, the DART ionization source was set to a temperature of 175°C and the discharge gas was running at 2 L min^{-1}.

2.3 Flow Injection Gradient Ratio Standard Addition Method for MS

2.3.1 Solvents, Standards, Instrumentation

Artesunate, an important and widely used antimalarial medication, was used to develop the flow injection analysis technique. In all experiments, artesunate was extracted directly from tablets, so any matrix effects due to tablet excipients were present in all experiments.

In order to quantitatively measure the amount of artesunate, a tablet (Mekophar Chemical Pharmaceutical JSC, Vietnam; Holley-Cotec Pharmaceuticals Co., Ltd., China, Guilin Pharmaceutical Co., China) was first homogenized using a mortar and pestle. The powder from the entire tablet was then placed in a vial and mixed with 10 mL of methanol (Sigma, St. Louis, MO, US). The solution of artesunate and methanol (and excipients that may have been extracted with the artesunate) was kept on ice for the entirety of the extraction process and all experiments. After being shaken every five minutes for a total of 40 minutes, the artesunate extract was filtered through a 0.45 μm PTFE membrane (MicroLiter Analytical Supplies, Inc., Suwanee, GA, US). This extract was then diluted to a concentration appropriate for ESI, in most cases, 1 μM.

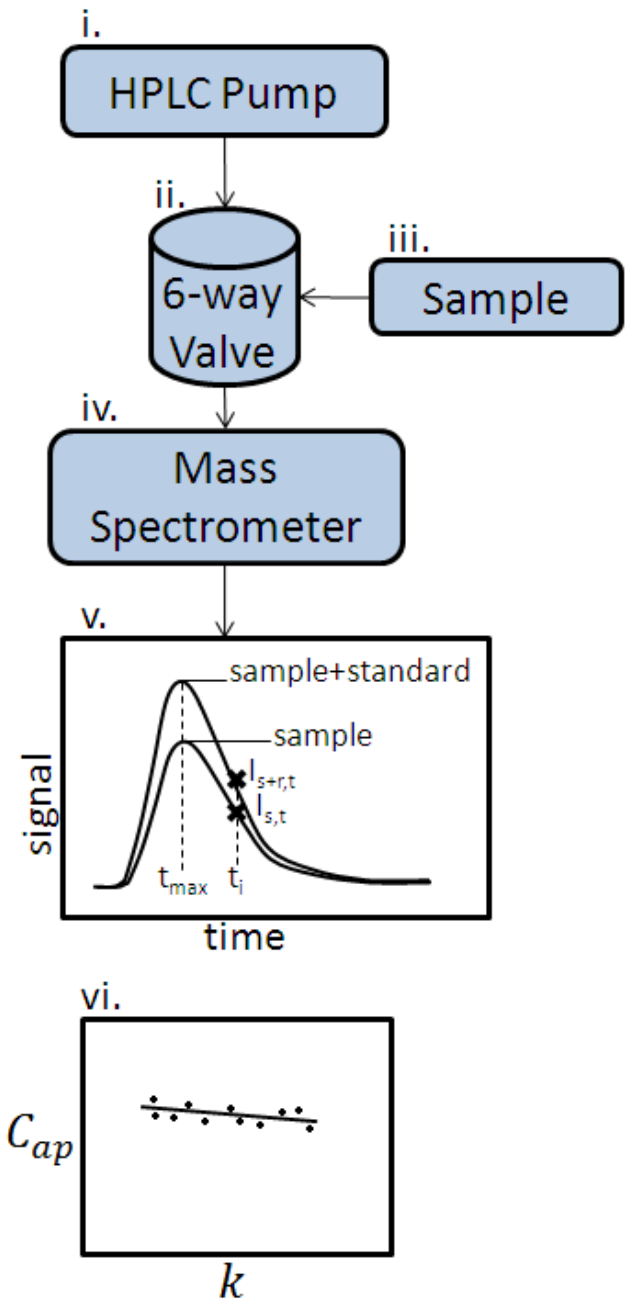

Figure 8: Workflow for flow injection gradient ratio standard addition mass spectral analysis.

2.3.2 Flow Injection Setup

The workflow used for FI-GR-SA-MS is shown in Figure 8. An HPLC pump (Agilent, Santa Clara, CA, US) delivering methanol at a rate of 150 μL min^{-1} was connected to the inlet of a software-controlled 6-way divert valve (Rheodyne (now IDEX Health and Science), Oak Harbor, WA, US), which was installed in the front panel of the mass spectrometer. The exit duct of the divert valve was connected to the mass spectrometer inlet. A syringe pump (Cole Parmer, Vernon Hills, IL, US) was used to load the sample into the loop of the divert valve in a reproducible manner. The sample coil used in this case was made of PEEK tubing and had a volume of 7.5 μL. Approximately 250 μL of sample solution were used to flush the sample loop and avoid carryover from previous samples. Six seconds into each MS run, the 6-way valve was switched, injecting the contents of the sample loop as a plug into the constant stream of methanol flowing into the electrospray ionization source. Each FI-GR-SA-MS run required 30 seconds of mass spectrometer acquisition time.

2.3.3 Mass Spectral Analysis

Mass spectral analysis was performed using a Bruker MicroTOF Q mass spectrometer. The settings were optimized for a mass-to-charge ratio of 570.4, the expected mass-to-charge ratio of the protonated artesunate/dodecylamine proton-bound complex. Specific instrumental settings used for these experiments can be found in Appendix A.6.

2.3.4 Data Analysis

Data was analyzed using the gradient ratio standard addition method. Equations 8 and 9, used for data analysis, were adapted from the work by Koscielniak[46] and can be found below.

$$C_{ap} = \frac{I_{s,t}}{I_{s+r,t} - I_{s,t}} C_r \quad \text{(Eq. 8)}$$

$$k(t) = \frac{I_{s+r}(t)}{I_{s+r}(t_{max})} \quad \text{(Eq. 9)}$$

C_{ap} is the apparent concentration of the sample without standard added. $I_{s,t}$ is the intensity of the sample signal at a certain point in time. $I_{s+r,t}$ is the intensity of the sample plus standard at a certain point in time. C_r is the concentration of the standard that was added to the sample. The first equation uses these variables to calculate the apparent concentration, which is plotted against the relative dilution at each time point, k(t). The relative dilution is calculated from $I_{s+r}(t)$, the intensity of the sample plus standard at a particular point, divided by $I_{s+r}(t_{max})$, the intensity of the sample plus standard at the maximum. The maximum of the sample plus standard trace is chosen as the first point for analysis and data is then analyzed point by point down to the 10% relative dilution value calculated with Equation 9.

2.3.5 Degraded Samples

In order to search for artesunate degradation products, genuine samples that had not yet reached their expiration date were artificially degraded in an oven heated to approximately 105°C. Samples were degraded for periods of 1, 2, 3, 4, 5, 6, 8, 10, and 12 hours.

2.3.6 HPLC Conditions

Samples were extracted in methanol and diluted to a theoretical concentration of 2 mg/mL. These extracts were run through a 0.45 μm nylon filter (MicroLiter Analytical Inc., Suwanee, GA, US), then placed in an HPLC vial (Agilent, Santa Clara, CA, US). The international pharmacopeia accepted method of artesunate analysis was the HPLC method followed. A potassium phosphate buffer was prepared using potassium dihydrogen phosphate (Sigma, St. Louis, MO, US) and deionized water. The buffer was adjusted to a pH of 3 using phosphoric acid (Sigma, St. Louis, MO, US). This buffer was used in a 50:50 ratio with acetonitrile for the mobile phase. A reverse phase C18 column (Supelco, St. Louis, MO, US) was used for analysis of the degraded artesunate. An artesunate standard (Sigma, St. Louis, MO, US) was used to prepare calibration curves for HPLC experiments. Calibrant solutions had concentrations of 1, 2 and 3 mg/ml. The UV detector was set to a wavelength of 216 nm. The mobile phase was flowed at 0.6 mL min^{-1}; each run lasted 15 minutes.

CHAPTER 3

RESULTS

3.1 Screening of Poor Quality Medicines

3.1.1 Survey of Poor Quality Artemisinin Combination Therapy and other Antimalarials in Africa

A large survey of drugs in Africa has been ongoing for the past five years. Hundreds of samples collected have been thoroughly analyzed in the context of this study. Sadly, many counterfeits have been uncovered. Figure 10 represents the results obtained for a study of drugs collected by INTERPOL. A specific detected counterfeit, for example, was uncovered in the tablets coded GH 09/01 (see Appendix A.1, Figure 9), the active pharmaceutical ingredient stated on the packaging was a co-formulation of artemether and lumefantrine, as can be seen in Figure 9. The upper panel of this figure displays the mass spectrum of the sample analyzed, while the lower panel is the mass spectrum of a genuine drug, with an zoomed inset of the peaks, revealing characteristic isotopic abundances of the genuine drugs. When the sample was screened using DART-MS, no artemether or lumefantrine was detected, however, pyrimethamine, another antimalarial was identified. Because lumefantrine is a yellow drug, the co-formulation of lumefantrine and artemether is a yellow tablet. The counterfeit tablet containing pyrimethamine appeared yellow, indicating the counterfeiters went to the trouble to camouflage the tablet in order to fool those they would sell the fake medicine to. The yellow dye used to disguise the counterfeit medicines has not yet been identified.

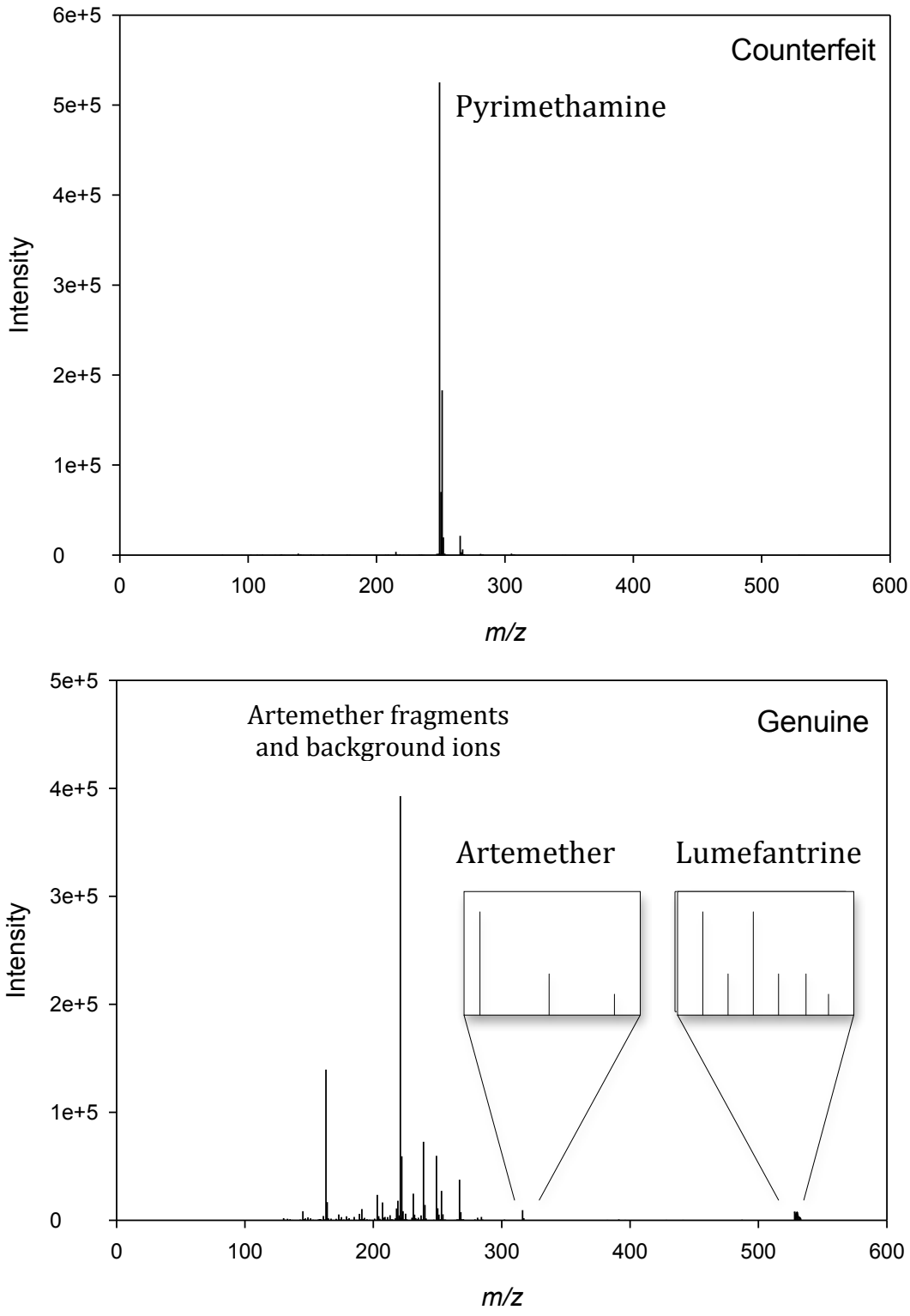

Figure 9: Example of genuine and counterfeit mass spectra for GH 09/01, a sample stated to contain artemether (*m/z* 316) and lumefantrine (*m/z* 528). Counterfeit contained pyrimethamine (*m/z* 249).

In the case of the medicine coded 4024 Nigeria (see Appendix A.1), the blisterpack indicated the contents being the antimalarial halofantrine, a drug sold by SmithKline as 'Halfan'. When screened using DART-MS, it was discovered that this medicine did not contain halofantrine, but contained acetaminophen instead. This type of formulation is especially dangerous because the infected patient will take the medicine, their fever will break, and they will begin to feel better. Unfortunately, the medicine is not fighting the parasite, it is only masking the symptoms of malaria, so the person will believe they are getting better, but ultimately, their condition will not have been treated.

Poor quality medicines can show a wide array of compositions, which is why analysis by so many methods is crucial to ensure the quality of a drug supply. In the case of the sample coded DRG 06/01 (Appendix A.1), when it was screened using MS and analyzed with HPLC, no active pharmaceutical ingredient was detected. This sample was composed exclusively of excipients, making it obviously counterfeit. In the case of sample UG 09/02, however, the expected active pharmaceutical ingredients were present in acceptable quantities and the majority of examined parameters appeared genuine, however no perforations were present across the blisterpack, which should be present in the genuine sample. The lack of this small detail suggested that this medicine was counterfeit. Samples like this demonstrate the lengths counterfeiters will go to for their medicines to appear genuine.

The most interesting samples examined in the course of this work were those coded CHINA 07/18- CHINA 07/21. The packaging stated these to be a co-formulation of dihydroartemisinin and piperaquine. When these medicines were analyzed by DESI-MS, analysts were surprised to detect the presence of sildenafil, the active pharmaceutical

ingredient in Viagra® in these antimalarials. The effect of this drug in patients with malaria is unknown, as sildenafil is most often taken by those who suffer from a very different ailment. This unexpected active pharmaceutical ingredient could have grave repercussions, as those with hypertension are warned against ingesting sildenafil. These samples also contained notable errors in the medicine's packaging.

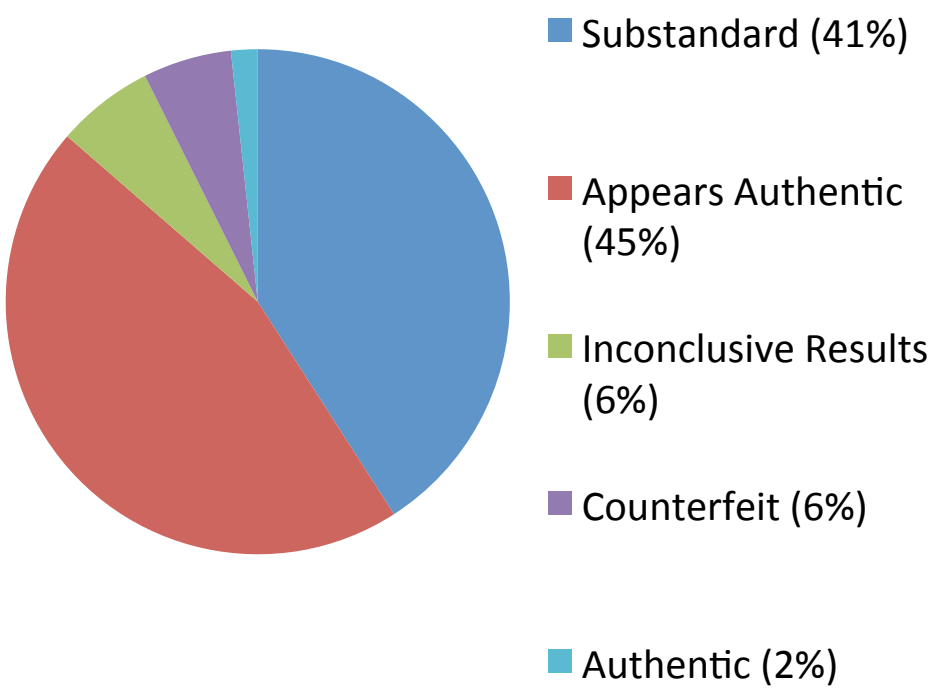

Figure 10: Pie chart representing proportions of sample set in each of the medicine quality groups. The analyzed medicines were collected by INTERPOL.

3.1.2 Randomized survey of antimalarial drug quality in Laos

Previous studies performed using convenience sampling in the Lao People's Democratic Republic (Laos) indicated that between 38 and 54 percent of all oral artesunate tablets collected in a four year time frame (2000-2003) were counterfeit. A follow-up study utilizing a random sampling method was carried out to verify this finding. Outlets were randomly chosen based on a statistician's random number tables from lists of provinces and districts within the selected sampling region.

One hundred and eighty outlets were sampled in the current study, representing 33.9% (180/531) of all pharmacies and shops selling medicines recorded in the study areas and 8.1% of all licensed pharmacies in Laos in 2003 (163/2,014). The majority of outlets sampled during the first collection were licensed pharmacies (81.5%). Shops selling artesunate were found in 7/ 12 (58.3%) districts. All pharmacies were Class 3 (i.e. 'with the licensee being neither pharmacist nor assistant pharmacist'. Artesunate was found in 25 of all 180 outlets (13.9%). Considering only the pharmacies, 15.3% (25/163) sold artesunate. No artesunate was purchased from shops selling medicines. Only one brand of artesunate was found in each pharmacy. Five pharmacies (20%) offered two blisterpacks of artesunate and the remaining 20 offered one.

All samples were sold in blisterpacks. By inspection of packaging, without knowledge of the chemical results, 26/ 30 (87% (95%CI 68–96%)) artesunate samples were counterfeit, three were genuine (10%) and the classification of one sample (12 Pas P2/1) could not be determined because key parts of the packaging were cut off before sale.

There was 100% agreement between the Fast Red dye test[14], HPLC, and MS analysis for the 30 samples labeled as artesunate[57]. All those classified as counterfeit based on the packaging contained no detectable artesunate. Chemical analysis of the sample with insufficient packaging (mentioned above) was shown by MS to contain pyrimethamine, sulphadoxine, and paracetamol, but no artesunate and was, therefore, counterfeit. The combination of packaging and chemistry demonstrates that 27/30 (90%) (95%CI 72–97%) of artesunate samples were counterfeit. In terms of outlets, 22/25 (88%) (95% CI 68–97%) sold fake artesunate. The three genuine samples contained a median (range) artesunate content/tablet of 49.2 (45.1– 50.3) mg (all had stated tablet content of 50 mg artesunate). The 27 counterfeit samples that underwent forensic MS analysis were found to contain paracetamol (16), sulphadoxine (12), dimethylfumarate (6), metamizole (5), pyrimethamine (8), erythromycin (5), artemisinin (4), 2-mercaptobenzothiazole (3), chloramphenicol (2), chloroquine (1) and erucamide (1). The concentrations of artemisinin as determined by HPLC were 0.26, 4.50, 6.50 and 115.7 mg/tablet, chloroquine 14.7 mg/tablet, pyrimethamine 17.1, 16.0, 16.6 mg/tablet and sulphadoxine 409.6, 385.9, 413.9 mg/tablet. Of 12 and 8 samples found by MS to contain sulphadoxine and pyrimethamine, respectively, sulphadoxine and pyrimethamine were found by HPLC in only three and three samples, respectively. The ratios of pyrimethamine to sulphadoxine, normally 1:20 in sulphadoxine- pyrimethamine (SP) coformulated tablets, were 1:24.0, 1:24.1 and 1:24.9 – suggesting that the counterfeits may have been formulated from powder after the co-drugs had been mixed to manufacture SP tablets. Of 4 samples examined with XRD, calcite was detected in three and starch in one. The stable isotope analysis of the calcite suggested a high temperature

or volcanic origin. The results from the pollen analysis are consistent with a source of the fake artesunate in southern China, but do not prove this geographical origin.

3.2 Internal Energy Deposition of DART-MS

3.2.1 Determination of the E_{int} *Deposition of DART Compared to ESI*

Various energy-depositing processes occur during DART ionization. For the thermometer compounds tested in this study, potential energy deposition pathways begin with the thermal desorption of the solid neutral salt into the gaseous phase (Scheme 1i). The neutral salt undergoes charge splitting to form the halide anion and the precursor cation via atmospheric pressure thermal desorption ionization (APTDI)[58], and/or the effect of the electric field established between the needle electrode, grid electrode, and the mass spectrometer inlet orifice (Scheme 1ii). Further activation of the precursor cation proceeds through additional heating (Scheme 1iii), reactive collisions with metastable He species (He^*) (Scheme 1iv), and/or deposition of excess energy released during proton transfer from protonated water clusters (Scheme 1v).

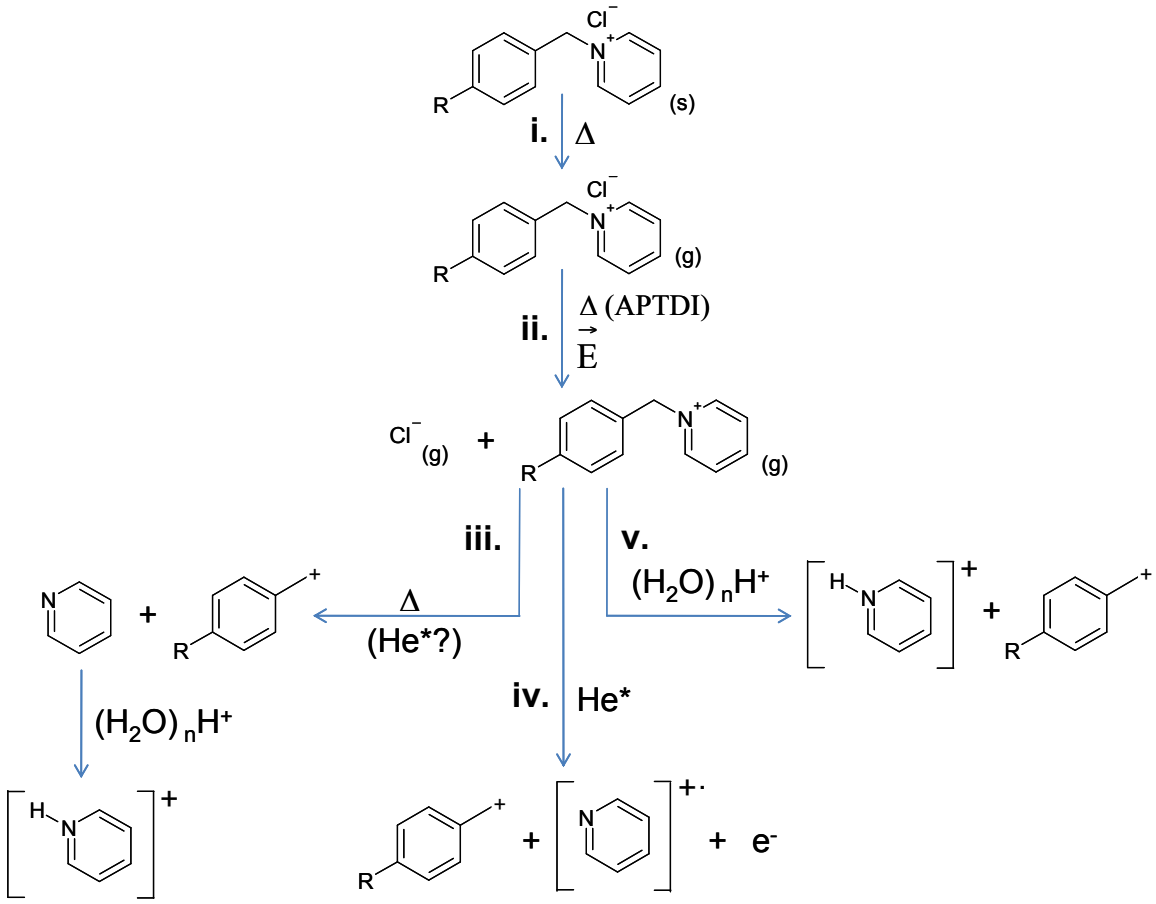

Scheme 1: Depiction of hypothesized fragmentation pathway for benzylpyridinium salts.

At the lowest assayed helium gas heater (DART) or desolvating chamber (ESI) temperature set point (175 ºC), both aqueous and 50% methanol solutions probed by ESI had lower $\langle E_o \rangle$ values (1.71 eV and 1.53 eV, respectively) compared to DART at all three gas flow rates tested (2 L min^{-1}: 1.92 eV, 4 L min^{-1}: 2.02 eV, and 6 L min^{-1}: 2.08 eV) (Figure 11a). In comparison to the softest ESI conditions with a 50% methanol solution, at 175 ºC, DART $\langle E_o \rangle$ values were higher by 25%, 32%, and 36% at 2, 4, and 6 L min^{-1}, respectively. The same trend followed at 250 ºC (Figure 11b), corresponding to DART $\langle E_o \rangle$ values that were higher than 50% methanol ESI values by 30%, 34%, and 38% at 2, 4, and 6 L min^{-1}, respectively. Furthermore, $\langle E_o \rangle$ values at 325 ºC for DART (2 L min^{-1}: 2.09 eV, 4 L min^{-1}: 2.18 eV, and 6 L min^{-1}: 2.21 eV) were higher than the comparable experiments for the 50% methanol ESI values by 28%, 33%, and 35% at 2, 4, and 6 L min^{-1}, respectively (Figure 11c). The shape of the E_{int} distributions displayed no asymmetric tailing at all temperatures tested[59]. These $\langle E_o \rangle$ values indicated that under the tested conditions, ESI is a "softer" ionization technique compared to DART.

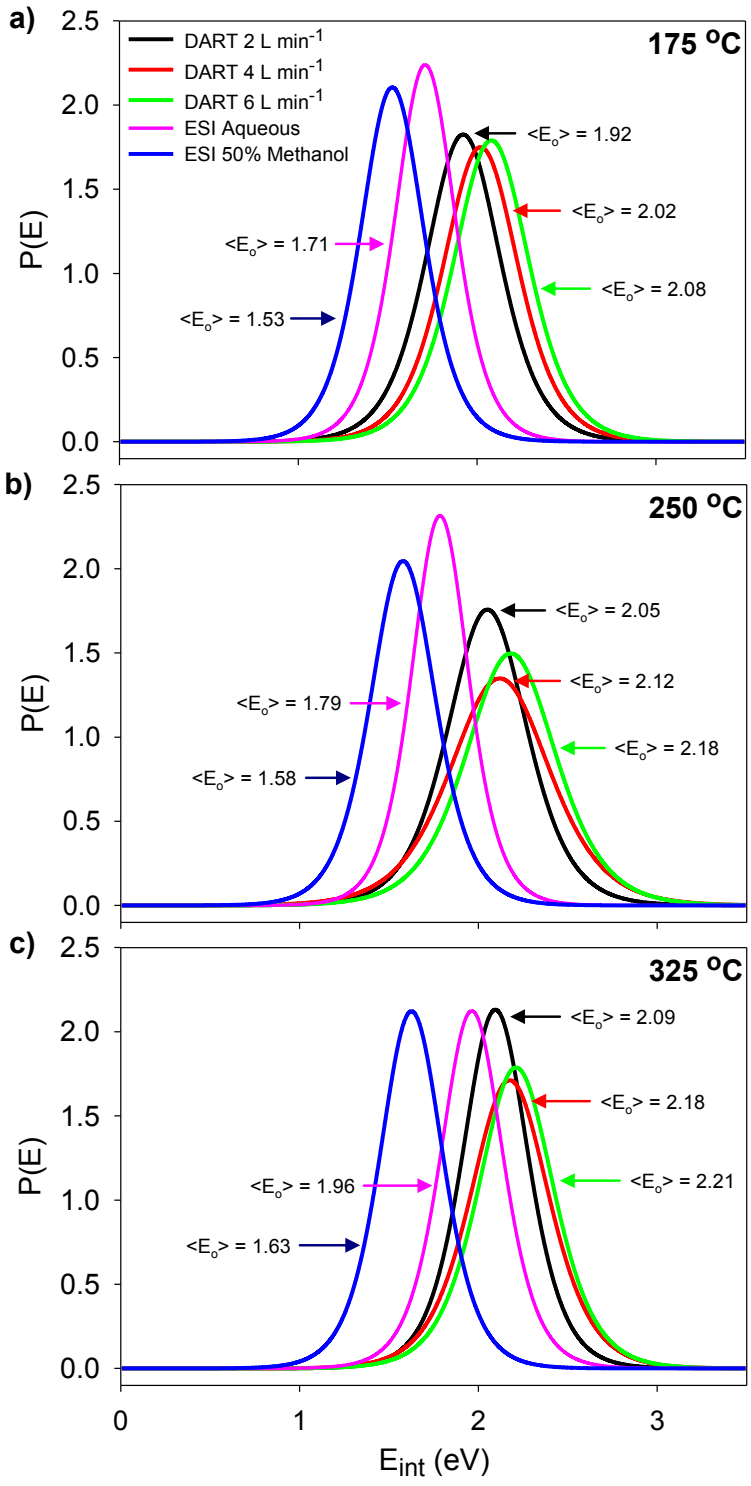

Figure 11: Mean E_{int} ($<E_o>$) distributions for DART and ESI with helium gas heater (DART) or desolvation chamber (ESI) temperature set points of a) 175 ºC, b) 250 ºC, and c) 325 ºC.

The aqueous solution analyzed by ESI had higher $<E_o>$ values in comparison to the 50% methanol solutions by 12%, 13%, and 20% at 175, 250, and 325 ºC, respectively. Due to the higher vapor pressure of methanol, droplets produced from a 50% methanol solution desolvate faster than aqueous droplets and cool more rapidly. The differences in E_{int} deposition observed between ESI experiments were consistent with prior investigations showing that P(E) could be altered by varying the solvent system vapor pressure, greatly affecting thermal and kinetic energy contributions[55]. Sprayed droplets acquire thermal energy by in-source heat conversion and friction with gas molecules to an extent that depends on droplet sizes[40, 55, 60, 61]. Kinetic energy from electric field-driven acceleration of charged droplets and ions can also be deposited into E_{int} modes, both in the atmospheric pressure region and within the various reduced pressure regions of the mass spectrometer interface[38, 40, 62].

3.2.2 Thermal Activation Pathways

In ESI, heated gas serves the role of improving charged droplet desolvation before entering the ion transfer optics region[48, 63]. This differs from the role of the heated gas used in DART experiments, which is to evaporate residual solvent and thermally desorb the analytes. If set high enough, temperatures induce unwanted fragmentation of labile species. It is quite important to distinguish between the DART temperature set by software, and the actual temperature within the ionization region. Measured gas temperatures at the bottom of the sample capillaries rapidly decreased upon increasing the flow rate setting as a result of rapid convective cooling of the ionization source environment. Direct temperature measurements (Figure 12) indicated that the actual gas

temperature was consistently lower than the set value, and that the difference between the two increased with increasing flow rates. When the heater was set at 175 ºC (Figure 12a), the average steady-state gas temperatures at 2, 4, and 6 L min^{-1} were 163 ºC, 145 ºC, and 136 ºC, respectively. This downward trend was the same for set temperatures of 250 ºC (2 L min^{-1}: 227 ºC, 4 L min^{-1}: 200 ºC, and 6 L min^{-1}: 187 ºC) (Figure 12b) and 325 ºC (2 L min^{-1}: 283 ºC, 4 L min^{-1}: 252 ºC, and 6 L min^{-1}: 236 ºC) (Figure 12c).

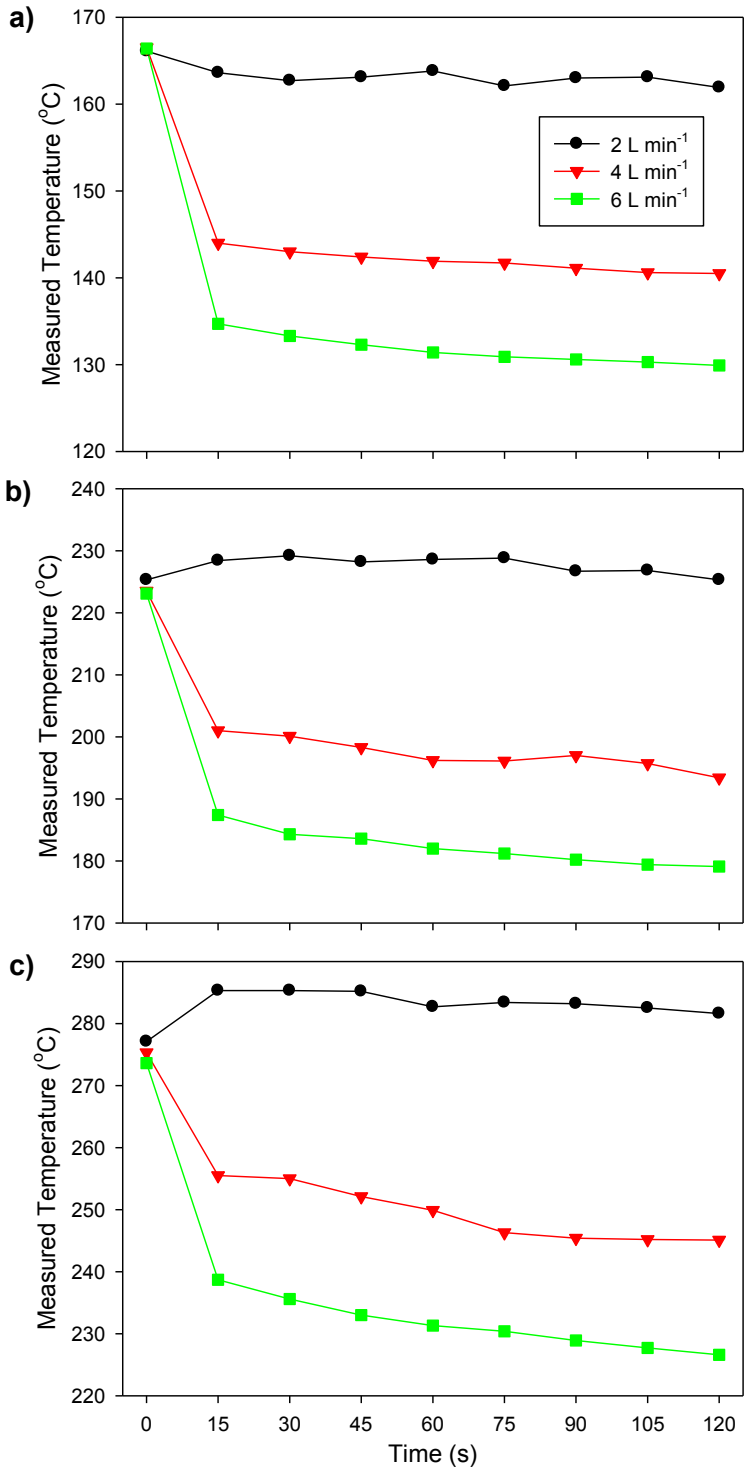

Figure 12: Measured gas temperature at the bottom of the sample capillary in the DART ionization region at experimental set temperatures of a) 175ºC, b) 250ºC, and c) 325ºC. Time t=0 sec corresponds to the instant the gas flow is turned on in the preheated DART source.

The measured "effective" temperatures strongly influenced the extent of E_{int} deposition. Ions generated at a high flow rate (4 and 6 L min^{-1}) at any set gas temperature were created in a thermally cooler environment compared to those created at low flow rates (2 L min^{-1}). Ion formation in a locally cooler environment is expected to lead to a decrease in thermal-induced fragmentation[59, 64, 65]. Contour maps for the data in Figure 11 were created to assist in understanding the E_{int} deposition trends observed experimentally (Figure 13). The E_{int} contour map for ESI indicates a decrease in E_{int} deposition with increasing concentrations of methanol at lower temperatures (Figure 13) as previously reported in similar work[55] and discussed above. The DART map shows that the least amount of energy was deposited at lower gas flow rates and temperatures (blue to green on the color scale), whereas the highest energy deposition occurred at high flow rates and set temperatures (yellow to red color scale, Figure 13). Because lower measured gas temperatures were detected at higher flow rates, thermal ion activation could not account for the increase in E_{int} observed under those conditions. Although ESI is clearly a 'cooler' ionization source, there is some overlap between the internal energy deposition of DART and ESI.

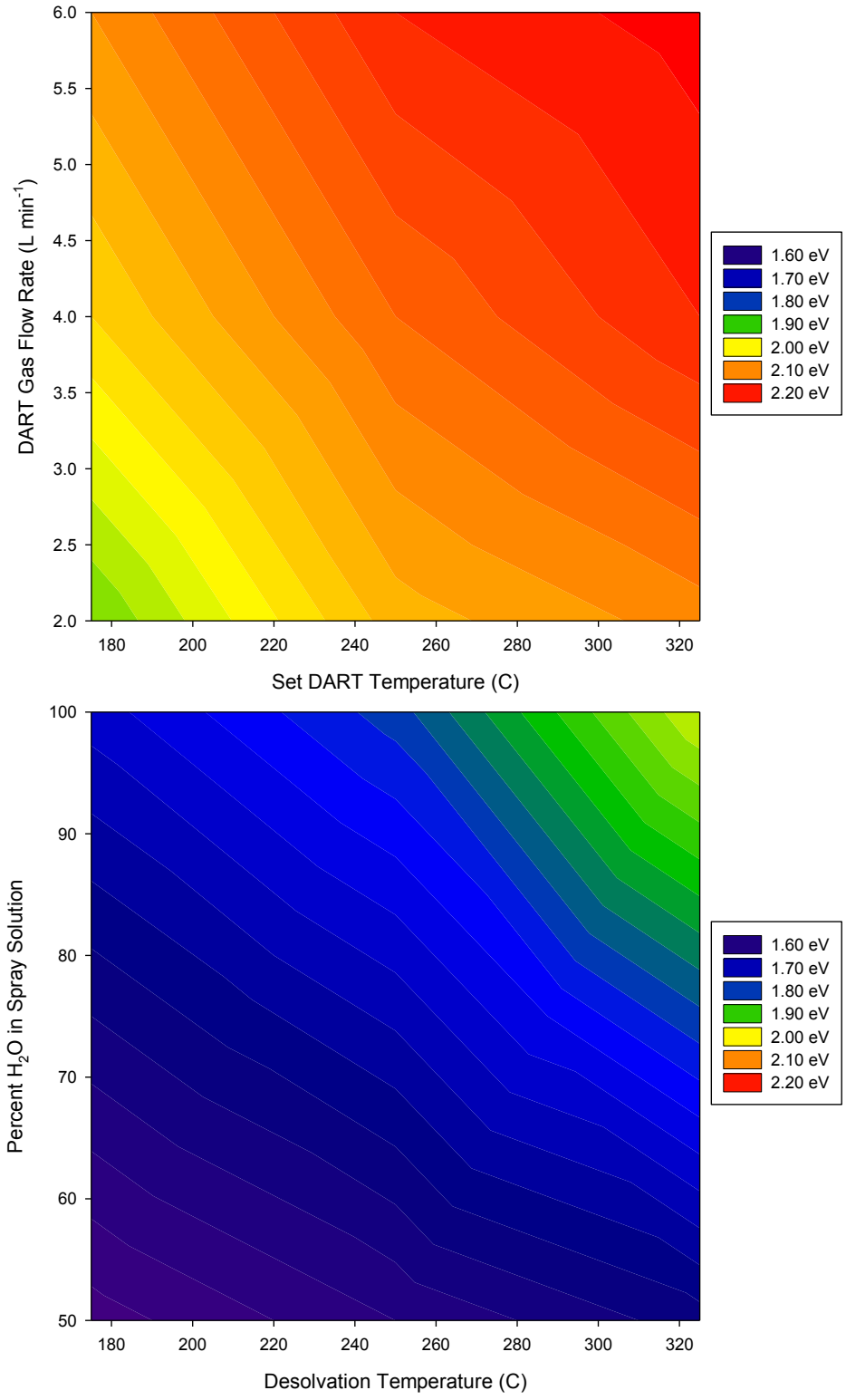

Figure 13: Mean E_{int} surface contour maps for DART (upper plot) and ESI (lower plot). Temperatures plotted on the x-axis correspond to set points in the ion source control software.

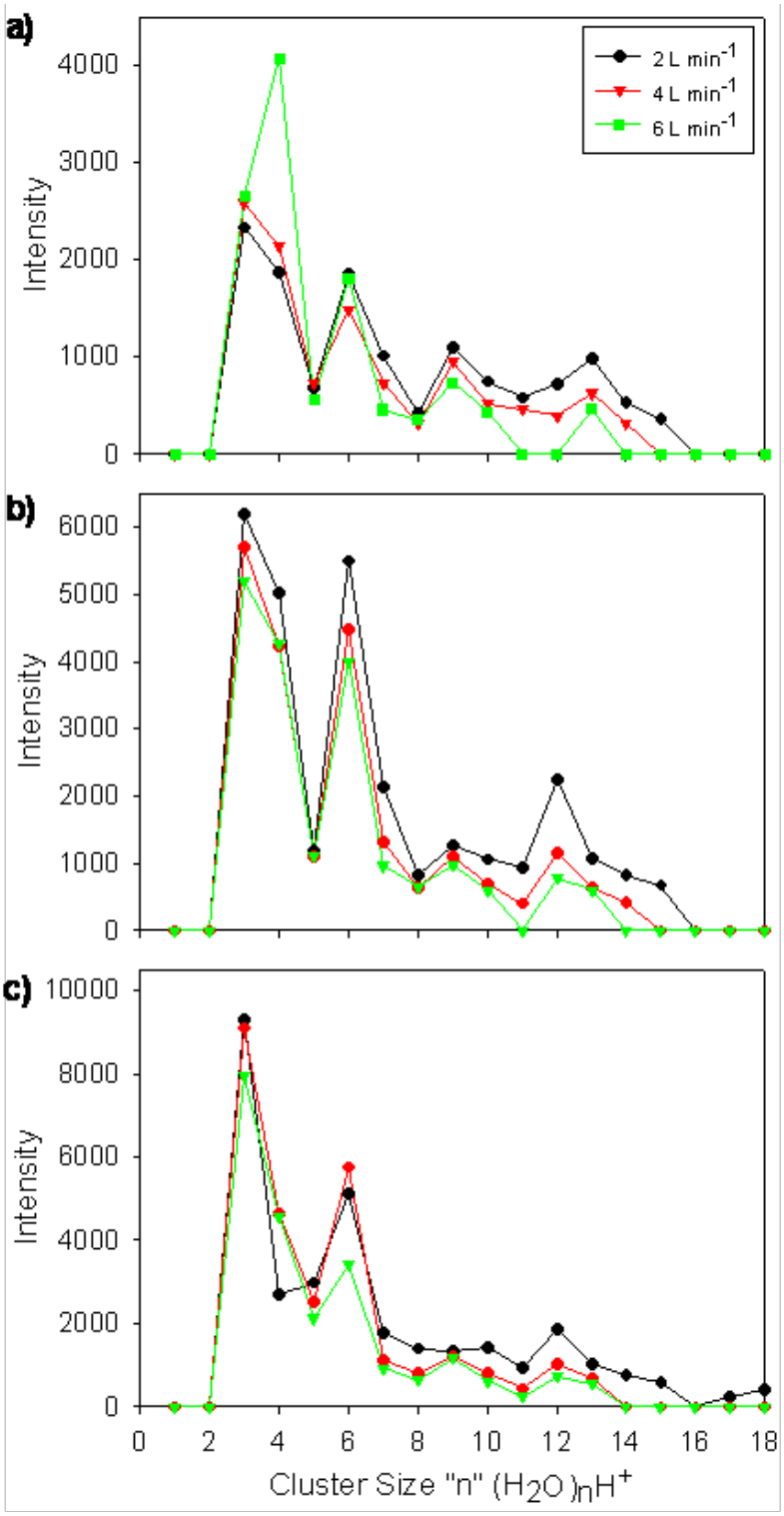

Figure 14: Observed absolute abundances of protonated water clusters with "*n*" water molecules ($(H_2O)_nH^+$) at set DART temperatures of a) 175 °C, b) 250 °C, and c) 325 °C and different glow discharge gas flow rates. The electrical current on the discharge needle monitored from the DART controller software remained constant throughout these experiments.

Increase in $<E_o>$ may also result from the excess energy released during dissociative proton transfer reactions with protonated water clusters (Scheme 1v)[66]. An increase in the intensities of protonated water cluster ions when increasing the set gas temperature was observed at all flow rates (Figure 14). At 175 °C (Figure 14a), 250 °C (Figure 14b), and 325 °C (Figure 14c), clusters with $n \leq 6$ were the most abundant. This suggests that the pathways shown in Scheme 1iii and 1v, may act concurrently. The abundance of clusters with $n \geq 8$ was observed to increase at low flow rates. This is to be expected, due to the increased hydrate thermodynamic stability at higher temperatures[67]. The trend was less clear for smaller hydrates. As a whole, however, the increase observed in protonated water cluster intensities as flow rate was decreased did not explain the changes in internal energy deposition. This suggests that additional collisional activation during transit through the ion optics or other pathways, such as that shown in Scheme 1iv, may play a significant role in further determining $<E_o>$. This alternative activation pathway involves direct Penning ionization of thermometer ions with He* producing pyridine molecular ions ($Py^{+\cdot}$). This ionization pathway is not expected to be prevalent at low exit grid voltages and high ambient humidity (45%)[64]. When DART mass spectra were examined in detail, $Py^{+\cdot}$ was detected in low abundance. As expected, protonation of the pyridine molecule was favored significantly over the formation of $Py^{+\cdot}$ at all tested flow rates and temperatures with a net increase in $Py^{+\cdot}$ abundance at higher effective temperatures. The relatively low abundance of $Py^{+\cdot}$ (0.61 % on average) suggests that under the present conditions, the pathway depicted in Scheme 1iv should not be considered a major contributor to changes in $<E_o>$.

3.2.3 Collisional Activation Effects.

In-source collision-induced dissociation (CID) is generally performed by increasing the acceleration voltages applied to orifices and skimmers in the first stage of a differentially-pumped mass spectrometric system. Higher potential differences in the first differentially pumped regions produce more energetic collisions with gaseous molecules, inducing higher fragmentation yields during ion transport towards the mass analyzer. In-source CID yields can also be influenced by the gas pressure in the spectrometer's interface[67]. As pressure (P) in this region increases, the mean free path (λ) decreases ($\lambda \alpha 1/P$) leading to a decrease in the collisional energy transfer[68]. Ultimately, this manifests into a reduction in ion fragmentation and a decrease in the E_{int} deposition[59]. To investigate the existence of this type of effect, the pressure of the first differentially-pumped region was monitored via a Pirani gauge for all DART and ESI experiments (Table 1).

Table 1: Pirani gauge pressure for first TOF differentially-pumped chamber under various experimental DART and ESI conditions.

Temperature Set Points	175 ºC	250 ºC	325 ºC
DART: 2 L min^{-1}	260 Pa	240 Pa	230 Pa
DART: 4 L min^{-1}	240 Pa	230 Pa	200 Pa
DART: 6 L min^{-1}	230 Pa	220 Pa	190 Pa
ESI: Aqueous blank	210 Pa	210 Pa	210 Pa
ESI: 50% methanol blank	210 Pa	210 Pa	210 Pa

*Pressure values listed here were constant for all experiments

A decrease in pressure was observed when both the DART ion source temperature and flow rate settings were increased. No changes were observed for ESI. It is thus highly likely that the increase in pressure in the first differentially pumped region as the DART gas flow rates were decreased is responsible for the lower E_{int} deposition observed a given set DART gas temperature.

3.2.4 Influence of Fluid Dynamics on E_{int} *Deposition.*

Previous ESI energy deposition studies have shown a correlation between the ion source design, and the mean value and width of the E_{int} distribution[55]. Using the DART ion source, design, and experimental variables such as sample positioning, gas temperature, and gas flow rates determine neutral and charged particle trajectories within the ionization region. Previous studies from our group have suggested that particle circulation may occur in some sampling geometries, decreasing experimental sensitivity[33]. In the present context, particle circulation may also lead to longer residence times in elevated temperature regions and/or cause more collisions with energetic metastables, reactive ions, and neutral molecules.

3.2.5 Metastable-stimulated Desorption Effects

Cody et al. have suggested that desorption in DART may include both thermal and non-thermal processes, such as bombardment of the sample surface by metastables or ions[32]. According to the results presented thus far, the former can be considered as being a predominant pathway for energy deposition. Example of the latter include reactive chemical sputtering[69], and metastable-stimulated desorption (MSD). In MSD metastable

rare gas atoms are directed at a surface *in-vacuo* and collide with the outermost surface of the sample, creating an electron hole via Auger de-excitation of the metastable species[70, 71]. This process can create a repulsive potential between the surface and analyte stimulating desorption. To investigate the presence of these non-thermal desorption processes, survival yield experiments were attempted using unheated helium metastables. Benzylpyridinium ions were not detected from either slurries, liquid solutions, or from completely dried salts under any of the conditions previously tested suggesting the absence of E_{int} deposition pathways involving non-thermal desorption processes.

3.3 Flow Injection Gradient Ratio Standard Addition Method for MS

3.3.1 Analysis of Artesunate-Dodecylamine Complexes by MS

Dodecylamine (DDA) was added in excess to sample solutions of artesunate prior to FI-GR-SA-MS analysis. DDA forms a proton-bound non-covalent complex with artesunate, resulting in a higher intensity ESI signal than that from a pure artesunate solution. The amine forms a complex by hydrogen bonding between the amine nitrogen and the ether like moieties in the artesunate lactone ring. The gain in ESI signal is due to the localization of the positive charge of the complex at the nitrogen atom of the dodecylamine[72]. Also, the addition of a positively charged hydrophobic ligand to the artesunate molecule enhances ion evaporation upon exiting the ESI needle. The result is a complex with higher ionization efficiency that also assists in impeding fragmentation of the artesunate molecule.

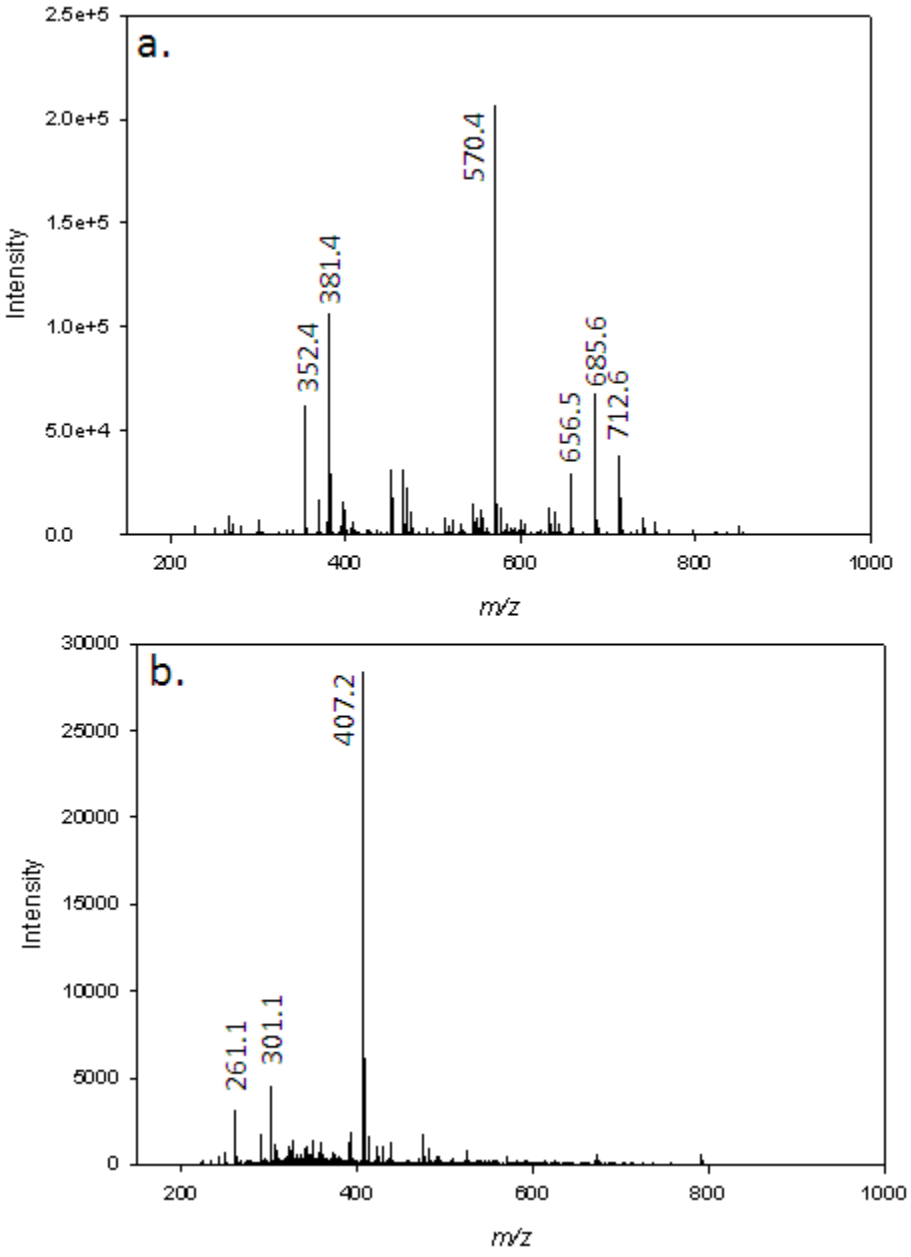

Figure 15: Representative mass spectra of artesunate with (a) and without (b) DDA added to the solution. The *m/z* of artesunate $[M+Na]^+$ is 407.2, as can be seen in panel b, while the *m/z* of the [artesunate+DDA+H]$^+$ complex is 570.4, as seen in panel a. Note the more complicated spectrum, but significantly more intense signal with the addition of DDA.

Figure 15 demonstrates the difference in signal when DDA is used as opposed to pure artesunate for FI-GR-SA-MS analysis. While the spectra with DDA appear much more complex due primarily to additional DDA species in the spectrum, the intensity of the signal for the artesunate-DDA complex is increased. In this case, distinguishing new peaks due to degradation products or contaminants in the artesunate tablet may be more difficult, especially if the degradation product or contaminant is present at very low concentration or is not preferentially ionized.

3.3.2 Matrix Effects

Although this method only requires a single point standard addition, the point by point analysis of the trailing dilution tail of the FIA peak results in a method that can still accurately account for matrix effects. Analysis of the extracted ion chronogram (EIC) traces results in multiple reproducible dilution ratios. Because any matrix that may be interacting with the analyte of interest is diluted as the peak decreases from the maximum, the effects of that matrix are also decreased as the solution is diluted. In this trailing portion of the signal, not only the matrix present is diluted, but the intensity of all ionic species of interest is decreasing as well, however, the ratio of the sample and sample plus standard traces converges to the correct apparent concentration, as demonstrated below.

3.3.3 Method Performance

The FI-GR-SA-MS method was analyzed for figures of merit that are most commonly evaluated in new analytical techniques. First, the linear range was evaluated.

This is an important parameter, as it limits the concentration interval that can be reliably investigating without incurring any bias. The corresponding results can be seen in Figure 16, below.

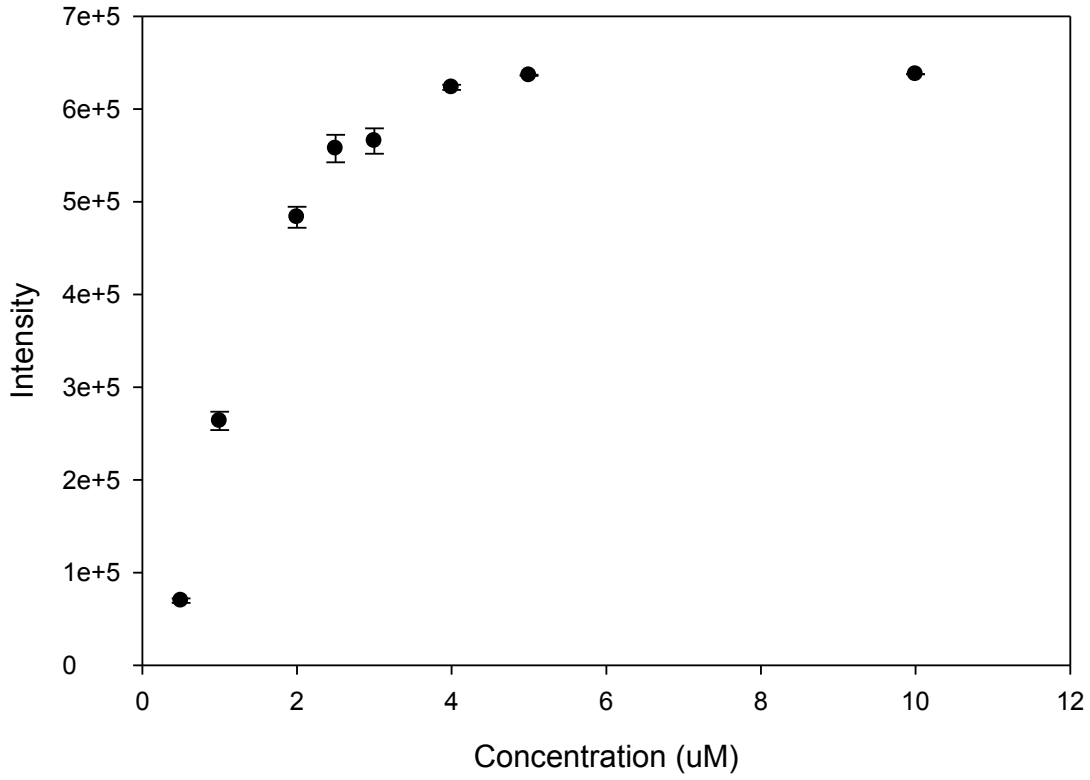

Figure 16: Electrospray response of the [artesunate+DDA+H]$^+$ complex. Experiments were run in triplicate. Error bars represent one standard deviation of the replicates collected.

The upper limit of the linear range for these experiments was approximately 2 μM, with a lower detection limit in the 30 nM range. To match the linear response range, unknown or degraded solutions were most often diluted to a theoretical concentration of 1 μM for all experiments, to ensure that the upper linear limit was not reached. This linear limit was determined using the artesunate+DDA complex. The linear limit for when the sodiated artesunate ion is used may differ significantly.

Initial investigations on the accuracy of the FI-GR-SA-MS method are shown in Figure 17. All standards prepared had a concentration below 2.5 μM to avoid exceeding the linear range. The x-axis represents the theoretical concentration of artesunate in the prepared unknown solutions, while the y-axis represents the concentration of the sample solution measured using the FI-GR-SA-MS method. If this method is accurate, the equation of the line fitting the theoretical concentration of the solutions versus the measured FIA concentrations in this plot should have a slope of one and a y-intercept of zero. The confidence intervals for the regression parameters were calculated at the 95% confidence level, showing that this technique is accurate within the experimental variance, and suggesting that it can accurately detect the concentration of artesunate in solution of varying concentration.

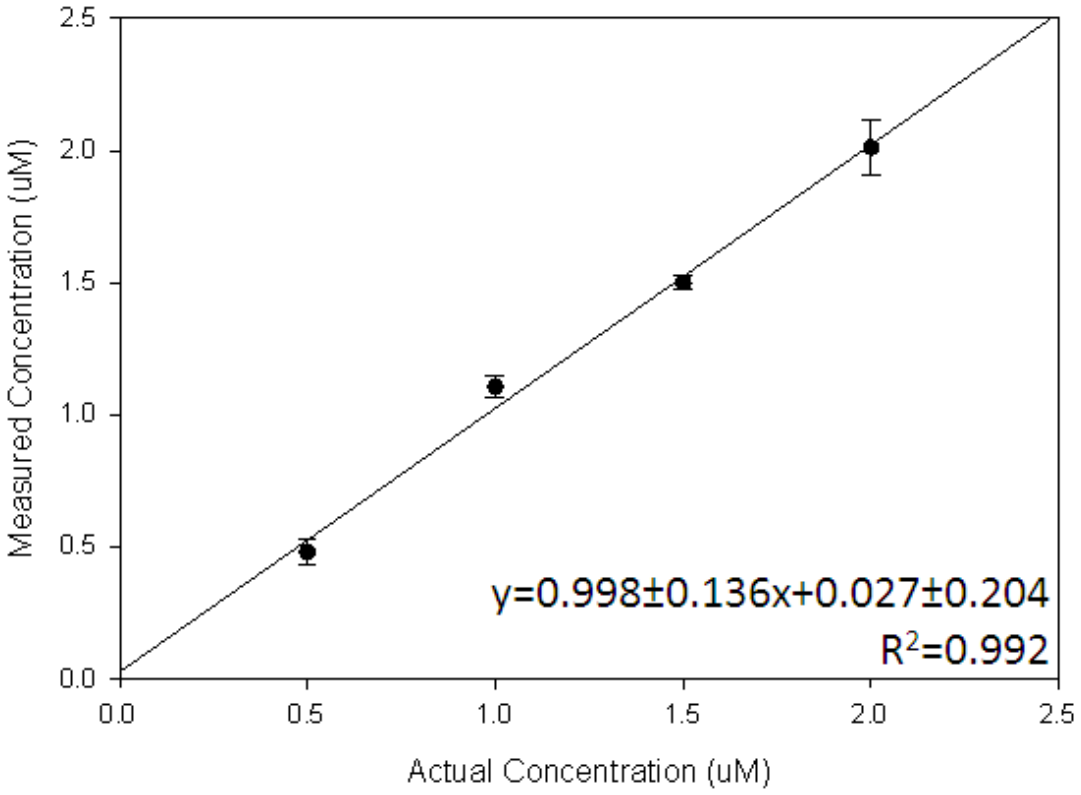

Figure 17: Accuracy of FI-GR-SA-MS analysis estimated by comparing measured concentrations to concentrations of synthetic unknown standards. Experiments were run in triplicate. Error bars represent one standard deviation of the data collected.

3.3.4 Identification of Degradation Products

Degradation products are formed in artesunate tablets as a result of exposure to high temperatures and/or high humidity conditions for extended periods of time. Because degradation products of artesunate have only been studied in suppositories[73], identification of artesunate degradation products in tablets was undertaken. A study was designed to progressively degrade artesunate tablets and investigate which products are produced using MS. First, genuine artesunate tablets were manually degraded in an oven at 100°C for different periods of time (between one and twelve hours) without any artificial atmosphere. These degraded tablets were examined by FI-GR-SA-MS for quantity of artesunate remaining in the tablet. Signals whose intensity increased in intensity with increased tablet degradation time were designated as possible artesunate degradation products. These species were then tentatively identified using accurate mass measurements. Figure 18 is the electrospray mass spectrum resulting from an artesunate tablet that has been heated in an oven for six hours. There was no DDA added to the solution in this run, to simplify the spectrum and allow for possible identification of any degradation products that may be present. As compared to Figure 15b, the most intense peaks in the mass spectrum of Figure 18 are degradation product adducts, as opposed to the previously observed base peak of undegraded artesunate ions (Figure 15b).

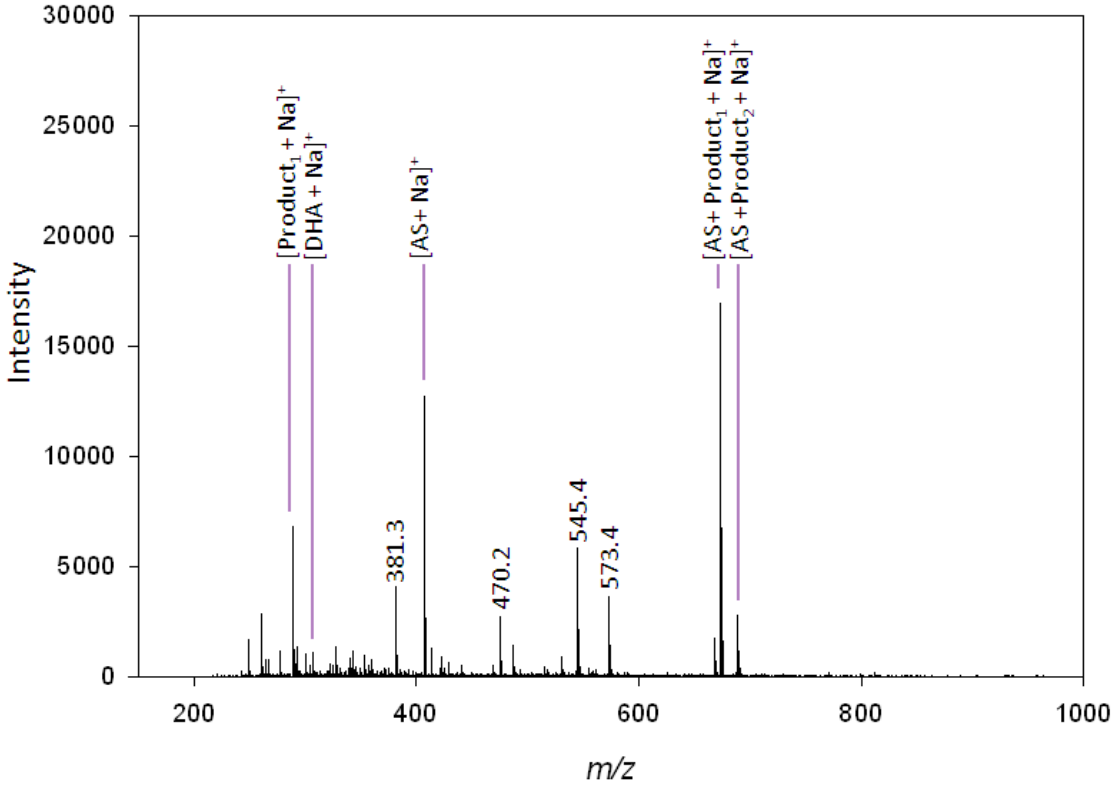

Figure 18: Mass spectrum of degraded artesunate, tablet extract without DDA addition. The tablet was artificially degraded for 6 hours.

While the intensity of some peaks changed significantly over a period of six hours of heating, the intensity of other peaks remained somewhat constant. The ion representative of dihydroartemisinin, for example, stayed relatively constant for the entire duration of the degradation experiment with only a slight increase as the artesunate was degrading more rapidly. The trace of the intensity of the ion indicative of artesunate concentration decreased significantly after approximately eight hours of heating. Dips in the artesunate trace could be indicative of tablets resulting from different blisterpacks containing different quantities of artesunate or, more likely, the dips in intensity seen at the one and four hour marks of time in the oven could be an artifact due to the changing sensitivity in the mass spectrometer over time. A trace of the intensities of three degradation products over time can be found in Figure 19, below.

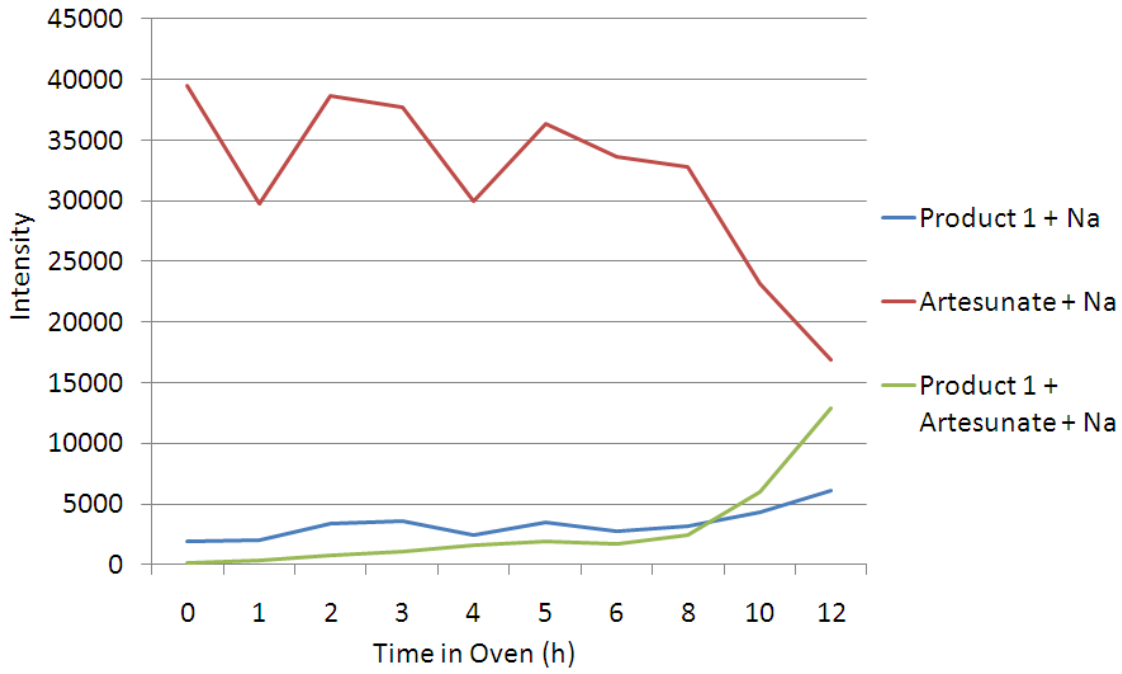

Figure 19: A trace of the intensities of three ions versus the length of time each sample was degraded in the oven. The intensities reported were an average of the intensity during the peak 30 seconds of the EIC trace for three FI-GR-SA-MS runs without the sample added to the solution.

Figure 19 suggests that many ongoing, perhaps parallel, reactions occur while the tablet is being degraded. The trace of the intensity of Product 1 appears to be somewhat stable until later stages of the degradation experiment, and it seems that the product is also able to bind to artesunate, perhaps during the electrospray process. Once the tablet has been degraded for nine hours, the formation of Product 1 seems to increase significantly. As the artesunate tablet was further degraded, a plethora of new peaks were observed in the mass spectrum. While effort was put forth to examine every peak, it was not possible to identify all species present. Because manufacturers do not fully disclose excipients used and because these excipients are most likely being degraded when exposed to high temperatures for extended periods of time, the possible structures are endless. The species that could be identified by their accurate mass measurements in the degraded artesunate mass spectrum are shown in Table 2, on the next page.

Table 2: Identified degradation products of artesunate.

Molecular Formula	Calculated Mass	Experimental Mass	Error (ppm)	Description
$C_{15}H_{22}O_4Na$	289.1416	289.1418	0.8197	$[Product\ 1+Na]^+$
$C_{15}H_{24}O_5Na$	307.1521	307.1522	0.2279	$[Dihydroartemisinin+Na]^+$
$C_{19}H_{28}O_8Na$	407.1682	407.1680	0.4593	$[Artesunate+Na]^+$
$C_{34}H_{50}O_{12}Na$	673.3200	673.3205	0.8050	$[Artesunate+Product\ 1+Na]^+$
$C_{34}H_{50}O_{13}Na$	689.3149	689.3112	5.4330	$[Artesunate+Product\ 2+Na]^+$

All accurate mass values and isotopic abundances of the proposed elemental formulas correspond very well with the theoretical values, suggesting correct identification of these compounds. The [Artesunate+ $Product_2$+ Na]$^+$ ion had a significantly higher error than the other components identified in Table 2, however, this discrepancy can be attributed to the fact that this signal is nearing the edge of the calibrated *m/z* region.

While Product 1 was identified in the mass spectrum both individually and as a complex with artesunate, Product 2 was found uncomplexed in the mass spectrum. It is possible that Product 2 did not ionize well by itself, or its affinity to artesunate was too strong. The fact that these degradation products preferentially bind to artesunate was not surprising, as artesunate is often detected as a dimer at high concentrations. For example, when artesunate tablets are analyzed by DART-MS, the artesunate ion is rarely seen intact, although the dimer is often detected. It is possible that formation of these clusters with artesunate adds stability to its structure.

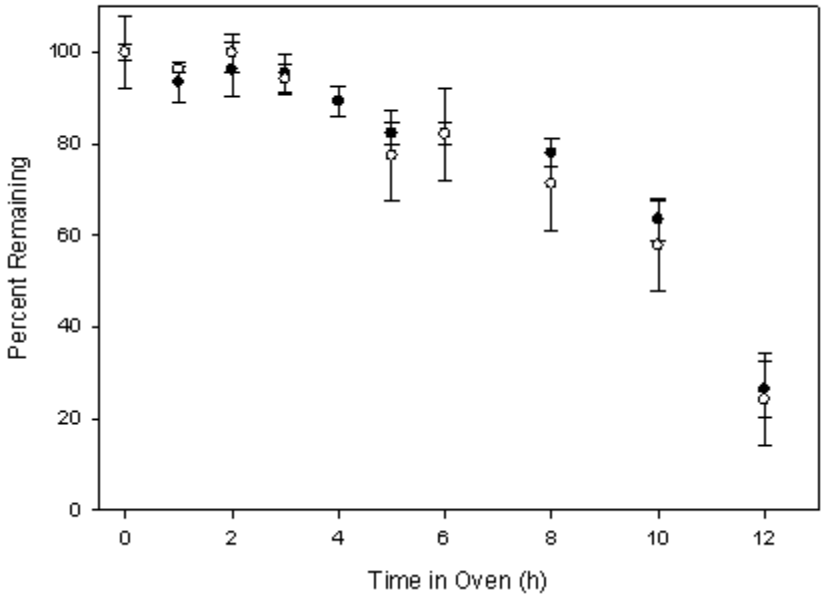

Figure 20: Percent of API remaining after artesunate tablets have been degraded in the oven at ~100ºC for 0-12 hours. Solid circles represent the values obtained using FI-GR-SA-MS analysis, while the open circles represent data obtained using HPLC. Error bars represent one standard deviation for the data set of 3 measurements.

Figure 20 displays the percent of artesunate remaining in each tablet versus the amount of time the tablet was left to degrade in the oven. FI-GR-SA-MS and HPLC were both used to analyze the artesunate content in these tablets. The solid circles represent the values obtained with FI-GR-SA-MS, while the open circles represent values obtained by using HPLC. Each sample was run in triplicate for each method and the error bars represent one standard deviation of the technical replicates. As can be seen in Figure 20, the results of these two analytical techniques overlapped in all cases, demonstrating that the comparable results can be achieved using both FI-GR-SA-MS and HPLC, a widely accepted method of quantitation. Figure 21 further compares the HPLC and FIA results. A confidence level of 95% was used in calculations of the confidence interval for the line fitted to the HPLC data versus the FI-GR-SA-MS data. Figure 21, indicates that the calculated confidence intervals encompass a slope of one and a y-intercept of zero, verifying that these data statistically overlap with one another. It should be noted that the data corresponding to the tablet degraded for eight hours was deemed a statistical outlier, and thus was removed from the data set.

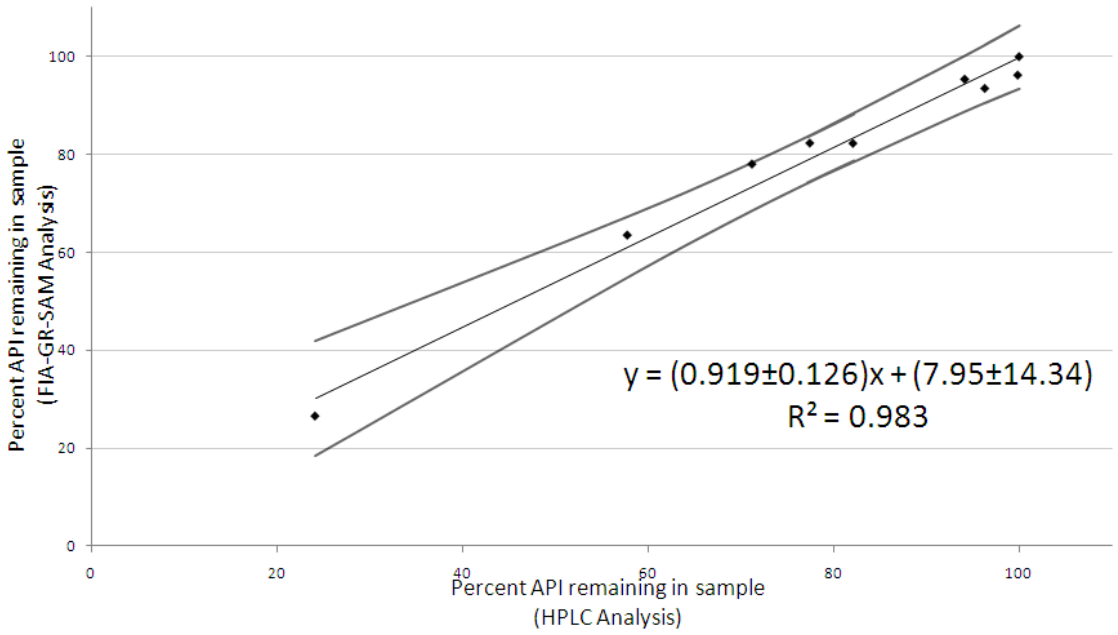

Figure 21: HPLC data versus FI-GR-SA-MS data with 95% confidence intervals added. Because the intervals include a slope of one and a y intercept of zero, the accuracy of the FI-GR-SA-MS results are verified against a standard method.

The degradation experiment was repeated using 50 mg artesunate oral tablets produced by Guilin Pharmaceuticals (see Appendix A.3), a different brand than the ones previously used (Holley-Cotec Pharmaceuticals, Figure 20). The degradation curves for these two brands of artesunate tablets were very dissimilar, with the tablets from Guilin Pharmaceuticals degrading approximately four times faster than the tablets from Holley-Cotec Pharmaceuticals. It is possible that a difference in excipients used contributed to the difference seen in the degradation curves. It is also possible that the pressure used to press the tablets differed, resulting in a harder or softer tablet, for which the rate of heat exchange would be much different.

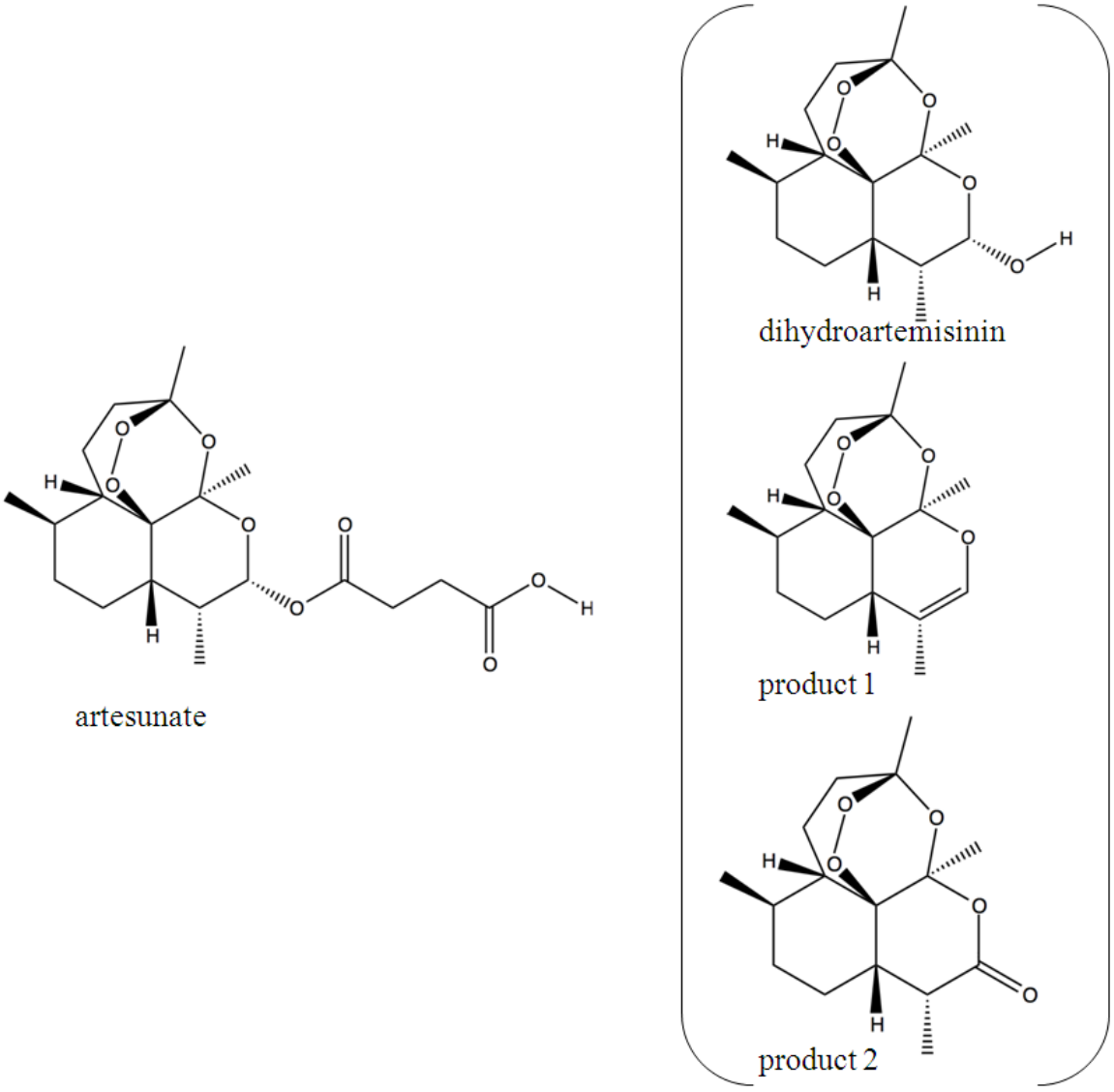

Scheme 2: Proposed structures for artesunate degradation products.

The degradation products that we propose are produced by thermal degradation, as the tablets were not exposed to sunlight, nor were they exposed to any high humidity levels besides the ambient humidity in the laboratory, approximately 9.2 grams per meter cubed. The degradation products proposed in Scheme 2, above partially match what Haynes *et al* observed in their investigation of artesunate suppositories. In Haynes's study of artesunate suppository degradation products, the most abundant degradation product was dihydroartemisinin[73]. In our experiments, dihydroartemisinin is consistently present for the entire duration of the artesunate degradation process, in a relatively consistent abundance. We have not yet performed experiments to elucidate the details of the artesunate degradation pathways in tablets, specifically whether artesunate is degraded to dihydroartemisinin and subsequently dihydroartemisinin is degraded to the products seen in Scheme 2, or if the artesunate is degrading directly into the dihydroartemisinin and the products seen simultaneously.

A very interesting experiment to pursue with artesunate antimalarial tablets would be to synthesize these tablets with different known excipients and using different pressures to press these tablets. The tablets could then be manually degraded and analyzed by the FI-GR-SA-MS method. This would allow researchers to better understand which excipients and tablet hardness cause more rapid degradation to artesunate, allowing observations to be made concerning what properties of the excipients may have accelerated or hindered degradation of the molecule.

CHAPTER 4

CONCLUSIONS

4.1 DART Screening of Poor Quality Medicines

Enormous effort is spent in determining the most efficacious antimalarials for country malaria programs, but it is essential that the quality of the drugs subsequently distributed is monitored and good quality of drug supply must be maintained. The drug screening methods presented here can be used to assure the quality of drugs, but many of these techniques are not available in the majority of the malarious world. Hence, there are few data to inform policy in situ or to rapidly intervene. Further research is needed to determine the extent of the drug quality problem, evaluations of appropriate methods for drug quality assessment, estimation of the impact of poor-quality medicines and the effectiveness of possible interventions must be evaluated.

A stronger alliance with pharmaceutical companies is a crucial step to ensure the drug quality in these less developed regions. Compliance of pharmaceutical companies with requests for genuine medicines to be analyzed by scientists would build a strong alliance. Because analysts would have a genuine for comparison, this would allow verification as to whether drugs are genuine or poor quality and which subset of poor quality drugs collected pharmaceuticals may fit into.

Enhanced regulation and quality assurance of the proliferating genuine manufacturers would help reduce the problematic presence of substandard drugs, while MRAs strengthening storage regulations would assist in decreasing the presence of degraded pharmaceuticals distributed to patients. Better collaboration between academic

research, the pharmaceutical industry, medicines regulatory authorities and the law-enforcement agencies will greatly help to ensure that the vulnerable are protected from poor-quality medicines.

4.2 Internal Energy Deposition of DART-MS

Utilizing the "survival yield" method, the E_{int} distribution of a series of p-substituted benzylpyridinium ions was compared between ESI and DART TOF MS. Although differences in some experimental settings were unavoidable to produce high quality data, ESI was the "softer" of the two ionization techniques with some overlap in energy distributions with DART. Thermal ion activation was a major contributor to E_{int} deposition in DART. Additionally, in-source CID in the first pumped region of the mass spectrometer contributed to DART E_{int} deposition as gas flow rates and set temperatures were increased. Although the work presented here improves our understanding of the fundamental desorption and ionization processes taking place when utilizing DART, more work in this area is still necessary. In particular, the effect of ambient humidity, nitrogen gas as a source of metastables, and the contributions of ambient ion transport fluid dynamics to ion activation under other configurations are likely to be worthwhile endeavors for future investigation.

4.3 Flow Injection Gradient Ratio Standard Addition Method for MS

The rapid method for quantification of active pharmaceutical ingredients presented here has the advantage of being much faster than traditional methods used for quantitative analysis of pharmaceuticals. Because an isotopically labeled standard is not

required, this method is more economical than common methods used for quantification in mass spectrometry. Additionally, this new method also allows the user to detect degradation products, enables the distinction between degraded and substandard pharmaceuticals. These types of poor quality medicines are a serious issue in developing countries, perhaps even more important than counterfeits.

APPENDIX A.1

Artesmisinin Combination Therapy Survey

Table 3: Investigation of artemisinin combination therapy quality in Africa.

Sample Code, Sample location, Formulation, Classification	**Packaging**	**Batch No Mfg. Date Exp Date (Putative Types)**	**Mass spectrometry**	**HPLC-UV mg/tablet**	**XRD/ XRF**	**Botany**
A. Counterfeit artesunate collected in Cameroon. All stated to contain 50mg artesunate/tablet						
Cameroon S5/07 12x50mg white tablets /blister with packet and leaflet. Collected July 2007 Counterfeit	'Artesunat' stated to be manufactured by 'Mekophar Chemical Pharmaceutical Joint-Stock Company' 'Neros Mekophar' hologram on packet NAFDAC 04-3397 Reg. N^{o}/N^{o} VNA-2892-99 Bar code 8934574010511 Marketed by; Neros Pharmaceuticals Ltd., Lagos Nigeria	0170805 08/2005 08/2008	chloroquine$^{\alpha\beta}$ sucrose$^{\alpha}$	56.0, 58.0 mg/tablet chloroquine	XRD–starch (C), organic compounds (C)	Fungal spores, plant cells, pollen grains of *Typha angustifolia*, charcoal, black chips
Cameroon S5 1/08 12x50mg white tablets /blister with packet and leaflet. Collected January 2008 Counterfeit	'Artesunat' stated to be manufactured by 'Mekophar Chemical Pharmaceutical Joint-Stock Company' 'Neros Mekophar' hologram on packet NAFDAC REG N^{o} : 04-3397 Reg. N^{o}/N^{o} VNA-2892-99 Bar code 8934574010511 Marketed by; Neros Pharmaceuticals Ltd., Lagos Nigeria	06027FX 07/2006 07/2009	chloroquine$^{\alpha,\beta}$ no sucrose	--------	XRD – starch (M), dextrose (A), talc (T)	Fungal spores, fern spores, *Pinus* pollen grain, traces of charcoal, black chips, cellular and amorphous organic debris

Cameroon S5 2/08 12x50mg white tablets /blister with packet and leaflet. Collected January 2008 Counterfeit	'Artesunat' stated to be manufactured by 'Mekophar Chemical Pharmaceutical Joint-Stock Company' and 'Marketed by; Neros Pharmaceuticals Ltd., Lagos Nigeria' 'Neros Mekophar' hologram on packet NAFDAC REG N^{o} : 04-3397 Reg. N^{o}/N^{o} VNA-2892-99 Bar code 8934574010511	06027FX 07/2006 07/2009	chloroquine$^{\alpha,\beta}$ no sucrose	--------	XRD - starch (M), dextrose (A), talc (T)	Fungal spores, fern spores, *Ulmus* pollen grain, cellular and amorphous debris
Cameroon S5 3/08 12x50mg white tablets /blister with packet and leaflet. Collected January 2008 Counterfeit	'Artesunat' stated to be manufactured by 'Mekophar Chemical Pharmaceutical Joint-Stock Company' and 'Marketed by; Neros Pharmaceuticals Ltd., Lagos Nigeria' 'Neros Mekophar' hologram on packet NAFDAC REG N^{o} : 04-3397 Reg. N^{o}/N^{o} VNA-2892-99 Bar code 8934574010511	06027FX 07/2006 07/2009	chloroquine$^{\alpha,\beta}$ no sucrose	--------	XRD – starch (M), dextrose (A), talc (T)	Fungal spores (~20 µm), rare Asteraceae (daisies), Chenopodiaceae and a folded tricolporate pollen grain, fungal hyphae, cellular and amorphous debris
Cameroon S5 4/08 12x50mg white tablets/blister with packet and leaflet. Collected January 2008 Counterfeit	'Artesunat' stated to be manufactured by 'Mekophar Chemical Pharmaceutical Joint-Stock Company' and 'Marketed by; Neros Pharmaceuticals Ltd., Lagos Nigeria' 'Neros Mekophar' hologram on packet NAFDAC REG N^{o} : 04-3397 Reg. N^{o}/N^{o} VNA-2892-99 Bar code 8934574010511	06027FX 07/2006 07/2009	chloroquine$^{\alpha,\beta}$ no sucrose	--------	XRD – starch (M), dextrose (A), talc (T)	Fungal spores, pollen grain?, charcoal, black chips, cellular and amorphous organic debris, plant cellular material (up to ~160 µm)
Cameroon S5 5/08 12x50mg white tablets /blister with packet and leaflet. Collected	'Artesunat' stated to be manufactured by 'Mekophar Chemical Pharmaceutical Joint-Stock Company' and 'Marketed by; Neros	06027FX 07/2006 07/2009	chloroquine$^{\alpha,\beta}$ no sucrose	--------	XRD - starch (M), dextrose (A), talc (T)	Fungal spores, charcoal, black chips, Myrtaceae and Poaceae

January 2008 Counterfeit	Pharmaceuticals Ltd., Lagos Nigeria' 'Neros Mekophar' hologram on packet NAFDAC REG N^{o} : 04-3397 Reg. N^{o}/N^{o} VNA-2892-99 Bar code 8934574010511					(grass) pollen, cellular and amorphous organic debris, plant cellular material
Lao 07/24-1, 07/24-2, 07/24-3, 07/24-4 12x50mg white tablets /blister with packet and leaflet Genuine	'Artesunat' stated to be manufactured by 'Mekophar Chemical Pharmaceutical Joint-Stock Company' No hologram SDK/Reg. No: VNB-2339-04 Bar code 8934574010245	06004FN 07/08/06 08/2009	artesunate	52.0, 51.0, 52.0, 52.0, 52.0 mg/tablet	XRD - Organic compounds (A), starch (M), talc (T)	Very rare charcoal, ?*Ulmus*, Cyatheaceae fern spores, Poaceae, Brassicaceae, Myrtaceae, Chenopodiaceae,
Lao 07/25-1, 07/25-2, 07/25-3, 07/25-4 12x50mg white tablets /blister with packet and leaflet Genuine	'Artesunate' stated to be manufactured by 'Mediplantex 358 Giai Phong Road – Hanoi- Viet Nam' No hologram Reg. No. VNA – 2820-05 Myanmar Reg. No: 0907A7304 Bar code 893504100035 Packet circular seal	061106 31/11/06 11 2009	artesunate	50.5, 52.5, 48.0 mg/tablet	XRD – Starch (A), talc (M)	Charcoal (some wood derived), Poaceae, *Pinus, Betula,* Palmae, *Trema, Alnus, Fraxinus,* Cyperaceae (sedges), Chenopodiaceae pollen, Cyatheaceae and Hymenophyllaceae fern spores
S 66 12x50mg white tablets /blister with packet and leaflet Genuine	'Artesunat' stated to be manufactured for 'AA Medical Products Ltd., by Mekophar, Vietnam' MYN Reg. No. : R0906A3639	07038FX 09/2007 09/2010	artesunate	52.5 mg/tablet	XRD - Organic compounds (A), starch (M), talc (T)	Poaceae with fungal spores inside, *Pinus, Typha*, Apiaceae (carrot family), Asteraceae, Chenopodiaceae pollen

S 67 12x50mg white tablets /blister with packet and leaflet Genuine	'Artesunate' stated to be manufactured for 'AA Medical Products Ltd., by Mekophar, Vietnam' MYN Reg. No. : 0406A3639	06038FX 09/2006 09/2009	artesunate	51.5 mg/tablet	XRD – Organic compounds (A), starch (M), talc (T)	Black chips, hyaline "cysts", Poaceae, ?Sapotaceae pollen
Mek 10/03, 10/05 Genuine, direct from manufacturer 12x50mg white tablets /blister with packet and leaflet Genuine	'Artesunat' stated to be manufactured by 'Mekophar Chemical Pharmaceutical Joint-Stock Co.' and marketed by : 'NEROS PHARMACUETICALS LTD., LAGOS, NIGERIA.' 'MKP' hologram	10005FX 25/03/10 25/03/13	artesunate	artesunate 51.0, 50.0, 49.0 and 51.0, 51.0, 52.0 mg/tablet	-------	----------
B. Counterfeit dihydroartemisinin (DHA) collected in Kenya and Nigeria. All samples stated to contain 60mg DHA. All stated to be manufactured by 'Jiaxing Nanhu Pharmaceutical Co. Ltd. Jiaxing City, under license of Beijing Holley-Cotec Pharmaceuticals (PR China)' with stated trade name 'Cotecxin'						
Kenya 07/01, Genuine 8x60mg white tablets/blister with packet and leaflet Genuine	Tablet diameter 9.22 mm & thickness=3.98 mm	MFD 10112006; EXP 11/2009; LOT 031106	dihydroartemisinin[α, β]	60.6 mg/tablet dihydroartemisinin	XRD – Organic compounds (C), lactose (M), glucose (M), starch (M)	Charcoal fragments, isolated plant cells, very rare fungal spores and hyphae, *Picea*, Malvaceae (probably *Hibiscus* spp.), Moraceae (cannabis family)
Kenya 07/02 8x60mg white tablets/blister with packet and leaflet Counterfeit	Tablet diameter= 9.14 mm & thickness=5.27 mm. Differences in color of packaging	MFD 10042006; EXP 04/2009; LOT 030406	No AI detected	No dihydroartemisinin detected	XRD - Starch (A), dolomite (M), calcite (M), quartz (M)	Abundant fine charcoal, rare fungal hyphae, occasional fungal cellular clusters and at least 4 different types of abundant, relatively large (up to 37 μm),

						mainly thick walled, brown fungal spores, totaling over 3,300 on the 22 slides (i.e. ~ 1000 grains per tablet). *Pinus*, Asteraceae, Chenopodiaceae, Fagaceae, *Quercus*?, Rubiaceae
Private hospital, Nigeria [1] 8x60mg white tablets/blister Counterfeit	-------	MFD 2003; EXP November 2005 Lot Number 02110	acetaminophen [β]	No dihydroartemisinin detected (LSHTM)	---------	---------
C. Counterfeit halofantrine collected in West Africa and China. Tablets stated to contain 250mg halofantrine						
BN 694 Genuine 6 tablets/blister Direct from manufacturer Genuine	'Halfan' stated to be manufactured by 'SmithKline Beecham Laboratoires Pharmacetiques'	694 Mfg. Apr02 Exp Apr05 (Genuine)	halofantrine[α, β]	250 mg/tablet halofantrine [γ]	XRF-multiple elements	---------- ---------- ------
2007 Sierra Leone 6 tablets/blister Counterfeit	'Halfan' stated to be manufactured by 'SmithKline Beecham Laboratoires Pharmacetiques'	550 Mfg. Jun99 Exp Jun02 (A)	artemisinin[α, β]	25.0 mg/tablet artemisinin	XRF – Titanium, Ferric	---------- ---------- ------
2008 Sierra Leone 6 tablets/blister Counterfeit	'Halfan' stated to be manufactured by 'SmithKline Beecham Laboratoires Pharmacetiques'	605 Mfg. May00 Exp May03 (A)	artemisinin[α, β]	21.0 mg/tablet artemisinin	XRF - Titanium, Ferric	---------- ---------- ------
2015 Nigeria 6 tablets/blister Counterfeit	'Halfan' stated to be manufactured by 'SmithKline Beecham Laboratoires	613 Mfg. Jan00 Exp Jan03	artemisinin[α, β]	35.0 mg/tablet artemisinin	XRF - Titanium, Ferric	---------- ---------- ------

	Pharmacetiques'	(A)				
4020 Nigeria 6 tablets/blister Counterfeit	'Halfan' stated to be manufactured by 'SmithKline Beecham Laboratoires Pharmacetiques' Same blister design (apart from use of different batch data), same rudimentary 'GSK' holographic label and same leaflet as 4023. However, blister strip is not from the same tooling as 4023.	709 Mfg. Jun02 Exp. Jun05 (D)	acetaminophen[α, β]	317 mg/tablet acetaminophen	XRF - Multiple elements	----------
4021 Nigeria 6 tablets/blister Counterfeit	'Halfan' stated to be manufactured by 'SmithKline Beecham Laboratoires Pharmacetiques' No holographic label	550 Mfg. Jun99 Exp Jun04 (A)	artemisinin[α, β]	35.0 mg/~1/2 tablet artemisinin	XRF - Titanium, Ferric	----------
4023 Nigeria 6 tablets/blister Counterfeit	'Halfan' stated to be manufactured by 'SmithKline Beecham Laboratoires Pharmacetiques'' See 4020	710 Mfg. May02 Exp May05 (D)	acetaminophen[α, β]	128 mg/~1/2 tablet acetaminophen	XRF - multiple elements	----------
4024 Nigeria 6 tablets/blister Counterfeit	'Halfan' stated to be manufactured by 'SmithKline Beecham Laboratoires Pharmacetiques' Rudimentary 'SB' holographic label (enhancement to label present on 5106)	710 Mfg Jun02 Exp Jun05 (B)	acetaminophen[β]	0.1 mg/~1/2 tablet acetaminophen	XRF – Calcium, Ferric	----------
5029 Tanzania 6 tablets/blister Counterfeit	'Halfan' stated to be manufactured by 'SmithKline Beecham Laboratoires Pharmacetiques' Genuine sample but year of Mfg. and Exp altered to extend shelf life by 2 years	666 Mfg. May03 Exp May06	halofantrine hydrochloride[ε]	250 mg/tablet halofantrine[γ]	XRD - Organic compounds (A), starch (C)	One fungal spore, rare, very small charcoal fragments, pitted plant cells, very common starch granules

5070 Nigeria 6 tablets/blister Counterfeit	'Halfan' stated to be manufactured by 'SmithKline Beecham Laboratoires Pharmacetiques'. Same blister design as 5312 with rudimentary (but more sophisticated than 4020 & 4023) 'GSK' holographic label	735 Mfg. Jan03 Exp Jan06	acetaminophen[ε, β]		XRD - Talc (A), starch (M), quartz, chlorite and organic compounds	Fungal spores and hyphae, very small charcoal fragments, *Fagopyrum*, *Pinus*, *Artemisia*, Chenopodiaceae, *Sesamum* pollen grains. No wind blown grass pollen suggests seasonally arid area
5106 Cameroon 6 tablets/blister Counterfeit	'Halfan' stated to be manufactured by 'SmithKline Beecham Laboratoires Pharmacetiques' Very rudimentary 'SB' holographic label.	690 Not listed (D)	acetaminophen[α, β]	302 mg/tablet acetaminophen	XRF - multiple elements	----------
5176 Democratic Republic of Congo 6 tablets/blister Counterfeit	'Halfan' stated to be manufactured by 'SmithKline Beecham Laboratoires Pharmacetiques' Refined version of 'GSK' holographic label with increased clarity in comparison to those on 5070 & 5312 - with finer design elements e.g. micro text (see also 6227, 7103 & 7135E).	768 Mfg. Jan04 Exp Jan07 (B)	No AI detected[α, β]	No AI detected	XRF - Calcium, Ferric	----------
5312 Liberia 6 tablets/blister Counterfeit	'Halfan' stated to be manufactured by 'SmithKline Beecham Laboratoires Pharmacetiques' Same design as 5070 with rudimentary (but more sophisticated than 4020 & 4023)' GSK' holographic	735 Mfg. Jan03 Exp Jan06 (E)	acetaminophen[α, β]	58.0 mg/tablet acetaminophen	XRF - Ferric	----------

	label					
6227 China 6 tablets/blister Counterfeit	'Halfan' stated to be manufactured by 'SmithKline Beecham Laboratoires Pharmacetiques' Similar holographic label design to 5176, 7103 & 7135E. Same blister as 7073B apart from changed Mfg. and Exp date data and different (enhanced detailed design elements on 7073B) version of 'GSK' holographic label	803 Mfg. Sep04 Exp Sep07 (C)	acetaminophen[β]	< 1mg/tablet acetaminophen	XRF - Titanium	---------- ---------- ------
7103 Nigeria 6 tablets/blister Counterfeit	'Halfan' stated to be manufactured by 'SmithKline Beecham Laboratoires Pharmacetiques' Similar holographic label design to 5176, 6227 & 7135E	781 Mfg. Jan05 Exp Jan08	dipyrone[α, β]	------	-----	---------- ---------- ------
7073b Nigeria 6 tablets/blister Counterfeit	'Halfan' stated to be manufactured by 'SmithKline Beecham Laboratoires Pharmacetiques'. Same blister design as 6227 apart from changed Mfg. and Exp date data and different (more rudimentary on 6227) version of 'GSK' holographic label	803 Mfg. Sep06 Exp Sep09	No AI detected[ε α]	-------	XRD - Calcite (A), Starch (C), Talc (M), organic compounds	*Betula* pollen grain and *Stenochlaena* fern spore, fungal spores, very small charcoal fragments, calcite slivers and starch grains, *Pinus* sacci
7135a Nigeria 6 tablets/blister Genuine	'Halfan' stated to be manufactured by 'SmithKline Beecham Laboratoires Pharmacetiques'	820 Mfg. Dec05 Exp Dec08	halofantrine hydrochloride[ε]	250 mg/tablet halofantrine hydrochloride[γ]	XRD - Organic compounds (A), starch (C)	Rare, very small charcoal fragments, pitted plant vessels. No pollen
7135e Nigeria 6 tablets/blister Counterfeit	'Halfan' stated to be manufactured by 'SmithKline Beecham Laboratoires	817 Exp Dec05 Mfg. Dec08	pyrimethamine[ε]	-------	XRD - Talc (A), Starch (M),	Pollen grains of Cyperaceae and Chenopodia

	Pharmacetiques' Similar holographic label design to 5176, 6227 & 7103				chlorite	ceae, rare fungal spores, rare, very small charcoal and plant cellular fragments
D. Counterfeit co-formulated dihydroartemisinin-piperaquine collected in China, destined for Africa. Tablets stated to contain co-formulated dihydroartemisinin-piperaquine (40mg & 320mg). All stated to be manufactured by 'Zheijiang Holley Nanhu Pharmaceutical Group Ltd Under license of HolleyPharm' with stated trade name 'Duo-Cotecxin'						
China 07/14, Genuine 8 blue tablets/blister with packet and leaflet Direct from manufacturer Genuine	'Composition per tablet' in English text on packet edge Text transverse across blisterpack Hologram	0806 0908200 6 08/2008	dihydroartemisinin[α, β], piperaquine[α]	Dihydroartemisinin 38.0, 37.8 mg/tablet, 291, 286 piperaquine mg/tablet	XRD – starch (A), quartz (T), clay minerals (T), talc (M)	Fungal spores, black chips, *Pinus*, Poaceae, Moraceae pollen grains, black synthetic thread
China 07/15 Genuine 8 blue tablets/blister with packet and leaflet Direct from manufacturer Genuine		0806 0908200 6 08/2008	dihydroartemisinin[α, β], piperaquine[α]	Dihydroartemisinin 37.0, 37.7 mg/tablet, 303, 302 piperaquine mg/tablet	XRD – starch (A), clay minerals (T), talc (M)	Rare *Cibotium* fern (Dicksoniaceae) spores, Oleaceae pollen, organic material (~160 μm), numerous black chips
China 07/16 Genuine 8 blue tablets/blister with packet and leaflet Direct from manufacturer Genuine		0806 0908200 6 08/2008	dihydroartemisinin[α, β], piperaquine[α]	Dihydroartemisinin 37.3, 37.7 mg/tablet, 292, 299 piperaquine mg/tablet	XRD – starch (A), clay minerals (T), talc (M)	Fungal spores, *Cibotium* fern (Dicksoniaceae) spores, *Pinus* pollen, organic debris, numerous black chips
China 07/17 Genuine 8 blue tablets/blister Direct from manufacturer Genuine		0806 0908200 6 08/2008	dihydroartemisinin[α, β], piperaquine[α]	Dihydroartemisinin 37.8, 37.0 mg/tablet, 295, 301 piperaquine mg/tablet	XRD – starch (A), clay minerals (T), talc (M)	Fungal spores, *Cibotium* fern (Dicksoniaceae) spores, *Pinus* pollen, organic debris,

						numerous black chips
China 07/18 8 blue tablets/blister with packet and leaflet Counterfeit	'Composition par tablet', 'Dihydroartemisinine' and Pipéraquine' in English text on packet edge (Fig 1E). Text less clearly printed and longitudinal across blisterpack Blisterpack 'Oral taken' incorrect English No hologram Packet MFD, EXP and LOT codes printed using dot matrix printer	010106 11 04 2007 04/ 2009	sildenafil[α]	18.4 mg/tablet sildenafil	XRD – starch (A), quartz (T), dolomite (M), calcite (T), talc (T)	Abundant fungal spores, rare *Cibotium* fern (Dicksoniaceae) spores, Poaceae pollen grain, organic debris, numerous black chips
China 07/19 8 blue tablets/blister with packet and leaflet Counterfeit		010106 11 04 2007 04/ 2009	sildenafil[α]	7.3 mg/tablet sildenafil	XRD – starch (C), quartz (M), dolomite (C), calcite (M), talc (M)	Abundant fungal spores, hyphae, rare *Cibotium* fern (Dicksoniaceae) spores, *Quercus* pollen grain, organic debris, charcoal, numerous black chips, fragments of an insect exoskeleton
China 07/20 8 blue tablets/blister with packet and leaflet Counterfeit		010106 11 04 2007 04/ 2009	sildenafil[α]	9.6 mg/tablet sildenafil	XRD – starch (C), quartz (M), dolomite (C), calcite (M), talc (M)	Abundant fungal spores, hyphae, *Cibotium* fern (Dicksoniaceae) spores, *Quercus* and Chenopodiaceae pollen grains, organic debris, charcoal, numerous black chips, fragments of an insect exoskeleton, mammalian hair

China 07/21 8 blue tablets/blister with packet and leaflet Counterfeit		010106 11 04 2007 04/ 2009	sildenafil[α]	6.1 mg/tablet sildenafil	XRD – starch (C), quartz (M), dolomite (C), calcite (M), talc (M)	Abundant fungal spores, hyphae, *Cibotium* fern (Dicksoniaceae) spores, *Quercus,* Chenopodiaceae, *Pinus*, Poaceae, ?*Artemisia*, ?Euphorbiaceae pollen grains, organic debris, charcoal, numerous black chips, blue and red synthetic threads
E. Counterfeit artemether-lumefantrine collected in Ghana and Cameroon. All tablets stated to contain co-formulated artemether-lumefantrine (20mg & 120mg)						
Gh 09/01 8 yellow tablets/blister with packet and leaflet Counterfeit	'Coartem' stated to be manufactured by 'Beijing Novartis Pharma Ltd, Beijing, China for Novartis Pharma AG, Basle, Switzerland, under licence from the PRC.' Packet text in English, French, German and Spanish. German spelling error 'Unter 30^{o}C lagem'. No blisterpack codes. Blisterpack corners angled	M1200 01 2009 05 2011	Pyrimethamine Yellow pigment of unknown identity	Pyrimethamine 6.2 & 7.7 mg/tablet Yellow pigment of unknown identity	XRD - starch (A)	Remained yellow during acetolysis. Rare fungal hyphae and spores, Asteraceae and Poaceae pollen, other broken unidentifiable pollen
Gh 09/02 8 yellow tablets/blister with packet and leaflet Counterfeit	'Coartem' stated to be manufactured by 'Beijing Novartis Pharma Ltd, Beijing, China for Novartis Pharma AG, Basle, Switzerland, under licence from the PRC.' Packet text in English, French, German and Spanish.	X0089 07 2008 08 2010	Pyrimethamine Yellow pigment of unknown identity	Pyrimethamine 24.0 & 25.0 mg/tablet Yellow pigment of unknown identity	XRD - talc (A), starch (M)	Remained yellow during acetolysis. Large quantity of starch grains that did not dissolve. Rare fungal remains. A

	Differences in packet size and color. Text in different font. Correct German phrase ‘‘Unter 30^{o}C lagern’. Different widths and colors of packet color tab bars, Blisterpack size different, codes smudged, foil duller and corners curved. Leaflet size different and paper color different					few *Pinus* pollen grains
CAM 10/01 Camero on, from Novarti s via INTER POL 6 yellow tablets/b lister with packet and leaflet Counter feit	‘Coartem’ stated to be manufactured by ‘Beijing Novartis Pharma Ltd, Beijing, China for Novartis Pharma AG, Basle, Switzerland, under licence from the PRC.’ Packet text in English, French, German and Spanish. NAFDAC Reg. No. 04-3275 Blisterpack corners angled	X1257 06 2008 05 2011 Indistinct printing on blister	Pyrimethamin e and sulfadiazine	No artemether or lumefantrin e Pyrimetham ine 148 & 139 mg/tab	XRD - starch (A)	A lot of very fine organic and non-organic debris. The organic debris consists of very finely disarticulate d plant material, black specks and rare fragments of charcoal. The only spores and pollen are one *Pinus* grain and two Chenopodia ceae grains (*Chenopodi um*?). Suggests an arid climate. The combination of *Pinus* plus chenopod pollen on their own is consistent with, but do not prove, a source in India. Fungal

						spores very common and varied in morphology - single celled, multicellar, clumps and variously ornamented
CAM 10/02 Camero on, from Novarti s via INTER POL 6 yellow tablets/b lister with packet and leaflet Counter feit	'Coartem' stated to be manufactured by 'Beijing Novartis Pharma Ltd, Beijing, China for Novartis Pharma AG, Basle, Switzerland, under licence from the PRC.' Packet text in English, French, German and Spanish. NAFDAC Reg. No. 04-3275 Blisterpack corners angled	X1257 06 2008 05 2011 Indistinct printing on blister	Pyrimethamin e and sulfadiazine	No artemether or lumefantrin e Pyrimetham ine 148 & 145 mg/tablet	XRD - starch (A)	Identical to CAM 10/01 except contains much less finely dispersed organic and inorganic material and no chenopod pollen. One *Pinus* grain is present. Fungal spores and hyphae rare.
Ken 06/01 From Novartis agent in Kenya 8 yellow tablets/blister with packet and leaflet Genuine	'Coartem' stated to be manufactured by 'Beijing Novartis Pharma Ltd, Beijing, China for Novartis Pharma AG, Basle, Switzerland, under licence from the PRC.' Packet text in English, French, German and Spanish	X0124 08 2005 07 2007	Artemether, lumefantrine	Artemether 35.0 & 35.0 mg/tab and lumefantrin e 314 & 317 mg/tablet	XRD - starch (C), organic compou nds (C), calcium sulphate (C), anhydrit e (M), talc (T)	Turned dark brown during acetolysis. Very little seen, apart from some fragmentary conifer pollen grains and rare fungal remains. Similar to Lao 09/06

NOV 10/43 Direct from manufacturer. 6 tablets/blister with packet and leaflet Genuine	'Riamet' stated to be manufactured by 'Beijing Novartis Pharmaceutical Ltd.'	X0095 09 2007 08 2009	Artemether, lumefantrine	Artemether 19.3, 19.5, 19.5 mg/tablet & 120, 117, 117 lumefantrine mg/tablet	------	----------
NOV 10/44. Direct from manufacturer. 6 tablets/blister with packet and leaflet Genuine	'Riamet' stated to be manufactured by 'Beijing Novartis Pharmaceutical Ltd.'	X0102 11 2008 10 2010	Artemether, lumefantrine	Artemether 19.3, 19.4, 19.3 mg/tablet & 119, 120, 120 lumefantrine mg/tablet	------	----------
NOV 10/45. Direct from manufacturer. 6 tablets/blister with packet and leaflet Genuine	'Riamet' stated to be manufactured by 'Beijing Novartis Pharmaceutical Ltd.'	X0106 11 2009 10 2011	Artemether, lumefantrine	Artemether 19.4, 19.6, 19.3 mg/tablet & 119, 120, 119 lumefantrine mg/tablet	------	----------
Lao 09/06, 09/07 & 09/09. From CMPE stock, Government of Laos sourced from Novartis 24 yellow tablets/blister Genuine	'Coartem' stated as manufactured by 'Novartis Pharmaceutical Corporation, Suffern, New York, USA for Novartis Pharma AG, Basle, Switzerland, under licence.' Text in English	F1350 02 2009 01 2011	Artemether, lumefantrine for Lao 09/09	Artemether 45.2 & 44 mg/tablet and 287 & 280 lumefantrine mg/tablet for Lao 09/09	XRD - starch (C), organic compounds (C), calcium sulphate (C), anhydrite (M), talc (T)	Lao 09/06 and Lao 09/07. Turned dark brown during acetolysis. Rare starch grains, very rare fungal hyphae. Conifer pollen, including *Pinus* and *Dacrydium pierrei*, Cyatheaceae and smooth unidentifiable monolete spores and pollen of *Betula*, *Trifolium*, *Alnus, Carpinus*, ?*Quercus*, Proteaceae,

						Rubiaceae (coffee family) and unidentifiable tricolporate grains.
F. Counterfeit co-formulated sulphamethopyrazine and pyrimethamine collected in Tanzania and Uganda. Tablets stated to contain co-formulated sulphamethopyrazine and pyrimethamine (500mg & 25mg). All stated to be manufactured by 'Pharmacia Italia S.p. A. Ascoli Piceno under authority of Pfizer INC. N/Y.' with stated trade name 'Metakelfin'						
Tan 09/01 Each packet contains 5 blisters of 6 tablets each, with leaflet Stated to contain co-formulated sulphamethopyrazine and pyrimethamine (500mg & 25mg) Counterfeit	Packet text ''malaria , use' NAFDAC NO: 04-3861. Batch No, expiry and manufacture date printed without indentation. Foil of blisterpack shiny, text very hard to read and Batch No, expiry and manufacture date embossed. Leaflet different color and dimensions with errors – 'Pyrimethamine, 25mg', '1 tabletand..', 'presdisposea', 'both,as in'	E378A 10/06 10/2010	pyrimethamine	Pyrimethamine 1.4 and 2.3 mg/tablet	XRD - gypsum (A), starch (M), anhydrite (T), calcite, cristobalite. The sulphur isotope analysis suggests gypsum of Permian age	Rare small black chips and fine organic cellular matter. Fern spores, including *Lycopodium* spp. and a Cyatheaceae. Pollen from *Pinus*, *Betula*, ?Chenopodiaceae, Chloranthaceae, Poaceae, *Potamogeton*, Ericaceae (heather family), Asteraceae, Myrtaceae. A possible *Dacrydium pierrei*.
Tan 09/02 Each packet contains 5 blisters of 6 tablets each, with leaflet Genuine	Different packet colours and dimensions and weight. Different fonts and superscript alignments. Batch No., expiry and manufacture date printed without indentation Packet text 'malaria, use'. Foil of blisterpack matt and Batch No, expiry and manufacture date printed. Leaflet paper whiter and	G 894A 01/08 01/2012	Sulphamethopyrazine, pyrimethamine	Sulphamethopyrazine 520 & 520 mg and pyrimethamine 24.9 & 25.3 mg/tablet	XRD - organic compounds (A), meta-alunogen (C), starch (M)	Very rare organic material, small black chips, short fungal hyphae, *Pinus* pollen grains, mainly pollen wings (sacci)

	dimensions different					
Ug 09/01 Each packet contains 5 blisters of 6 tablets each, with leaflet Genuine	2D barcode perforations across blister NAFDAC NO: 04-3861	G466A 10/2007 10/2011	Sulphamethopyrazine, pyrimethamine	Sulphamethopyrazine 425mg and pyrimethamine 31.3 mg/tablet	----	
Ug 09/02 Each packet contains 5 blisters of 6 tablets each, with leaflet Counterfeit	2D barcode no performations across blister NAFDAC NO: 04-3861	F824A 01/2009 01/2013	Sulphamethopyrazine, pyrimethamine	Sulphamethopyrazine 245, 265 mg and pyrimethamine 24.5, 32.0 mg/tablet	----	
Ug 09/03 Each packet contains 5 blisters of 6 tablets each, with leaflet Counterfeit	2D barcode no perforations across blister No NAFDAC No	C827A 02/2007 02/2011	Pyrimethamine, trace amounts of Sulphamethopyrazine detected	No sulphamethopyrazine and pyrimethamine 25.3, 28.0 mg/tablet	-----	
Ug 09/04 Each packet contains 5 blisters of 6 tablets each, with leaflet Counterfeit	2D barcode no perforations across blister NAFDAC NO: 04-3861 Packet text 'malaria,use'. Batch No, expiry and manufacture date printed without indentation. Foil of blisterpack shiny, text very hard to read and Batch No, expiry and manufacture date embossed. Leaflet different color and dimensions with errors – 'Pyrimethamine, 25mg', '1 tabletand..', 'presdisposea', 'both,as in'	E378A 10/2010 10/2006	Trace amounts pyramethamine detected, no Sulphamethopyrazine detected.	No sulphamethopyrazine or pyrimethamine detected	----	

G. Convenience sampling of antimalarials in the Democratic Republic of the Congo (DRC)						
DRC 08/01. Central market Kananga, Lulua Province, DRC. 6x100mg white artesunate tablets/blister with packet Substandard/degraded	'Marinate' No manufacturers details on the packet or blister. Only GUJ/DRUGS/1407 *	RET. 008 JAN.2006 DEC.2008	artesunate	artesunate 79.0, 88.0 mg/tablet	----	----
DRC 08/02. Central market Kananga, Lulua Province, DRC. 12x50mg white artesunate tablets/blister with packet Genuine	'Artesunate' Stated to be manufactured by 'Mekophar Chemical Pharmaceutical Joint-Stock Company, HCMC Vietnam.' 'Fabrique pour "AMT Inc. USA" Text on packet in English, Spanish and French	07011FX 03/2007 03/2010	artesunate	artesunate 45.0, 52.5, 53.5, 52.5 mg/tablet	-----	-----
DRC 08/03. Central market Kananga, Lulua Province, DRC. 12x50mg white artesunate tablets/blister with packet Genuine	'Artesunat' Stated to be manufactured by 'Mekophar Chemical Pharmaceutical Joint-Stock Company, HCMC Vietnam.' 'Fabrique pour "AMT Inc. USA" Text on packet in English, Spanish and French	07013FX 03/2007 03/2010	artesunate	artesunate 49.0, 49.0, 55.0, 53.0 mg/tablet	-----	-----
DRC 08/04. Central market Kananga, Lulua Province, DRC. 6x100mg white artesunate tablet/blister with packet Genuine	'ARTSUN-100' Stated to be 'Made for euromedi Pharma 99, Carmelite Road, Middlesex, London' Text in English and French Code No. MP/DRUGS/25/23/2001 *	AK-02 FEB-07 JAN-10	artesunate	artesunate 80.0, 90mg/tablet	-----	-----
DRC 08/05. Central market Kananga, Lulua Province, DRC. 12x50mg white artesunate	'Sunat' Stated to be manufactured by 'SHALINA LABORATORIES PVT. LTD. 96,	006 NOV.06 SEP.09	artesunate	artesunate 45.0, 50.0, 54.0, 52.0	-----	-----

tablet/blister with packet Genuine	Maker Chamber VI, Nariman Point, Mumbai-Inde' Code No. MH/DRUGS/KD-1392A *			mg/tablet		
DRC 08/06. Central market Kananga, Lulua Province, DRC. 3x306.2mg amodiaquine tablets and 3x100mg white artesunate tablets/blister with packet Genuine	'Sunat-A' Stated to be manufactured by 'SHALINA LABORATORIES PVT. LTD. 96, Maker Chamber VI, Nariman Point, Mumbai-Inde' Code No. MH/DRUGS/KD-1392A *	002 OCT.07 SEP.10	1. amodiaquine $^{\alpha}$ 2. artesunate, disaccharide$^{\alpha, \beta}$	1. Amodiaquine 242, 288 mg/tablet 2. Artesunate 87.0, 101 mg/tablet	-----	-----
DRC 08/07. Central market Kananga, Lulua Province, DRC. 12x50mg white artesunate tablets/blister with packet Genuine	'Artesunat' Stated to be manufactured by 'Mekophar Chemical Pharmaceutical Joint-Stock Company, HCMC Vietnam.' 'Fabrique pour "AMT Inc. USA" Text on packet in English, Spanish and French	07014FX 03/2007 03/2010	artesunate acid$^{\beta}$	artesunate 45.0, 54.0, 54.0, 52.0 mg/tablet	-----	-----
DRC 06/01, Kivu, DRC. 1 30ml bottle of suspension with spoon, packet and leaflet Counterfeit	'HALFAN' Suspension Stated to be manufactured by 'SmithKline Beecham Laboratoire Pharmaceutiques Esplanade Charles de Gaulle 92731 NANTERRE Cedex,' NAFDAC REG NO. 04-2181 *	BN 3006 Mfg. 07/2003 Exp 07/2006	No active ingredients	---------	--------	Abundant extremely fine black material, less than 0.25µm in diameter. Rare fungal remains, all of the same type, and 8 pollen grains including 5 small *Pinus* grains, and one Poaceae
DRC 07/01, Kinshasa, DRC. 6 x100mg artesunate tablets/blister Counterfeit	Astrinate on one face of leaflet and Arinate on reverse Stated to be 'Manufactured for AT17 RUE POISSONNIERS	Lot: 110705 Exp: 06/08 Mfg.: 07/05	artesunate	88.5, 70.9 mg artesunate/tablet	----	-----

	75018 PARIS' *					
H. Convenience sampling of antimalarials in West Africa						
BF 08/01 8 x coformulated dihydroartemisinin-piperaquine (40mg & 320mg) tablets/blister with packet Pharmacy, Ouagadougou, Burkina Faso Genuine	'DUO-COTECXIN' Stated to be manufactured by 'Zheijiang Holley Nanhu Pharmaceutical Group Co. Ltd. Under license of HolleyPharm'	020207 2700220 07 02/2009	dihydroartemisinin[β], piperaquine[β]	Dihydroartemisinin 53.0, 32.0 mg/tablet, piperaquine 240 mg/tablet	-----	-----
BF 08/02 6 x 100mg artesunate tablet/blister with packet Pharmacy, Ouagadougou, Burkina Faso Genuine	'Arinate' Stated to be manufactured by 'Dafra Pharma nv / sa Turnhout (Belgium)' *	07C261 26 Mar 2007 03 2010	artesunate[β]	artesunate 98.0, 106 mg/tablet	-----	-----
BF 08/03 6x50mg artesunate tablets/blister Pharmacy, Ouagadougou, Burkina Faso Genuine	'Artesunate' Stated to be manufactured by 'Ubithera, Adam Pharm Comp Ltd, Anhui, China' *	B. N.: 030906 MFG: 09/06 EXP: 08/09	artesunate[β]	artesunate 44.0, 50.0 mg/tablet	-----	-----
TOG 08/01 12x50mg artesunate tablets/blister with packet Pharmacy, Lome, Togo Genuine	'Artesunate' Stated to be manufactured by 'TONGMEI LABORATOIRE, Lomé-TOGO' *	010307 03 2007 03 2010	artesunate[β]	artesunate 44.0, 51.0, 50.0, 48.0 mg/tablet	-----	-----
TOG 08/02 12x50mg artesunate tablets/blister with packet Pharmacy, Lome, Togo	ARTESUNATE' Stated to be from 'Arthésis Nyd Pharma, Genéve-Suisee. Manufactured by Laboratoires Cipla	K60703 07/2008	artesunate[β]	artesunate 50.0, 53.0, 55.0, 50.0 mg/tablet	-----	-----

Genuine	Ltd MH/DRUGS/845' *					
BEN 08/01 12x50mg artesunate tablets/blister with packet Market, Cotonou, Benin Genuine	'ARTESUNATE' Stated to be manufactured by 'NSW Pharmaceutical Co. Ltd. Under the License of Imperial Botanical CJS INT'L.' Company logo on packet similar design to Guilin Pharmaceutical Co. Ltd hologram but with 'IMPERIAL BOTANICAL' across the mountains *	070522 05 / 2007 04 / 2010	artesunate[β]	artesunate 43.0, 47.0, 46.0, 46.0 mg/tablet	-----	-----
BEN 08/02 3x200mg white artesunate tablets and 3x pink tablets of 500mg sulfamethoxypyrazine and 25mg pyrimethamine/ blister with packet Pharmacy, Cotonou, Benin Genuine	'AsunateDenk 200 Plus' Stated to be manufactured by 'Artesan Pharma GmbH & Co. KG, Lüchow, Germany for DENK PHARMA GmbH & Co. KG, Muenchen, Germany' 'Reg. No. NAFDAC…,ZAM 130/032-POM'	14861 08 / 2006 08 / 2009	1. artesunate[α, β] 2. sulfamethoxypyrazine[α], pyrimethamine[α, β]	1. Artesunate 182, 230 mg/tablet 2. sulfamethoxypyrazine 495, 501, 718 mg/tablet, pyrimethamine 9.3, 30.0, 36.0 mg/tablet	-----	-----
BEN 08/03 6 coformulated tablets of 100mg artesunate and amodiaquine 270mg (base)/blister with packet Pharmacy, Cotonou, Benin	'Coarsucam' Stated to be manufactured for 'sanofi Aventis, Casablanca, Morocco, manufactured by Maphar Casablanca, Morocco'	5010 06 / 2007 06 / 2009	artesunate[α, β], amodiaquine[α]	artesunate 105, 99.0 and amodiaquine 227, 265 mg/tablet	-----	-----

Genuine						
BEN 08/04 8x 60mg dihydroartemisinin in tablets/blister with packet Pharmacy, Cotonou, Benin Genuine	'ARTEMAX' Stated to be manufactured by 'G.A. Pharmaceuticals S.A. Athens, Greece' *	6060 1 2008 1 2010	dihydroartemisinin[β]	dihydroartemisinin 65.0, 28.0 mg/tablet	-----	-----
BEN 08/05 3x4 x 50mg artesunate tablets, 4 tablets/ blister, three blisters with packet Pharmacy, Cotonou, Benin Genuine	'Artemal-S' Stated to be manufactured by 'Plethico Pharmaceuticals Limited Indore (MP), India ML. 25/39/85' *	7450 06/2007 05/2010	artesunate[β]	artesunate 46.8mg/ tablet	-----	-----
GH 08/01 12x 50mg artesunate tablets/blister with packet Pharmacy, Tamale, Ghana Genuine	MALASATE 50'' Stated to be manufactured by 'ERNEST CHEMISTS LIMITED, Accra, Ghana' *	0810G 10-07 10-10	artesunate[β]	artesunate 50.0, 47.0, 50.0, 47.0 mg/tablet	-----	-----
GH 08/02 3x4 x 50mg artesunate tablets, 4 tablets/blister, three blisterpacks with packet Pharmacy, Tamale, Ghana Genuine	'ARTESUNATE XL' Stated to be manufactured by 'XL LABORATORIES PVT. LTD, Bhiwadi, Rajasthan, India for KAMA INDUSTRIES LTD. ACCRA-NORTH, GHANA' Mfg. Lic. No. : Raj. 2059 *	7002 05/2007 05/2010	artesunate[β]	artesunate 45.0, 48.5, 52.5, 50.0 mg/tablet	-----	-----
GH 08/03 12x50mg artesunate and 12x 150mg amodiaquine (base) tablets/blister Pharmacy, Navrongo, Ghana	'MALATEX' Stated to be manufactured by 'KINAPHARMA LIMITED Accra, Ghana' *	B • N001 02/11	1. artesunate[α, β] 2. amodiaquine[α]	1. artesunate 47.0, 53.0, 53.0, 54.0 mg/tablet 2. amodia	-----	-----

Genuine				quine 151, 140, 144, 152 mg/tablet		
GH 08/04 6x100mg artesunate and 6x 300mg amodiaquine (base) tablets/blister with packet Pharmacy, Bolgatanga, Ghana Genuine	'GSUANTE 100 KIT' Stated to be manufactured by 'GVS LABS Dombivili, India' Mfg. Lic. No.: KD-1562 A	G0-01 16/01/2006 15/01/2009	1. artesunate[α, β] 2. amodiaquine[α]	1. artesunate 81.0, 90.0 mg/tablet 2. amodiaquine 260, 246 mg/tablet	-----	-----
GH 08/05 3x50mg artesunate powder sachets and 3x150mg amodiaquine powder sachets in packet Pharmacy, Bolgatanga, Ghana Genuine	'CAMOSUNATE PED' Stated to be manufactured by 'DANPONG-ADAMS PHARMACEUTICAL INDUSTRY (GHANA) LIMITED ACCRA, GHANA' *	0702006 02/07 02/10	1. artesunate[β] 2. amodiaquine[β]	1. artesunate 52.0 mg/tablet 2. amodiaquine 131 mg/tablet	-----	-----
GH 08/06 6x200mg artesunate tablets/blister with packet Pharmacy, Kumasi, Ghana Genuine	'ARTENEX 200' Stated to be manufactured by 'KINAPHARMA LIMITED, Accra, Ghana' *	007 SEP 05 SEP 09	artesunate[β]	artesunate 173, 212 mg/tablet	-----	-----
GH 08/07 8x60mg dihydroartemisinin tablets/blister with packet Pharmacy, Kumasi, Ghana	'COTECXIN'. Stated to be manufactured by 'Jiaxing Nanhu Pharmaceutical Co. Ltd. Jiaxing City, under license of Beijing Holley-Cotec Pharmaceuticals'	010106 19012006 01/2009	dihydroartemisinin[β]	dihydroartemisinin 58.0, 13.0 mg/tablet	-----	-----

Genuine						
GH 08/08 12x50mg artesunate tablets/blister with packet Pharmacy, Kumasi, Ghana Genuine	'ACUMAL' Stated to be manufactured by 'JCPL Pharma Pvt. Ltd, Jalgaon for KOJACH LIMITED KUMASI-GHANA' Mfg. Lic. No. 514 For Batch No, Mfd and exp. Date packet states 'See on Strip' *	B/No.ET 504 DEC.2005 NOV.2009	artesunate[β]	artesunate 44.0, 45.0, 45.0, 46.0 mg/tablet	-----	-----
GH 08/09 8x60mg dihydroartemisinin tablets/blister with packet Pharmacy, Akisombo, Ghana Genuine	'ALAXIN' Stated to be manufactured by 'GVS LABS, Dombivili, INDIA' Mgf. Lic. : KD 1562 A	GO – 26 02/01/2007 01/01/2010	dihydroartemisinin[β]	dihydroartemisinin 63.0, 37.0 mg/tablet	-----	-----
GH 08/10 12x50mg artesunate tablets/blister with packet Pharmacy, Akisombo, Ghana Genuine	'ARTESUNATE' Stated to be manufactured by 'Guilin Pharmaceutical Co. Ltd., Guilin, Guangxi, China'	070506 05/2007 05/2010	artesunate[β]	artesunate 49.0, 50.0, 52.0, 53.0 mg/tablet	-----	-----
GH 08/11 6x100mg artesunate tablets/blister with packet Pharmacy, Hohoe, Ghana Genuine	'GSUNATE FORTE' Stated to be manufactured by 'BLISS GVS PHARMA LTD. Palghar, Maharasthra, INDIA' Marketed by: 'TOBINCO PHARMACEUTICAS LTD. Accra, Ghana' Mfg. Lic. No. : 1040	GE – 08 08 / 2007 07 / 2010	artesunate[β]	artesunate 88.0, 100 mg/tablet	-----	-----
GH 08/12 12x50mg white artesunate tablets and 12x153.1mg	'GSUNATE 24 KIT' Stated to be manufactured by 'BLISS GVS	KF – 05 12 / 2007 11 / 2010	1. artesunate[β] 2. amodiaquine[β]	1. artesunate 42.0, 48.0,	-----	-----

amodiaquine (base) yellow tablets/blister with packet Pharmacy, Hohoe, Ghana Genuine	PHARMA LTD. Palghar, Maharasthra, INDIA' Mfg. Lic. No. : 1040			51.0, 52.0 mg/tablet 2. amodiaquine 137, 156, 162, 156 mg/tablet		
GH 08/13 6 Artesunate100mg tablets and 6 amodiaquine 300mg tablets/blister with packet Pharmacy, Ho, Ghana Substandard/degraded	'AMONATE-400' Stated to be manufactured for 'Pharmanova Limited, Accra, Ghana. Manufactured by: Atlantci Pharmaeucticals Limited Accra, Ghana' *	7004 10-07 10-10	1. artesunate[α, β] 2. amodiaquine[α]	1. artesunate 92.0, 103 mg/tablet 2. amodiaquine 237, 240 mg/tablet	-----	-----
GH 08/14 coformulated 8 tablets of dihydroartemisinin 40mg and piperaquine 320mg/ blister with packet Pharmacy, Aflao, Ghana Genuine	'P-ALAXIN' Stated to be manufactured by 'GVC LABS, Dombivili, INDIA' Mfg. Lic.: KD-1485A Blisterpack M•I•KD•1485A	Packet Batch No.: GB-01 Mfg.Date : 08/ 2005 Exp. Date : 07/ 2008 Blister GB•01.08/05.07/08	dihydroartemisinin, piperaquine, disaccharide	dihydroartemisinin 49.0, 21.0 mg/tablet, piperaquine 243 mg/tablet	-----	-----
GH 08/15 12x50mg artesunate tablets/blister with packet Pharmacy, Bremen-Asikuma, Ghana Substandard/degraded	'LEVER Artesunate' Stated to be manufactured by 'ADAMS PHARAMCEUTICAL (ANHUI) CO., LTD. ANHUI, CHINA Division of Sunflower Int'l Group' NAFDAC REG. NO.: 04-5865	040207 02/07 01/10	artesunate[β]	artesunate 39.0, 43.0, 47.0, 47.0 mg/tablet	-----	-----

	Marketed by GENEITH GLOBAL LIMITED *					
GH 08/16 3x50mg artesunate and 3x153mg amodiaquine (base) tablets /blister with packet Pharmacy, Accra, Ghana Genuine	'ARSUCAM' Stated to be manufactured by 'Sanofi~synathelabo Manufacturer MAPHAR – Casablanca – Morocco'	0244 02/06 02/08	1. artesunate$^{\beta}$ 2. amodiaquine$^{\beta}$	1. artesunate 47.0, 55.0 mg/ tablet 2. amodiaquine 134, 144 mg/ tablet	-----	-----

* Genuine sample from manufacturer not available for comparison $^{\alpha}$Active Pharmaceutical Ingredient (API) detected by DESI-MS, $^{\beta}$API verified by DART-MS, $^{\gamma}$API detected by FTIR and verified when necessary by HPLC-ESI-MS. A (abundant, > 60%), C (common, 20-60%), M (minor, 5-20%), T (trace < 5%). Clay minerals are probably smectite and chlorite. HPLC-UV = high performance liquid chromatography with ultraviolet detection, FI-ESI-MS = flow injection electrospray ionization mass spectrometry, XRD = X-ray diffraction, XRF= X-ray fluorescence, FTIR = Fourier Transform Infra Red spectroscopy, HPLC-ESI-Ms = high performance liquid chromatography with electrospray ionisation and mass spectrometry detection, ACT = artemisinin-based combination therapy, GSK = GlaxoSmithKline, SB = SmithKline Beecham, LSHTM – HPLC analysis performed ny HK at London School of Hygiene and Tropical Medicine – see Ioset & Kaur (2009).

[1] Reported in Ioset & Kaur (2009) Meta-alunogen is aluminium sulphate hydrate

Acetaminophen is paracetamol

APPENDIX A.2

CODFIN Database

Below is a sample screenshot of the CODFIN database. This database contains information about each investigated sample, identified by a unique sample code. In the entry for each sample are links to documents containing a barcode, photos of the sample, and ASCII data, which may be used to plot spectral information (MS, Raman, NIR).

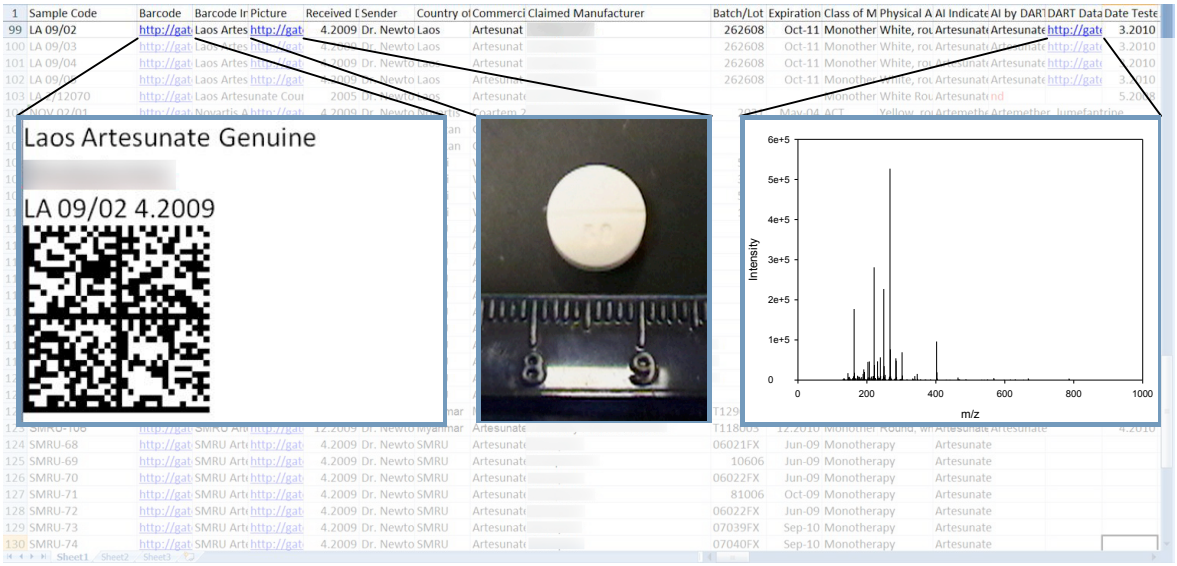

Figure 22: A snapshot of the CODFIN database with inlays of the barcode, picture, and MS data that is linked to the database.

Microsoft SharePoint Server is the program used to host the database. A quad-core computer was purchased and is maintained solely for the use of the database information. This server allows for anyone to access the database, provided they have a valid username and password, from all over the world. Users have the ability to update the database or upload new data. All database information is kept in the documents portion of the SharePoint Server website and organized either by country where the

medicines were collected or a particular study name, if the location of medicine collection is no known. Barcodes are generated based on the code name of each sample. The barcode also includes stated manufacturer, claimed active ingredients, and whether the medicine contains that claimed active ingredient based on MS screening of that medicine. Barcodes are created using TBarcode, a software purchased for this particular task. DataMatrix barcodes was the type of barcode used, as this type holds the most information. If a user is unsure what medicine they are examining, in the open database excel sheet, a find function can be opened, then the barcode scanned with a 2D barcode scanner. This allows the computer to immediately find all the gathered data on that particular medicine, assisting the user in identification of a barcoded medicine.

APPENDIX A.3

Degradation Curve for Guilin Pharmaceuticals Artesunate Tablet

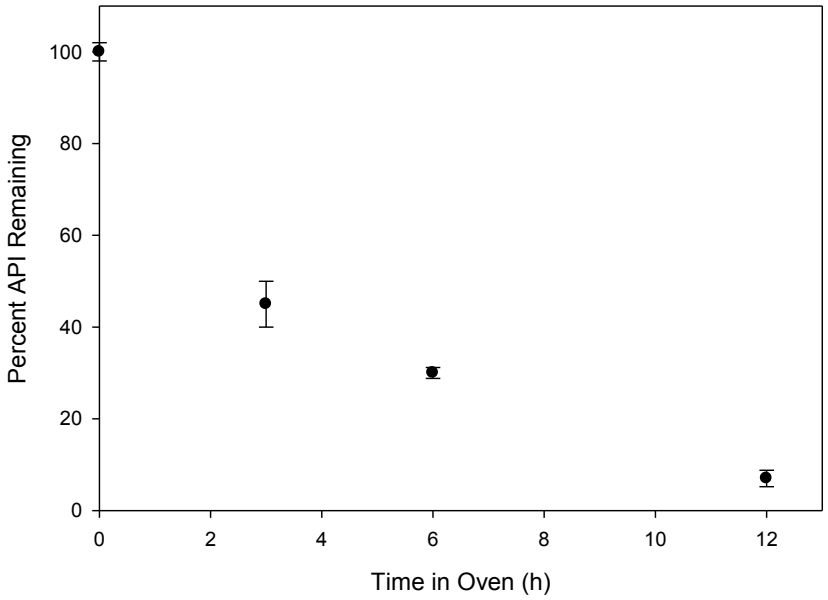

Figure 23: Percent of API remaining after artesunate tablets have been degraded in the oven at ~100ºC for 0-12 hours. Analysis was performed using the FI-GR-SA-MS method. Error bars represent one standard deviation for the data set of three measurements selected as the best out of seven runs.

APPENDIX A.4

Mass Spectrometer Settings for DART Screening of Poor Quality Drugs

Jeol AccuTOF:

Ring Lens: 5 V

Orifice 1: 20 V

Orifice 2: 25 V

Peaks Voltage: 300 V

Bias Voltage: 27 V

Pusher Bias Voltage: -0.27 V

Focus Voltage: -135 V

Focus Lens Voltage: 1.0 V

Quadrupole Lens Voltage: -5.0 V

Right/Left Voltage: 13.7 V

Top/Bottom Voltage: 3.7 V

Reflectron: 917.7 V

Detector Voltage: 2750 V

DART Conditions:

Temperature: 200°C

Discharge gas and flow rate: Helium at 4 L/min

Needle Voltage: 3600 V

Discharge Electrode: 200 V

Grid Electrode: 100 V

Bruker MicroTOF Q:

Scan Begin: 22 *m/z*

Scan End: 1000 *m/z*

Ion Polarity: Positive

Set Nebulizer Gas: 0.0 Bar

Set Dry Heater: 150°C

Set Dry Gas: 2.0 L/min

Set Capillary: 1500 V

Set End Plate Offset: -500V

Set Hexapole Storage: 41.0 V

Set Hexapole Extraction: 32.0 V

Set Lens 2: -4.0 V

Set Lens 3: 35.0 V

Set Lens 4: 28.0 V

Set Lens 5: -27.0 V

Set Lens 6: 23.0 V

Set Collision Storage: 35.0 V

Set Collision Extraction: 19.6 V

Set Lens 7: 7.0 V

Set Lens 8: -18.0 V

Set Lens 9: 0.0 V

Set Lens 10: -10.0 V

Set Funnel 1 RF: 250.0 Vpp

Set Funnel 2 RF: 300.0 Vpp

Set Hexapole RF: 300.00 Vpp

Set Collision Cell RF: 250.0 Vpp

Set Transfer Time: 77.0 µs

Set Pre Pulse Storage Time: 1.0 µs

Set Corrector Fill: 55.0 V

Set Pulser Pull: 0.1 V

Set Pulser Push: 804.0 V

Set Reflector: 1800.0 V

Set Flight Tube: 8600.0 V

Set Corrector Extract: 683.0 V

Set Detector TOF: 2007.2 V

DART Conditions:

Temperature: 200°C

Discharge gas and flow rate: Helium at 1 L/min

Needle Voltage: 3600 V

Discharge Electrode: 150 V

Grid Electrode: 50 V

APPENDIX A.5

Mass Spectrometer Settings for IE Deposition of DART

Ring Lens: 5 V

Orifice 1: 20 V

Orifice 2: 5 V

Peaks Voltage: 300 V

Bias Voltage: 27 V

Pusher Bias Voltage: -0.27 V

Focus Voltage: -135 V

Focus Lens Voltage: 1.0 V

Quadrupole Lens Voltage: -5.0 V

Right/Left Voltage: 13.7 V

Top/Bottom Voltage: 3.7 V

Reflectron: 917.7 V

Detector Voltage: 2750 V

APPENDIX A.6

Mass Spectrometer Settings for Flow Injection Gradient Ratio Standard Addition Method

Source Type: ESI

Focus: Not active

Scan Begin: 150 *m/z*

Scan End: 1000 *m/z*

Ion Polarity: Positive

Set Capillary: 4500 V

Set End Plate Offset: -500 V

Set Nebulizer: 1.0 Bar

Set Dry Heater: 200°C

Set Dry Gas: 5.0 L/min

Set Hexapole Storage: 42.5

Set Hexapole Extraction: 33.5 V

Set Lens 2: -2.5 V

Set Lens 3: 36.5 V

Set Lens 4: 23.5 V

Set Lens 5: -31.5 V

Set Lens 6: 18.5 V

Set Collision Storage: 35.0 V

Set Collision Extraction: 19.6 V

Set Lens 7: 7.0 V

Set Lens 8: -18.0 V

Set Lens 9: 0.0 V

Set Lens 10: -30.0 V

Set Funnel 1 RF: 400.0 Vpp

Set Funnel 2 RF: 400.0 Vpp

Set Funnel 3 RF: 460.0 Vpp

ISCID Energy: 0.0 V

Set Collision Cell RF: 450.0 Vpp

Set Transfer Time: 90.0 µs

Set Pre Pulse Storage Time: 10.0 µs

Set Corrector Fill: 55.0 V

Set Pulser Pull: 0.1 V

Set Pulser Push: 804.0 V

Set Reflector: 1800.0 V

Set Flight Tube: 8600.0 V

Set Corrector Extract: 683.0 V

Set Detector TOF: 1950.0 V

REFERENCES

1. K. A. Hall, P. N. Newton, M. D. Green and e. al, *Am. J. Trop. Med. Hyg.*, 2006, **75**.
2. *WHO, Geneva, Switzerland*, 2006.
3. P. N. Newton, M. D. Green, F. M. Fernandez, N. J. P. Day and N. J. White, *Lancet Infect. Dis.*, 2006, **6**, 602-613.
4. P. N. Newton, S. Proux, M. D. Green, F. Smithius, J. Rozendaal, S. Prakongpan, K. Chotivanich, M. Mayxay, S. Looareesuwan, J. Farrar, F. Nosten and N. J. White, *Lancet*, 2001, **357**, 1948-1950.
5. R. N. Price, A. C. Uhlemann, A. Brockman, R. McGready, E. Ashley, L. Phaipum, R. Patel, K. Laing, S. Looareesuwan, N. J. White, F. Nosten and S. Krishna, *Lancet*, 2004, **364**, 438-447.
6. N. J. White, *J. Clin. Invest.*, 2004, **113**, 1084-1092.
7. S. Yeung, W. Pongtavornpinvo, I. M. Hastings, A. J. Mills and N. J. White, *Am. J. Trop. Med. Hyg.*, 2004, **71**, 179-186.
8. P. N. Newton, F. M. Fernandez, A. Plancon, D. C. Mildenhall, M. D. Green, L. Ziyong, E. M. Christophel, S. Phanouvong, S. Howells, E. McIntosh, P. Laurin, N. Blum, C. Y. Hampton, K. Faure, L. Nyadong, C. W. R. Soong, B. Santoso, W. Zhiguang, J. Newton and K. Palmer, *PLoS Med.*, 2008, **5**, E32.
9. M. Dimou, G. Goras and A. Thrasyvoulou, *Grana*, 2007, **46**, 118-122.
10. J. R. Ioset and H. Kaur, *PLoS ONE*, 2009, **4**, E7270.
11. P. G. Risha, Z. Msuya, M. Clark, K. Johnson, M. Ndomondo-Sigonda and T. Layloff, *Health Policy*, 2008, **87**, 217-222.
12. Z. Takats, J. M. Wiseman, B. Gologan and R. G. Cooks, *Science*, 2004, **306**, 471-473.
13. M. D. Green, L. M. Dwight, R. A. Wirtz and N. J. White, *J. Pharmaceut. Biomed.*, 2000, **24**, 65-70.
14. M. D. Green, D. L. Mount and R. A. Wirtz, *Trop. Med. Int. Health*, 2001, **6**, 980-982.
15. M. D. Green, H. Nettey, O. V. Rojas, C. Pamanivong, L. Khounsaknalath, M. G. Ortiz, P. N. Newton, F. M. Fernandez, L. Vongsack and O. Manolin, *J. Pharmaceut. Biomed.*, 2007, **43**, 105-110.
16. C. Ricci, L. Nyadong, F. Yang, F. M. Fernandez, C. D. Brown, P. N. Newton and S. G. Kazarian, *Anal. Chim. Acta*, 2008, **623**, 178-186.
17. W. L. Yoon, R. D. Jee, A. Charvill, G. Lee and A. C. Moffat, *J. Pharmaceut. Biomed.*, 2004, **34**, 933-944.
18. P. N. Newton, S. J. Lee, C. A. Goodman, F. M. Fernandez, S. Yeung, S. Phanouvong, H. Kaur, A. A. Amin, C. J. M. Whitty, G. O. Kokwaro, N. Lindegardh, P. Lukulay, L. J. White, N. J. P. Day, M. D. Green and N. J. White, *PLoS Med.*, 2009, **6**, E52.
19. P. N. Newton, M. D. Green, D. C. Mildenhall, A. Plancon, H. Nettey, L. Nyadong, D. M. Hostetler, K. Powell, J. C. Wolff, A. E. Timmermans, A. A. Amin, U. MRA, T. MRA, G. FDB, S. Barbereu, C. Faurant, C. Eckers, S. Smith,

J. Thecanayagam, P. Fernandes, H. Kaur, N. J. White and F. M. Fernandez, In Preparation.
20. K. P. Board, Editon edn., 2004.
21. P. N. Newton, R. McGready, F. M. Fernandez, M. D. Green, M. Sunjio, C. Bruneton, S. Phanouvong, P. Millet, C. J. M. Whitty, A. O. Talisuna, S. Proux, E. M. Christophel, G. Malenga, P. Singhasivanon, K. Bojang, H. Kaur, K. Palmer, N. J. P. Day, B. M. Greenwood, F. Nosten and N. J. White, *PLoS Med.*, 2006, **3**, E197.
22. M. A. Atemnkeng, K. D. Cock and J. Plaizier-Vercammen, *Trop. Med. Int. Health*, 2007, **12**, 68-74.
23. M. Oyeniran, in *Nigerian Tribune*, Editon edn., 2006.
24. M. Oyeniran, in *Nigerian Tribune*, Editon edn., 2007.
25. O. Onwujekwe, H. Kaur, N. Dike, E. Shu, B. Uzochukwu, K. Hanson, V. Okoye and P. Okonkwo, *Malaria J.*, 2009, **8**, 22.
26. R. Bate, P. Coticelli, R. Tren and A. Attaran, *PLoS ONE*, 2008, **3**, E2132.
27. W. H. Organization, Editon edn., 2009.
28. K. E. Hope, in *The Ghanaian Times*, Editon edn., 2009.
29. U. S. Pharmacopeia, Editon edn., 2009.
30. F. Udoh, in *AllAfrica.com*, Editon edn., 2010.
31. F. Udoh, in *AllAfrica.com*, Editon edn., 2010.
32. R. B. Cody, J. A. Laramee and H. D. Durst, *Anal. Chem.*, 2005, **77**, 2297-2302.
33. G. A. Harris and F. M. Fernandez, *Anal. Chem.*, 2009, **81**, 322-329.
34. K. Kpegba, T. Spadaro, R. B. Cody, N. Nesnas and J. A. Olson, *Anal. Chem.*, 2007, **79**, 5479-5483.
35. F. M. Fernandez, R. B. Cody, M. D. Green, C. Y. Hampton, R. McGready, S. Sengaloundeth, N. J. White and P. N. Newton, *ChemMedChem*, 2006, **1**, 702-705.
36. C. Y. Pierce, J. R. Barr, R. B. Cody, R. F. Massung, A. R. Woolfitt, H. Moura, H. A. Thompson and F. M. Fernandez, *Chem. Commun.*, 2007, **8**, 807-809.
37. J. A. Laramee, H. D. Durst, T. R. Connell and J. M. Nilles, *Am. Lab.*, 2008, **40**, 18-20.
38. V. Gabelica and E. De Pauw, *Mass Spectrom. Rev.*, 2004, **24**, 566-587.
39. C. Y. Hampton, C. J. Silvestri, T. P. Forbes, M. J. Varady, J. M. Meacham, A. G. Federov, F. L. Degertekin and F. M. Fernandez, *J. Am. Soc. Mass Spectr.*, 2008, **19**, 1320-1329.
40. M. Nefliu, J. N. Smith, A. Venter and R. G. Cooks, *J. Am. Soc. Mass Spectr.*, 2008, **19**, 420-427.
41. A. R. Katritzky, C. H. Watson, Z. Dega-Szafran and J. R. Eyler, *J. Am. Soc. Mass Spectrom.*, 1990, **112**, 2471-2478.
42. H. I. Kenttamaa and R. G. Cooks, *Int. J. Mass. Spectrom.* , 1985, **64**, 79-83.
43. K. Vekey, *J. Mass Spectrom.*, 1996, **31**, 445-463.
44. A. G. Harrison, *Rapid Commun. Mass Sp.*, 1999, **13**, 1663-1670.
45. D. J. Burinsky, J. D. Williams, A. D. Thornquest Jr. and S. L. Sides, *J. Am. Soc. Mass Spectr.*, 2001, **12**, 385-398.
46. P. Koscielniak and P. Kozak, *Anal. Chim. Acta*, 2002, **460**, 235-245.
47. J. B. Fenn, M. Mann, C. K. Meng, S. F. Wong and C. M. Whitehouse, *Science*, 1989, **246**, 64-71.

48. P. Kebarle and U. H. Verkerk, *Mass Spectrom. Rev.*, 2009, **28**, 898-917.
49. J. V. Iribarne and B. A. Thompson, *J. Chem. Phys.*, 1976, **64**, 2287-2294.
50. M. Dole, L. L. Mack, R. L. Hines, R. C. Mobley, L. D. Ferguson and M. B. Alice, *J. Chem. Phys.*, 1968, **49**, 2240-2249.
51. B. K. Choi, A. I. Gusev and D. M. Hercules, *Int. J. Environ. An. Ch*, 2000, **77**, 305-322.
52. Y. O. Karatasso, I. V. Logunova, M. G. Sergeeva, E. N. Nikolaev, S. D. Varfolomeev and V. V. Chistyakov, *Pharm. Chem. J.*, 2007, **41**, 166-169.
53. V. H. Wysocki, H. I. Kenttamaa and R. G. Cooks, *Int. J. Mass. Spectrom.*, 1987, **75**, 181-208.
54. K. Vekey, A. G. Brenton and J. H. Beynon, *J. Phys. Chem.*, 1986, **90**, 3569-3577.
55. C. Collette and E. De Pauw, *Rapid Commun. Mass Sp.*, 1998, **12**, 1673-1678.
56. C. Collette, L. Drahos, E. De Pauw and K. Vekey, *Rapid Commun. Mass Sp.*, 1998, **12**, 1673-1678.
57. S. Sengaloundeth, M. D. Green, F. M. Fernandez, O. Manolin, K. Phommavong, V. Insixiengmay, C. Y. Hampton, L. Nyadong, D. C. Mildenhall, D. M. Hostetler, L. Khounsaknalath, L. Vongsack, S. Phompida, V. Vanisaveth, L. Syhakhang and P. N. Newton, *Malaria J.*, 2009, **8**, 172.
58. W. P. Peng, M. P. Goodwin, H. Chen, R. G. Cooks and J. Wilker, *Rapid Commun. Mass Sp.*, 2008, **22**, 3540-3548.
59. V. Gabelica, E. De Pauw and M. Karas, *Int. J. Mass. Spectrom.* , 2004, **231**, 189-195.
60. L. Drahos, R. M. A. Heeren, C. Collette, E. De Pauw and K. Vekey, *J. Mass Spectrom.*, 1999, **34**, 1373-1379.
61. S. P. Fisenko, W. N. Wang, W. Lenggoro and K. Okyuama, *Chem. Eng. Sci.*, 2006, **61**, 6029-6034.
62. V. L. Campbell, Z. Guan and D. A. Laude Jr., *J. Am. Soc. Mass Spectr.*, 1994, **5**, 221-229.
63. P. Kebarle, *J. Mass Spectrom.*, 2000, **35**, 804-817.
64. R. B. Cody, *Anal. Chem.*, 2009, **81**, 1101-1107.
65. J. A. Laramee and R. B. Cody, in *Encyclopedia of Mass Spectrometry*, eds. R. M. Caprioli and M. L. Gross, Elseivier, Amsterdam, Editon edn., 2007, vol. 6, pp. 377-387.
66. D. B. Milligan, P. F. Wilson, C. G. Freeman, M. M. N. Mautner and M. J. McEwan, *J. Phys. Chem. A*, 2002, **106**, 9745-9755.
67. G. Nicol, J. Sunner and P. Kebarle, *Int. J. Mass. Spectrom.*, 1988, **84**, 135-155.
68. A. Schmidt, U. Bahr and M. Karas, *Anal. Chem.*, 2001, **73**, 6040-6046.
69. R. G. Cooks, T. Ast and M. A. Mabud, *Int. J. Mass. Spectrom.*, 1990, **100**, 209-265.
70. M. Kurahashi and Y. Yamauchi, *Phys. Rev. Lett*, 2000, **84**, 4725-4728.
71. M. Kurahashi and Y. Yamauchi, *Surf. Sci.*, 2000, **454-456**, 300-304.
72. L. Nyadong, S. Late, A. Banga, M. D. Green, P. N. Newton and F. M. Fernandez, *J. Am. Soc. Mass Spectr.*, 2008, **19**, 380-388.
73. R. K. Haynes, H. W. Chan, C. M. Lung, N. C. Ng, H. N. Wong, L. Y. Shek, I. D. Williams, A. Cartwright and M. F. Gomes, *ChemMedChem*, 2007, **2**, 1448-1463.